2018

Kv7 Channels Of The Urinary Bladder Smooth Muscle: Functional Roles And Therapeutic Potential

Aaron Provence
University of South Carolina

K_V7 Channels of the Urinary bladder Smooth Muscle: Functional Roles and Therapeutic potential

by

Aaron Provence

Bachelor of Science
University of South Carolina, 2012

Submitted in Partial Fulfillment of the Requirements

For the Degree of Doctor of Philosophy in

Pharmaceutical Sciences

College of Pharmacy

University of South Carolina

2018

Accepted by:

Lorne J. Hofseth, Major Professor

Jun Zhu, Chair, Examining Committee

Mark Hamann, Committee Member

Jill Turner, Committee Member

Kenneth B. Walsh, Committee Member

Cheryl L. Addy, Vice Provost and Dean of the Graduate School

DEDICATION

To my mother and father.

ACKNOWLEDGEMENTS

I thank the members of my PhD Advisory Committee: Drs. Lorne J. Hofseth, Jun Zhu, Jill Turner, Mark Hamann, and Kenneth B. Walsh. I would like to thank Dr. Kiril L. Hristov for his mentorship and training during the course of my PhD. I also thank Drs. Shankar P. Parajuli, Vitor S. Fernandes, Wenkuan Xin, Gary P. Schools, Damiano Angoli, and Biao Chen for their support and teamwork. I further thank Dr. Eric S. Rovner for his mentorship and the Department of Urology at the Medical University of South Carolina (MUSC). Specifically, I thank the MUSC Urology staff surgeons: Drs. Thomas Keane, Harry Clarke, Stephen Savage, Ross Rames, Sandip Prasad, and Jonathan Picard, as well as the MUSC Urology Residents: Ryan Levey, Austin Younger, Mark Currin, Nima Baradaran, Olugbemisola McCoy, Alyssa Greiman, Sarah Starosta, Bryce Wyatt and Tracy Tipton for their help with human tissue collection. I thank my Graduate Program Director, Dr. Lorne Hofseth and Department Chair Dr. Kim Creek for their unwavering support and guidance throughout my PhD.

ABSTRACT

Overactive bladder (OAB) is a pervasive and debilitating condition for which effective therapeutic modalities are lacking. As potential novel pharmacological targets for lower urinary tract dysfunction, our recent studies have demonstrated voltage-gated K_V7 channels ($K_V7.1$-$K_V7.5$) to be functionally expressed in detrusor smooth muscle (DSM) of the urinary bladder. Nonetheless, the specific roles of individual K_V7 channel subtypes remains poorly understood. Using Western blot, immunocytochemistry, isometric DSM tension recordings, ratiometric fluorescence Ca^{2+} imaging, and patch-clamp electrophysiology, we demonstrated expression and key physiologic roles for the $K_V7.2$/$K_V7.3$ channels in guinea pig DSM using the novel and selective $K_V7.2$/$K_V7.3$ channel opener *N*-(2-Chloro-5-pyrimidinyl)-3,4-difluorobenzamide (ICA-069673). We further sought to pharmacologically target $K_V7.4$- and $K_V7.5$-containing channels, which evidence suggests are the prominent subtypes expressed in smooth muscle, to determine their involvement in regulating DSM excitation-contraction coupling. The novel $K_V7.4$/$K_V7.5$ channel activator *N*-(2,4,6-Trimethylphenyl)-bicyclo[2.2.1]heptane-2-carboxamide (ML213) was shown to enhance K_V7 channel currents in isolated DSM cells, hyperpolarize the DSM cell membrane potential, and attenuate the contractile activity of DSM isolated strips via a Ca^{2+}-dependent mechanism. ML213 exhibited significantly greater potency for inhibition of DSM contractility in comparison to $K_V7.2$/$K_V7.3$ channel opener ICA-069673. Using *in situ* proximity ligation assay (PLA), it was further revealed $K_V7.4$ and $K_V7.5$ channel α-subunits co-localize to form

heteromeric $K_V7.4/K_V7.5$ channel complexes in DSM isolated cells. These studies suggest $K_V7.4/K_V7.5$ channels are functionally expressed in guinea pig DSM, where they critically regulate DSM excitability and contractility.

Finally, to ascertain the translational implications of our aforementioned findings from experimental animals, we examined K_V7 channel expression and function in human DSM. K_V7 channel activators and inhibitors were shown to attenuate and potentiate, respectively, human DSM excitability and contractility in normal and OAB samples. Noteworthy, using *in situ* PLA, we confirmed the molecular interaction between $K_V7.4$ and $K_V7.5$ channel α-subunits, suggesting heteromeric $K_V7.4/KV7.5$ channel subtype expression at the cellular level in human DSM cells. These findings are consistent with our findings in guinea pig DSM and provide strong support to suggest $K_V7.4/K_V7.5$ channels are among the key subtypes regulating human DSM function.

In conclusion, our combined studies reveal novel insights into the expression, subunit composition, and physiological roles of K_V7 channel in DSM, providing critical information for directing future research efforts concerning the utility of K_V7 channels as therapeutic targets for OAB.

TABLE OF CONTENTS

LIST OF TABLES

LIST OF FIGURES

LIST OF ABBREVIATIONS

BK……...large-conductance voltage- and Ca^{2+}- activated K^+ channel

CCh .....Carbachol

DAPI.....4′,6-Diamidine-2′-phenylindole dihydrochloride

DMSO .....dimethyl sulfoxide

EFS.....electrical field stimulation

HEPES..... 4-(2-hydroxyethyl)piperazine-1-ethanesulfonic acid

K_V..... voltage-gated K^+ channel

ML213.....N-(2,4,6-Trimethylphenyl)-bicyclo[2.2.1]heptane-2-carboxamide

mAChR..... muscarinic acetylcholine receptor

PLA .....proximity ligation assay

RCA.....rolling circle amplification

TTX.....tetrodotoxin

XE991.....10,10-*bis*(4-pyridinylmethyl)-9(10H)-anthracenone dihydrochloride

OAB .....Overactive Bladder

CHAPTER 1

INTRODUCTION

Urinary Bladder Structure, Function, and Regulation

The urinary bladder facilitates two major functions: the storage and voiding of urine. Under physiological conditions, parasympathetic nerves release ACh and ATP to activate muscarinic ACh receptors (mAChRs) and purinergic receptors, respectively, to trigger bladder contraction and micturition (i.e. urine voiding)[1-3]. Within the walls of the urinary bladder detrusor smooth muscle (DSM), the main muscular component of the bladder, facilitates bladder contraction in response to mAChR activation. In human DSM, ACh-induced activation of mAChRs constitutes the primary mechanism initiating bladder contraction in urine voiding [1]. In addition to these nerve-mediated mechanisms, human DSM also exhibits spontaneous action potentials, intrinsic activity of the DSM cells which underlies the spontaneous phasic contractility of the bladder.

DSM contractility is mainly dependent upon an increase in global intracellular Ca^{2+} concentrations ($[Ca^{2+}]_i$) as the rise in $[Ca^{2+}]_i$ leads to the activation of myosin-light chain kinase pathways which underlies smooth muscle contractility (23, 44). As exemplified by Figure 1.2, ACh-induced activation of mAChRs can increases global intracellular Ca^{2+} concentrations via phospholipase C-mediated activation of sarcoplasmic reticulum IP3 receptors, which results in the release of Ca^{2+} from internal stores. Release of Ca^{2+} from the sarcoplasmic reticulum results in a dramatic increase in the *local* Ca^{2+} concentration, which can result in the activation of adjacent cation channels at the cell membrane.

Critically involved in the regulation of bladder contractility, K^+ channels function to regulate Ca^{2+} entry through L-type voltage-gated Ca^{2+} (Ca_v) channels, and thus intracellular Ca^{2+} levels, by virtue of their influence upon the cell membrane potential[4]. While the etiology and pathophysiology of overactive bladder (OAB) is not fully known, it has been directly linked to DSM dysfunction. As such, the pivotal role of the K^+ channels in controlling DSM cell membrane excitability has generated interest in their potential therapeutic utility for various forms of DSM dysfunction and OAB.

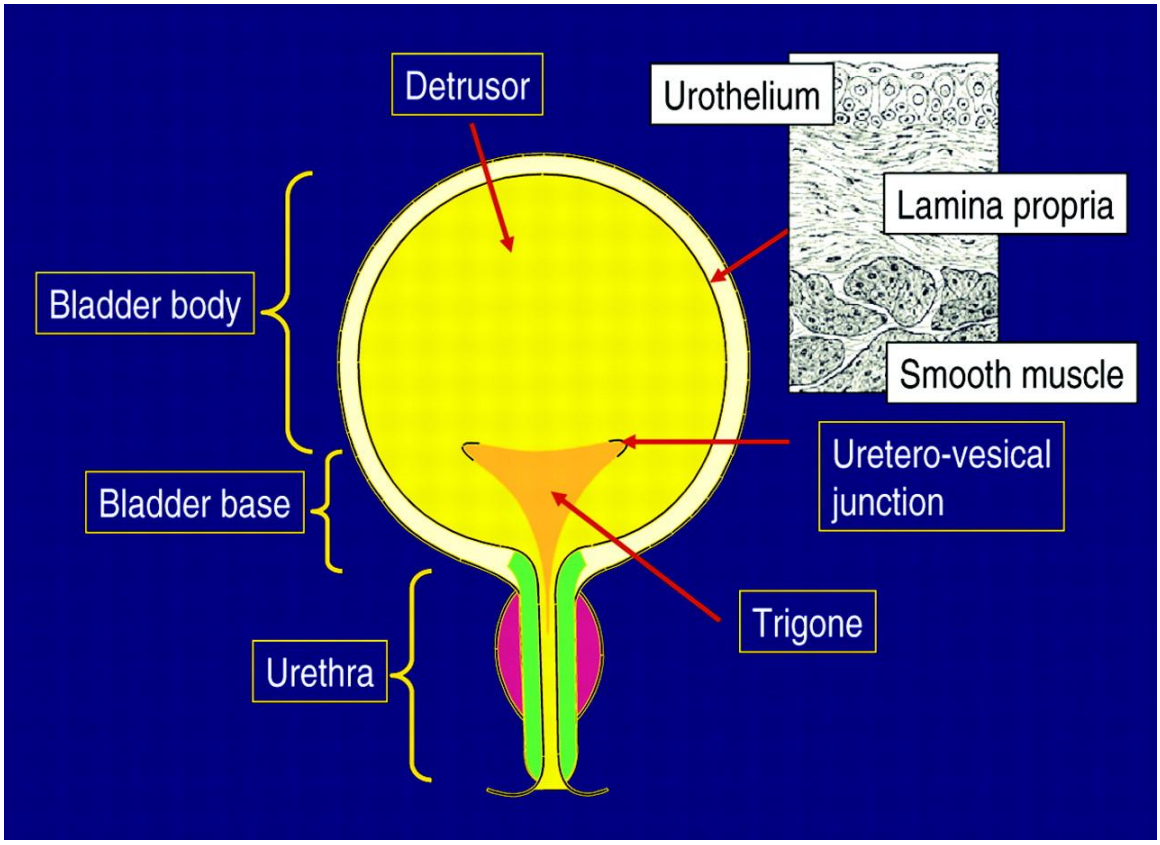

[1]Figure 1.1 Schematic drawing of the bladder.

[1] Reprinted from Andersson & Arner, 2004[1] with permission.

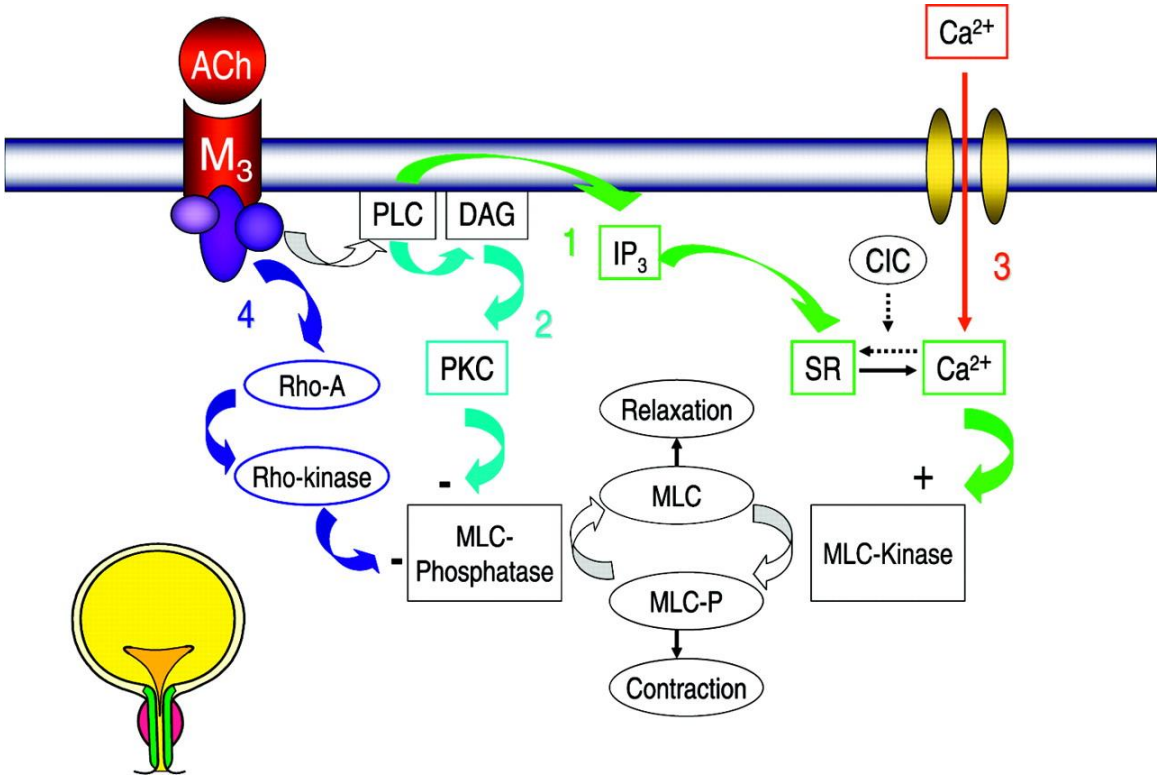

[2]Figure 1.2. Signal pathways (*1–4*) involved in activation of detrusor contraction via muscarinic M_3 receptors. ACh, acetylcholine; PLC, phospholipase C; DAG, diacylglycerol; PKC, protein kinase C; MLC, myosin light chain; IP_3, inositol trisphosphate; SR, sarcoplasmic reticulum; CIC, calcium-induced calcium release. There seem to be differences between species in the contribution of the different pathways in contractile activation. In human detrusor, Ca^{2+} influx (*3*) is of major importance.

[2] Reprinted from Andersson & Arner, 2004[1] with permission.

Overactive bladder

Overactive bladder (OAB) is currently among the most prevalent chronic health conditions in the United States with significant economic and health-related implications (47). As a syndrome, OAB is characterized by the lower urinary tract symptoms (LUTS) experienced by the individual, which includes urinary urgency, frequency, with or without urge urinary incontinence and nocturia (22). Despite the negative physical, social, and economic impact of OAB, evidence demonstrates this condition to have a detrimental impact upon individual's mental health and quality of life by interfering with their sleep, work, and social interactions (33, 34). Affecting ~16.5% of the population, the increasing prevalence of OAB is expected to continue and by the year 2018, it will impact an estimated 20.1% of the population at a cost of $82.6 billion (13, 27). However, these estimations underscore the widespread impact of OAB because as little as 25% of individuals affected actually pursue medical care (16).

The primary treatment for OAB involves antimuscarinics (i.e. anticholinergics); however, these agents are not tissue- or organ-specific in their mechanism of action and thus give rise to bothersome side-effects including blurred vision, dry-mouth, and tachycardia (16, 19). This is evidenced by the current patient discontinuation rates of 80-90% within the first year of treatment (18) with one report indicating the average time for patient discontinuation to be 31 days (15). More recently, a β3-adrenoceptor agonist known as mirabegron was approved by the FDA to treat OAB; however, its long-term efficacy is inconclusive (19). Likewise, intradetrusor botulinum toxin type A (OnabotulinumtoxinA) injections approved by the FDA in 2013 have shown to provide some effective symptomatic relief, yet this method of treatment is both invasive, requires IV sedation, and may call for recurrent injections to maintain clinical effectiveness (16). Therefore, the

considerable negative effects OAB has upon individual health, both physically and psychologically, dictates an urgent need for improved pharmacological therapeutics.

The storage and periodical release of urine describes the two major functions of the urinary bladder (5), a process facilitated by the contraction and relaxation of urinary bladder smooth muscle (UBSM) (39). UBSM contractility is mainly dependent upon increased intracellular Ca^{2+} concentrations ($[Ca^{2+}]_i$) as the rise in $[Ca^{2+}]_i$ leads to the activation of myosin-light chain kinase pathways which underlies smooth muscle contractility (23, 44). Therefore, if the goal of OAB therapeutics is to promote UBSM relaxation, it is essential therefore to consider the key mechanisms controlling Ca^{2+} influx within human UBSM cells. This precisely defines the fundamental role of UBSM K^+ channels, which by promoting cell membrane hyperpolarization, precludes Ca^{2+}-influx through L-type (long-lasting) voltage-gated Ca^{2+} (Ca_v) channels to promote membrane hyperpolarization and thus UBSM relaxation (6, 9).

Voltage-gated K_V7 Channels

Among all K^+ channels, the voltage-gated KCNQ family has been shown to serve functional roles in rat, guinea pig (3,12 25) and human UBSM (26); however, among the 40 genes encoding these channels, a subfamily of five channels encoded by KCNQ genes (KCNQ1-KCNQ5) have sparked great interest as potential pharmacological targets based on increasing evidence suggesting their involvement in a number of pathophysiological conditions including epilepsy, hypertension, chronic pain, and cardiac dysfunction (11, 20, 35, 40). The KCNQ (or K_V7) channel family (KCNQ1-KCNQ5) attains vast heterogeneity as their five α subunits form distinct homo- or hetero-tetrameric complexes (see Figure 1.3a) (42, 50). Further, KCNQ channels associate with KCNE-encoded β-regulatory

subunits (KCNE1-KCNE5), which may alter KCNQ channel biophysical properties including subcellular localization, pharmacology, and selectivity (1, 14, 30, 42, 48).

The knowledge of KCNQ channel expression and function primarily arose from studies in the heart and brain, however physiological roles for KCNQ channels in other vascular and non-vascular tissues systems is now becoming more apparent (28, 29, 31, 32, 36, 43, 51). The important physiological roles KCNQ channels serve in various tissues has coincided with an increasing number of KCNQ channel pharmacological modulators, which has further heightened our understanding of these channels along with revealing some key distinctions between KCNQ channels and other smooth muscle K^+ channels (30). Previously, the therapeutic utility of K^+ channel pharmacological activators, specifically KATP channels activators, were unsuccessful due to concerns regarding drug selectivity[1]. However, this changed in 2011 with the FDA approval of the antiepileptic drug retigabine, which exerts its therapeutic effects by targeting KCNQ2-5 channels (21). This has led to retigabine being widely utilized throughout various tissues and animal models in order to elucidate KCNQ channel function in health and disease (30).

Noteworthy and pertinent to this work, KCNQ channel functional roles, including in studies from our laboratory (2), have recently been identified within UBSM tissues of the guinea pig (2, 4)**,** pig (46); and rat, where retigabine was shown to have pronounced effects in reducing UBSM contractility (41). This may elude to the increased micturition volume and voiding intervals observed in rats subjected to acute retigabine exposure *in vivo* (41, 45, 46). More relevant, clinical evidence has proven retigabine to be associated with the increased occurrence of urinary retention (9). This indicates a potential role for KCNQ channel activity in regulating bladder function and therefore targeting these

channels may potentially provide beneficial relief for patients with OAB. While retigabine is a potent activator of KCNQ2-5 channels, the selectivity towards KCNQ2/3 channels is significantly greater than that of KCNQ4/5 as evidenced by experimentally determined EC_{50} values of 0.6 µM for KCNQ2/3 and 5.2-6.4 µM for KCNQ4/5 (21). KCNQ4 and KCNQ5 channel expression is predominate in smooth muscle (44) with KCNQ2/3 channels important for neuronal function. This could be very significant as this may suggest the potential pharmacological efficacy of future selective KCNQ4/5 channel activators as effective treatments for OAB, while KCN2/3 selective modulators may prove better for the treatment of neurological conditions. Therefore, this may abolish the large number of adverse effects associated with current OAB treatments and thus the beneficial implications of this research is incredibly relevant to public health, clinical medicine, and most importantly, quality of life.

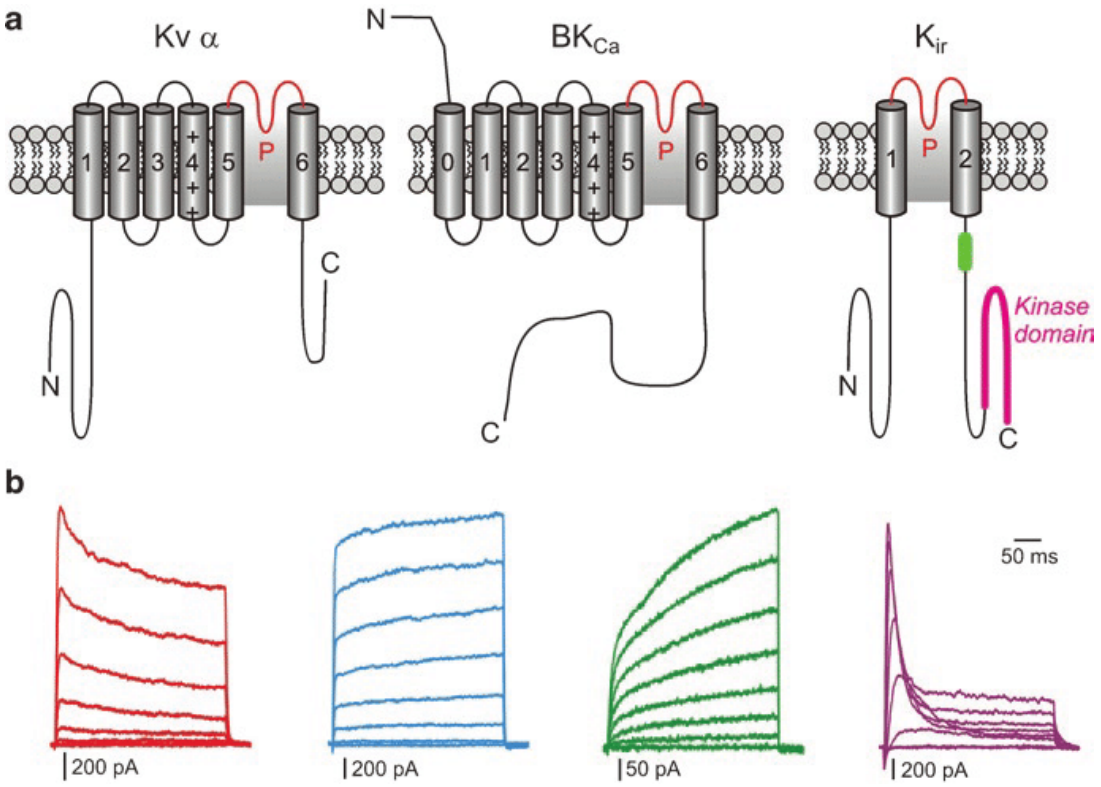

[3]Figure 1.3 Structure and function of K^+ channels. (a) Planar membrane topologies of single potassium channel subunits for KV , BK Ca , and K ir channels, respectively. The pore-forming loop and the voltage sensor in transmembrane unit 4 are indicated. (b) Representative current traces recorded in human pulmonary arterial smooth muscle cells indicating diversity in the Kv currents; from left to right, (1) rapidly activating and slowly inactivating I K(V), (2) rapidly activating and noninactivating I K(V) , (3) slowly activating and noninactivating I K(V) , and (4) rapidly activating and rapidly inactivating I K(V)K.

[3] Reprinted from Firth et al, 2011[5] with permission.

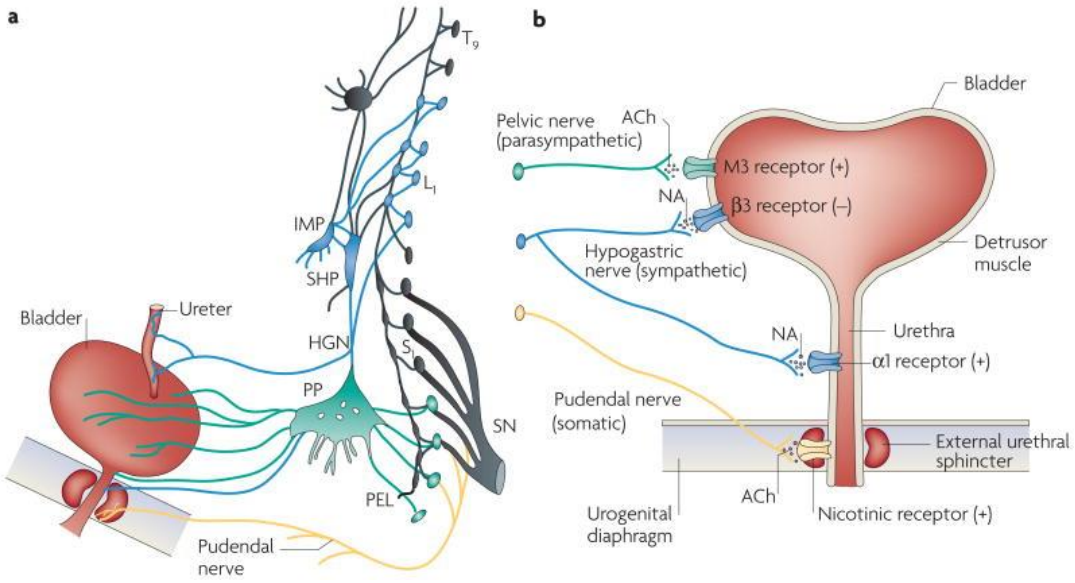

[4]Figure 1.4 Efferent pathways of the lower urinary tract

a | Innervation of the female lower urinary tract. Sympathetic fibres (shown in blue) originate in the T11–L2 segments in the spinal cord and run through the inferior mesenteric ganglia (inferior mesenteric plexus, IMP) and the hypogastric nerve (HGN) or through the paravertebral chain to enter the pelvic nerves at the base of the bladder and the urethra. Parasympathetic preganglionic fibres (shown in green) arise from the S2–S4 spinal segments and travel in sacral roots and pelvic nerves (PEL) to ganglia in the pelvic plexus (PP) and in the bladder wall. This is where the postganglionic nerves that supply parasympathetic innervation to the bladder arise. Somatic motor nerves (shown in yellow) that supply the striated muscles of the external urethral sphincter arise from S2–S4 motor neurons and pass through the pudendal nerves. **b** | Efferent pathways and neurotransmitter mechanisms that regulate the lower urinary tract. Parasympathetic postganglionic axons in the pelvic nerve release acetylcholine (ACh), which produces a bladder contraction by stimulating M_3 muscarinic receptors in the bladder smooth muscle. Sympathetic postganglionic neurons release noradrenaline (NA), which activates β_3 adrenergic receptors to relax bladder smooth muscle and activates α_1 adrenergic receptors to contract urethral smooth muscle. Somatic axons in the pudendal nerve also release ACh, which produces a contraction of the external sphincter striated muscle by activating nicotinic cholinergic receptors. Parasympathetic postganglionic nerves also release ATP, which excites bladder smooth muscle, and nitric oxide, which relaxes urethral smooth muscle (not shown). L_1, first lumbar root; S_1, first sacral root; SHP, superior hypogastric plexus; SN, sciatic nerve; T_9, ninth thoracic root. Part **a**modified, with permission, from REF. 144 © (1996) W. B. Saunders Company.

[4] Reprinted from Fowler et al., 2010[6] with permission.

CHAPTER 2

EXPERIMENTAL APPROACH

Rationale and Central Hypothesis

The important physiological role K_V7 channels serve in smooth muscle tissues, which evidence shows to be subtype- and tissue-specific, suggests these channels may provide a novel platform for future OAB pharmacological treatments. The achievement of this will require an improved understanding of K_V7 channel expression, subunit composition, and function in DSM excitability and contractility at both the single cell and whole-tissue level. *The central hypothesis of these studies is that K_V7 channels are critical regulators of human UBSM excitation-contraction coupling and thus K_V7 channels provide a novel target for the pharmacological treatment of OAB.*

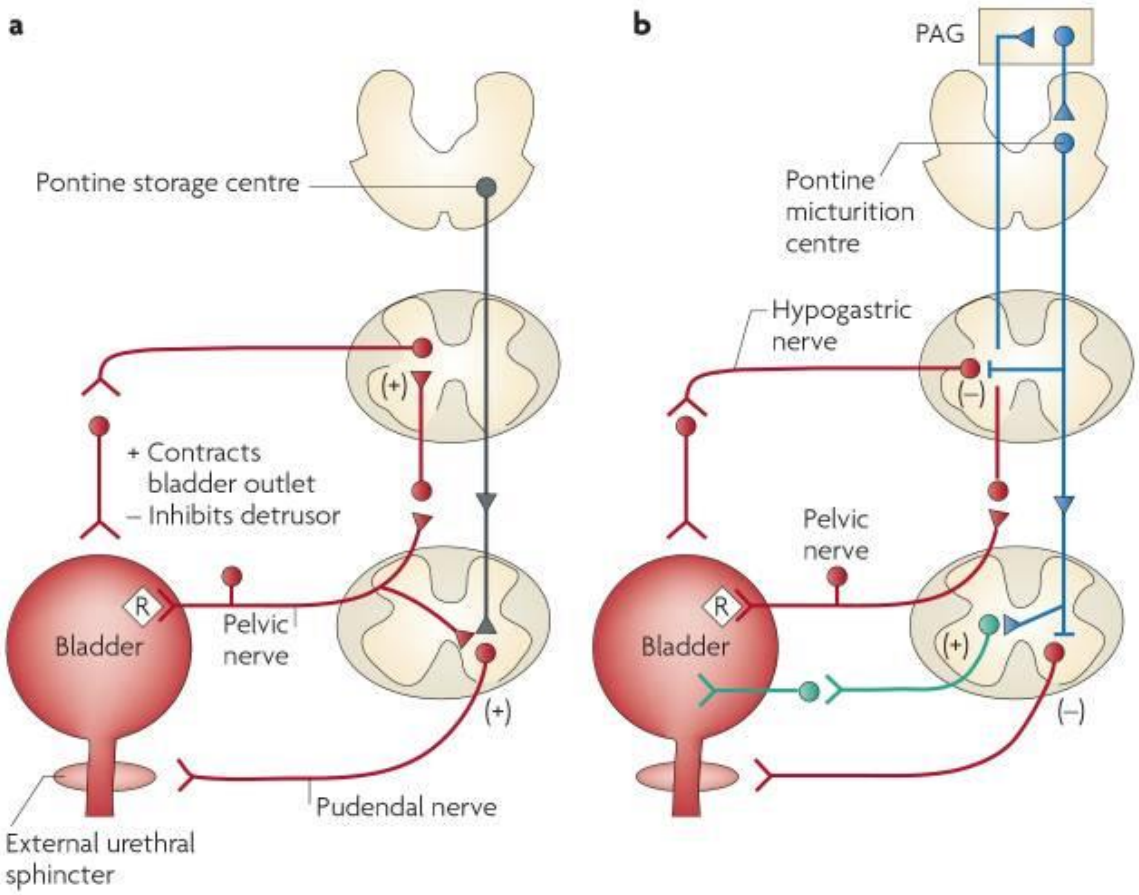

[5]Figure 1.5. Neural circuits that control continence and micturition

a | Urine storage reflexes. During the storage of urine, distention of the bladder produces low-level vesical afferent firing. This in turn stimulates the sympathetic outflow in the hypogastric nerve to the bladder outlet (the bladder base and the urethra) and the pudendal outflow to the external urethral sphincter. These responses occur by spinal reflex pathways and represent guarding reflexes, which promote continence. Sympathetic firing also inhibits contraction of the detrusor muscle and modulates neurotransmission in bladder ganglia. A region in the rostral pons (the pontine storage centre) might increase striated urethral sphincter activity. **b** | Voiding reflexes. During the elimination of urine, intense bladder-afferent firing in the pelvic nerve activates spinobulbospinal reflex pathways (shown in blue) that pass through the pontine micturition centre. This stimulates the parasympathetic outflow to the bladder and to the urethral smooth muscle (shown in green) and inhibits the sympathetic and pudendal outflow to the urethral outlet (shown in red). Ascending afferent input from the spinal cord might pass through relay neurons in the periaqueductal grey (PAG) before reaching the pontine micturition centre. Note that these diagrams do not address the generation of conscious bladder sensations, nor the mechanisms that underlie the switch from storage to voiding, both of which presumably involve cerebral circuits above the PAG. R represents receptors on afferent nerve terminals.

[5] Reprinted from Fowler et al., 2010[6] with permission

CHAPTER 3

[6]THE NOVEL $K_V7.2/K_V7.3$ CHANNEL OPENER ICA-069673 REVEALS SUBTYPE-SPECIFIC FUNCTIONAL ROLES IN GUINEA PIG DETRUSOR SMOOTH MUSCLE EXCITABILITY AND CONTRACTILITY

ABSTRACT

The physiological roles of voltage-gated K_V7 channel subtypes ($K_V7.1$-$K_V7.5$) in detrusor smooth muscle (DSM) are poorly understood. Here, we sought to elucidate the functional roles of $K_V7.2/K_V7.3$ channels in guinea pig DSM excitability and contractility using the novel $K_V7.2/K_V7.3$ channel activator N-(2-chloro-pyrimidin-5-yl)-3,4-difluoro-benzamide (ICA-069673). We employed a multi-level experimental approach using Western blot, immunocytochemistry with confocal microscopy, isometric DSM tension recordings, fluorescence Ca^{2+} imaging, and perforated whole cell patch-clamp electrophysiology. Western blot experiments revealed the protein expression of $K_V7.2$ and $K_V7.3$ channel subunits in DSM tissue. In isolated DSM cells, immunocytochemistry with confocal microscopy further confirmed protein expression for $K_V7.2$ and $K_V7.3$ channel subunits where they localize within the vicinity of the cell membrane. ICA-069673 inhibited spontaneous phasic, pharmacologically-induced, and nerve-evoked contractions in DSM isolated strips in a concentration-dependent manner. The inhibitory effects of ICA-069673 on DSM spontaneous phasic and tonic contractions were abolished in the presence

[6] Provence, A., J. Malysz, and G.V. Petkov, The Novel KV7.2/KV7.3 Channel Opener ICA-069673 Reveals Subtype-Specific Functional Roles in Guinea Pig Detrusor Smooth Muscle Excitability and Contractility. *The Journal of pharmacology and experimental therapeutics*, 2015. 354(3): p. 290-301.

of the K_V7 channel inhibitor XE991. Unlike nifedipine, under conditions of elevated extracellular K^+ (60 mM), the effects of ICA-069673 on DSM tonic contractions were significantly attenuated. ICA-069673 decreased global intracellular Ca^{2+} concentration in DSM cells, and this effect was blocked by nifedipine. ICA-069673 hyperpolarized the membrane potential and inhibited DSM spontaneous action potentials of isolated DSM cells, effects which were blocked in the presence of XE991. In conclusion, the current study using the novel $K_V7.2/K_V7.3$ channel activator ICA-069673, provides strong evidence for a critical role for the $K_V7.2$- and $K_V7.3$-containing channels in DSM function at both cellular and tissue levels.

INTRODUCTION

Voltage-gated K^+ (K_V7) channels ($K_V7.1$-$K_V7.5$), also known as KCNQ (KCNQ1-KCNQ5) channels, have recently been suggested as regulators of detrusor smooth muscle (DSM) excitability and contractility [7-9]. In DSM, the overall function of K_V channels, which includes the K_V7 channels, is to maintain and stabilize the resting membrane potential [4]. This is achieved by limiting the influx of Ca^{2+} through L-type voltage-gated Ca^{2+} (Ca_V) channels, which leads to DSM relaxation. The ability for DSM cells to generate spontaneous action potentials, which underlies DSM phasic contractility, allows this cell type to facilitate the function of the urinary bladder [4, 10, 11]. Under pathophysiological conditions such as overactive bladder (OAB), the contractile activity of DSM may be abnormally increased [12]. Thus, pharmacologically targeting bladder-specific K_V7 channel subtypes may represent a novel therapeutic strategy to control OAB.

The K_V7 channel family consists of five members ($K_V7.1$-$K_V7.5$), which form homomic or heteromeric tetramers of K_V7 α-subunits. The diversity of K_V7 channel combinations, such

as $K_V7.2/K_V7.3$ or $K_V7.3/K_V7.5$, expands their functional and biophysical properties [4, 13, 14]. For example, heteromeric $K_V7.2/K_V7.3$ channels produce whole cell currents 10-fold higher in amplitude than either homomeric $K_V7.2$ or $K_V7.3$ channels [14]. K_V7 channels can also associate with β-regulatory subunits (KCNE1-KCNE5), which may alter K_V7 channel properties and subcellular localization [15, 16]. This diversity of K_V7 channels expression and function, underlie their attractiveness as potential novel therapeutic targets for OAB.

K_V7 channel pharmacological modulators have proven useful for elucidating K_V7 channel functional roles in various tissues including vascular, bronchial, and gastrointestinal smooth muscle [17-24]. Such modulators include K_V7 channel activators retigabine ($K_V7.2$-$K_V7.5$) and L-364,363 ($K_V7.1$) as well as K_V7 channel inhibitors XE991 and linopiridine, which effectively block all K_V7 channels. Potential K_V7 channel functional role in DSM was suggested during the clinical trials of the antiepileptic drug retigabine. Patients undergoing treatment reported an increased occurrence of urinary retention compared to the placebo [25]. These findings correspond with *in vivo* studies in rodents, where retigabine increased bladder capacity while decreasing voiding frequency [26, 27].

In guinea pig DSM, mRNA transcripts for all K_V7 channel subunits have been identified [8], with qPCR studies indicating that $K_V7.1$, $K_V7.2$, and $K_V7.5$ channel α-subunits are most prevalent in DSM cells [7]. K_V7 channel inhibition with XE991 was associated with membrane depolarization and an increase in Ca^{2+} oscillations and phasic contractions in guinea pig DSM [7, 8]. K_V7 channel activation with retigabine caused membrane hyperpolarization and inhibition of DSM phasic contractions [7]. K_V7 channels

also regulate porcine DSM contractility, where the $K_V7.2$ and $K_V7.4$ channel activator ML213 displayed a comparable effect to retigabine in promoting DSM relaxation [28]. Despite emerging developments, K_V7 channel subtype-specific physiological roles remain poorly understood due to the lack of selective pharmacological modulators capable of distinguishing among K_V7 channel subtypes [29].

The novel compound N-2-chloro-5-pyrimidinyl-3,4-difluorobenzamide (ICA-069673) was developed by Icagen, Inc. (Durham, NC) – now part of Pfizer as Neusentis – in a screening program to identify subtype-selective K_V7 channel activators [30]. ICA-069673 demonstrated 20-fold greater selectivity for heteromeric $K_V7.2/K_V7.3$ channels over $K_V7.3/K_V7.5$ with EC_{50} values of 0.69 µM and 14.3 µM, respectively [30]. ICA-069673 did not affect $K_V7.1$ channels, which are predominately expressed in the heart [30]. A recent study on A7r5 smooth muscle cell line demonstrated that ICA-069673 was effective in activating recombinantly expressed $K_V7.4$ channels [31]. However, as $K_V7.4$ channel protein expression was not observed in guinea pig DSM [7], its functional relevance in DSM is unlikely.

Here, we aimed to investigate the functional roles of $K_V7.2$- and $K_V7.3$-containing channels in DSM excitability and contractility by targeting them with the novel $K_V7.2/K_V7.3$ channel activator ICA-069673. We applied a multi-level experimental approach including immunocytochemistry with confocal microscopy, Western blot, isometric DSM tension recordings, Ca^{2+} imaging, and perforated whole cell patch-clamp electrophysiology to test the hypothesis that $K_V7.2$- and $K_V7.3$-containing channels are among the K_V7 channel subtypes regulating DSM excitation-contraction coupling.

MATERIALS AND METHODS

Ethical approval for animal use. Experimental procedures involving the use of animals, as described in this study, were reviewed and approved by the Institutional Animal Care and Use Committee (IACUC) of the University of South Carolina (Columbia, SC, USA), protocol #1747.

Animal housing, euthanasia, and DSM tissue acquisition. A total of 38 adult male Hartley-Albino guinea pigs, ages ranging 3-12 months (Charles River Laboratories, Raleigh, NC, USA) and weights 310-575 g (average 463±16 g) were used in the present studies. Animals were housed at room temperature (22-23 ºC) within the Animal Resource Facilities at the University of South Carolina. Guinea pigs had free access to food and water and were exposed to 12 h light/dark cycles. Each animal was euthanized by CO_2 inhalation using a SMARTBOX™ Automated CO_2 Delivery System (Euthanex Corp, Palmer, PA, USA) followed by thoracotomy. The urinary bladder was subsequently removed by administering a transverse incision superior to the bladder neck.

DSM single-cell isolation and collection. DSM single cells were enzymatically isolated using a combination of papain and collagenase as previously described [7]. DSM cells were used for Ca^{2+} imaging or electrophysiological experiments within 12 h after isolation. Intact DSM strips with urothelium removed were used for single cell isolation.

Western blot analysis. Western blot experiments were performed according to previously described methods [10, 32]. For these experiments, the primary antibodies used were the anti-KCNQ2 (K_V7.2) (1:200 dilution, Santa Cruz Biotechnology, Dallas, TX, USA, cat. number: sc-7793) or anti-KCNQ3 (K_V7.3) (1:200 dilution, Santa Cruz Biotechnology, cat. number: sc-7794) polyclonal antibodies, respectively. The donkey anti-goat IgG-HRP

secondary antibody (1:500 dilution, Santa Cruz Biotechnology, cat. number: sc-2020) was used for all Western blot experiments. Experiments utilizing the competing peptides for K_V7.2 (Santa Cruz Biotechnology, cat. number: sc-7793P) or K_V7.3 (Santa Cruz Biotechnology, cat. number: sc-7794P) were pre-incubated with the K_V7.2 or K_V7.3 primary antibodies, respectively.

Immunocytochemistry. Immunocytochemical studies were conducted as previously described [10, 32]. Freshly-isolated DSM cells were incubated using either the anti-KCNQ2 (K_V7.2) primary antibody (1:300 dilution, Santa Cruz Biotechnology, cat. number: SC-7793), or the anti-KCNQ3 (K_V7.3) primary antibody (1:300 dilution, Santa Cruz Biotechnology, cat. number: SC-7795-R) diluted in 1% BSA/PBS overnight at 4°C. DSM cells that were incubated with the anti-K_V7.2 goat polyclonal antibody were then incubated with the secondary antibody Cy3-AffiniPure donkey anti-goat IgG (1:500 dilution; cat. number: 705-165-147, Jackson ImmunoResearch Laboratories, Inc., West Grove, PA, USA) overnight at 4°C. DSM cells that were incubated with the anti-K_V7.3 rabbit polyclonal primary antibody were then incubated with the secondary antibody Cy5-AffiniPure donkey anti-rabbit IgG (1:500 dilution; cat. number: 711-175-152, Jackson ImmunoResearch Laboratories, Inc.) overnight at 4°C. Subsequently, DSM cells were incubated in phosphate buffered saline (PBS) with the α-smooth muscle actin fluorescein isothiocyanate (FITC) antibody (cat. number: F3777, Sigma-Aldrich) for 2 h in a dark room. Nuclear staining was achieved by incubating DSM cells for 15 min in 4′,6-diamidino-2-phenylindole (DAPI, Invitrogen, Ltd., Grand Island, NY, USA; diluted in PBS 1:10,000). DSM cells were mounted with 1,4-Diazabicyclo[2.2.2]octane (DABCO).

Confocal images were obtained with a 63x oil immersion objective using a laser scanning LSM 700 confocal microscope (Carl Zeiss, Germany).

Isometric DSM tension recordings. Isometric DSM tension recordings were performed as previously described using DSM isolated strips free from urothelium [7, 10, 32, 33]. In urothelium-denuded DSM isolated strips showing spontaneous phasic contractions, the neuronal Na^+ channel blocker tetrodotoxin (TTX, 1 μM) was included prior to the application of increasing concentrations of ICA-069673 (100 nM-30 μM). Two separate protocols were conducted involving electric field stimulation (EFS)-induced DSM contractions, which were performed in the absence of TTX using a PHM-152I programmable stimulator (Med Associates, Inc., Georgia, VT, USA). For the first protocol, continuous stimulation of 10 Hz EFS frequency was delivered at 1 min intervals and a stable baseline and amplitude were reached prior to applying increasing concentrations of ICA-069673 (100 nM-30 μM). In the second EFS protocol, we applied incremental EFS stimulation frequencies (3.5, 5, 7.5, 10, 12.5, 15, 20, 30, 40, 50 Hz) at 3 min intervals for a control period, and then again in the presence of a single concentration of ICA-069673 (either 3 μM or 10 μM).

Ratiometric fluorescence Ca^{2+} imaging in freshly-isolated guinea pig DSM cells. We measured the global intracellular Ca^{2+} levels of freshly-isolated DSM cells using fura-2 AM, a ratiometric fluorescent Ca^{2+} probe, in accordance with previously described procedures [32].

Whole cell patch-clamp electrophysiology. Amphotericin-B perforated whole cell patch-clamp experiments were performed in current-clamp mode as previously described [7, 32].

All patch-clamp electrophysiological experiments were conducted at room temperature (22-23°C).

Solutions and drugs. Ca^{2+}-free dissection solution was composed of each of the following (in mM): 80 monosodium glutamate; 55 NaCl; 6 KCl; 10 glucose; 10 4-(2-hydroxyethyl)piperazine-1-ethanesulfonic acid (HEPES); 2 $MgCl_2$; NaOH was used to attain pH 7.3. PSS solution containing Ca^{2+} was freshly prepared each day and contained the following (in mM): 119 NaCl; 4.7 KCl; 24 $NaHCO_3$; 1.2 KH_2PO_4; 2.5 $CaCl_2$; 1.2 $MgSO_4$; 11 glucose; that was aerated with 95% O_2/5% CO_2 to attain pH 7.4. Physiological bath solution utilized for patch-clamp experiments was composed of the following (in mM): 134 NaCl; 6 KCl; 1 $MgCl_2$; 2 $CaCl_2$; 10 glucose; 10 HEPES; and NaOH was used to obtain pH 7.4. The patch-pipette solution contained (in mM): 110 potassium aspartate; 30 KCl; 10 NaCl; 1 $MgCl_2$; 10 HEPES; 0.05 ethylene glycol-bis(2-aminoethylether)-N,N,N',N'-tetraacetic acid (EGTA); NaOH was used to adjust the pH to 7.2. Amphotericin-B stock solution was freshly prepared daily in dimethyl sulfoxide (DMSO) and was included in the pipette solution (200-300 μg/ml) before the experiment and was subsequently replaced every 1-2 h. ICA-069673, XE991, fura-2 AM, and TTX were purchased from Tocris Bioscience (Minneapolis, MN) and were dissolved in DMSO, double distilled water, and acetate buffer at pH 4.8, respectively. Nifedipine was purchased from Sigma-Aldrich (St. Louis, MO, USA) and dissolved in DMSO.

Data Analysis and Statistics. Isometric DSM tension recording experiments were conducted using MyoMed software and analyzed as previously described[7]. Data for isometric DSM tension were normalized and expressed in %. For spontaneous phasic, carbachol-induced, KCl-induced, and 10 Hz EFS-induced contractions, the 5 min period

preceding the first application of ICA-069673 (100 nM-30 µM) was taken as the control (100 %). Maximal efficacy values were normalized to the control, with 0% of the control indicating full inhibition. The effects of ICA-069673 (100 nM-30 µM) on DSM phasic contraction parameters were determined by analysis of the 5 min period preceding the subsequent addition of a higher concentration. In 3.5-50 Hz EFS-induced contractions, the control period was defined as the contraction amplitude observed at 50 Hz EFS frequency before the addition of ICA-069673 (3 or 10 µM) and taken as 100%. Perforated whole cell patch-clamp experiments were performed and analyzed using pCLAMP 10.2. When ICA-069673 was applied in the presence of XE991, the control was defined as the 5 min period before the addition of ICA-069673 (in the presence of XE991 only). Where indicated in the summarized data, **n** represents the number of freshly-isolated DSM strips or cells, or individual immunocytochemistry/Western blot experiments, and **N** represents the number of guinea pigs. For spontaneous contraction experiments, statistical analysis for the comparison of ICA-069673 in the absence or presence of XE991, two-way ANOVA test was performed followed by Bonferroni post-hoc test. Remaining statistical analyses were performed using a two-tailed paired Students t-test. Summarized data are reported as means±SEM. P values <0.05 were considered statistically significant. Corel Draw Graphic Suite X3 software (Corel Co., Mountain View, CA) and GraphPad Prism 4.03 software (La Jolla, CA) was used for data illustration.

RESULTS

K_V7.2- and K_V7.3-containing channels are expressed in freshly-isolated DSM cells. To determine the protein expression of K_V7.2 and K_V7.3 channel subunits and their subcellular localization in DSM cells, we performed Western blot and immunocytochemical

experiments, respectively. Western blot data revealed the protein expression of $K_V7.2$ and $K_V7.3$ channel subunits in whole DSM tissue, which were not observed when the competing peptides for each $K_V7.2$ and $K_V7.3$ channel-specific antibodies were present (n=3, N=3, **Figure 3.1**). In freshly-isolated DSM cells, immunocytochemical experiments were conducted using antibodies specific for $K_V7.2$ or $K_V7.3$ channel subunits in combination with the α-smooth muscle actin-FITC antibody and DAPI nuclear stain **(Figure 3.1)**. The data demonstrated that $K_V7.2$ and $K_V7.3$ channel subunits are expressed in DSM cells and localized within the vicinity of the cell membrane (n=3, N=3, **Figure 3.1**). The detection of $K_V7.2$ and $K_V7.3$ channel protein expression in isolated DSM cells was abolished when the competing peptides for the $K_V7.2$ or $K_V7.3$ channel-specific antibodies were present (**Figure 3.1**). This confirms the specificity of the $K_V7.2$ and $K_V7.3$ channel-specific antibodies used in this study.

The Kv7.2/Kv7.3 chnanel activator ICA-069673 induces inhibition of spontanous phasic contrations in DSM isolated strips. In order to determine the functional roles of the $K_V7.2/K_V7.3$ channels on spontaneous phasic contractions in guinea pig DSM isolated strips, we conducted isometric DSM tension recordings using the novel $K_V7.2/K_V7.3$ novel activator ICA-069673. As shown in **Figure 3.2**, ICA-069673 (100 nM-30 μM) caused a concentration-dependent inhibition of spontaneous phasic contractions, an effect that recovered upon washout of ICA-069673. The IC_{50} and maximal efficacy values for ICA-069673 on spontaneous phasic DSM contraction parameters were the following: contraction amplitude, 4.5 (2.6-7.9, 95% confidence interval) μM and 3.3±1.8% of pre-compound control; muscle force integral, 3.2 (2.0-5.2) μM and 2.2±1.4%; contraction duration, 8.6 (4.3-17.3) μM and 9.8±5.2%, respectively. The IC_{50} value for the effect of

ICA-069673 on contraction frequency was 11.9 µM. The effect of ICA-069673 on contraction frequency resulted in maximal reduction of contraction frequency to 25.2±14.1% of the control (n=11, N=7; P<0.05; **Figure 3.2**). To confirm that concentration-dependent inhibition of spontaneous phasic contractions caused by ICA-069673 was mediated by K_V7 channels, we examined its effects in the presence of the K_V7 channel inhibitor XE991 (10 µM). In the presence of XE991 (10 µM), there were no measureable inhibitory effects of ICA-069673 on DSM phasic contractions (n=12, N=6; P>0.05; **Figure 3.2**). These results support the concept that $K_V7.2$- and $K_V7.3$-containing channels are important physiologically-relevant mediators of spontaneous phasic contractions in DSM isolated strips.

The Kv7.2/Kv7.3 chnanel activator ICA-069673 inhibits pharmacologically-induced contractions in DSM isolated strips. We examined the effects of ICA-069673 on DSM phasic contractions induced in response to either muscarinic receptor activation or sustained membrane potential depolarization using carbachol or KCl, respectively. ICA-069673 (100 nM-30 µM) caused a concentration-dependent inhibition of 0.1 µM carbachol-induced DSM contractions. For 0.1 µM carbachol-induced contractions, the IC_{50} and maximal efficacy values of ICA-069673 were: contraction amplitude, 5.5 (3.0-10.2, 95% confidence interval) µM and 20.8±8.9%; muscle force integral, 3.6 (1.9-7.0) µM and 18.9±8.2%; contraction duration, 13.3 (6.3-28.2) µM and 36.4±14.9%, respectively. DSM phasic contraction frequency was maximally reduced to a lesser extent to 46.5±18.2% of the control (n=10, N=7; P<0.05; **Figure 3.3**). ICA-069673 (100 nM-30 µM) concentration-dependently inhibited DSM phasic contractions induced by 20 mM KCl. For 20 mM KCl-induced contractions, the IC_{50} and maximal efficacy values for ICA-069673 on DSM

contraction parameters were as follows: contraction amplitude, 5.3 (2.6-11.0) µM and 10.4±5.6%; and muscle force integral, 4.2 (2.4-7.6) µM and 5.3±3.6%; contraction duration, 11.1 (2.8-36.7) µM and 31.8±13.0%; and contraction frequency, 12.2 (3.4-44.2) µM and 22.5±8.9% of the control, respectively (n=7, N=7; P<0.05; **Figure 3.4**). We then tested the effects of ICA-069673 (10 µM) on DSM tonic contractions induced by 60 mM KCl to determine the role of K^+ conductance in mediating the inhibitory effects of ICA-069673 as well to assess the functional interaction with the L-type Ca_V channels. As illustrated in **Figure 3.5**, under these experimental conditions, ICA-069673 (10 µM) decreased DSM tone to only 89.2±3.2% of the control (n=8, N=4; P<0.05) while the subsequent addition of the L-type Ca_V channel inhibitor nifedipine (1 µM) led to a more significant reduction in DSM tone to 28.7±3.8% of the control (n=8-9, N=4; P<0.001; **Figure 3.5**). There was a statistically significant difference between the inhibitory effects of ICA-069673 and nifedipine on DSM tonic contraction (n=8-9, N=4; P<0.001). These experiments support the concept that ICA-069673 does not directly inhibit L-type Ca_V channels

The Kv7.2/Kv7.3 chnanel activator ICA-069673 inhibits nerve-evoked contractions in DSM isolated strips. To assess the effects of ICA-069673 on nerve-evoked DSM contractions, we applied increasing concentrations of ICA-069673 to continuous 10 Hz EFS-induced contractions of DSM isolated strips. Under these experimental conditions, ICA-069673 (100 nM-30 µM) displayed a concentration-dependent inhibitory effect. For 10 Hz EFS-induced contractions, the IC_{50} and maximal efficacy values for ICA-069673 on nerve-evoked DSM contraction parameters were as follows: contraction amplitude, 9.8 (1.1-88.0) µM and 16.6±5.2%; and muscle force integral, 7.6 (0.6-97.8) µM and 19.0±5.4%

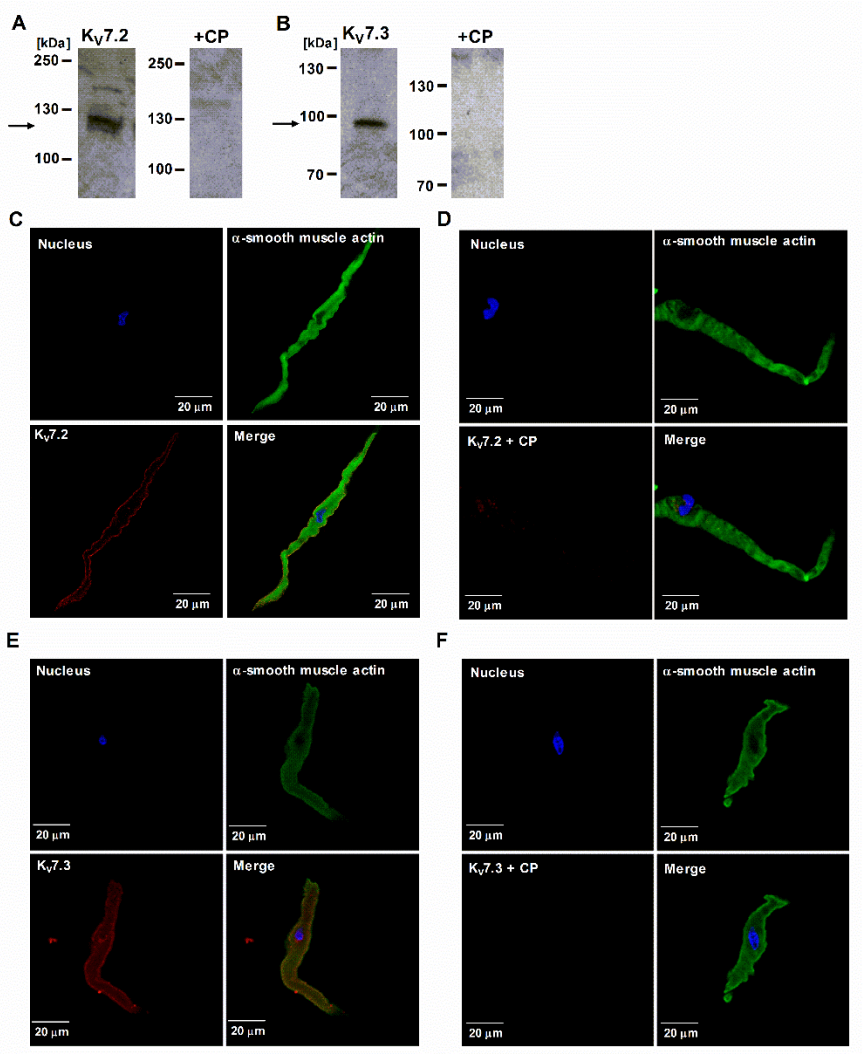

Figure 3.1. K_V7.2 and K_V7.3 channel subunits are expressed in freshly-isolated guinea pig DSM cells. Western blot analysis reveals the expression of **(A)** K_V7.2 and **(B)** K_V7.3 channel subunits at the protein level in DSM (n=3, N=3). The expected molecular weights of K_V7.2 and K_V7.3 channel proteins are 120 and 97 kDa, respectively (indicated by the arrows). No protein expression was detected in the presence of the competing peptides (CP) for each K_V7.2 and K_V7.3 channel antibodies, respectively. Confocal images from immunocytochemical experiments demonstrate the expression K_V7.2 (**C**) and K_V7.3 (**E**) channel subunits in freshly-isolated DSM cells along with membrane localization. Red staining indicates detection of either K_V7.2 or K_V7.3 channel subunits. Blue staining depicts the nucleus. Cells stained with the α-smooth muscle actin-FITC antibody are shown in green. The overlaid image for K_V7.2 or K_V7.3 with α-smooth muscle actin-FITC antibody and DAPI nuclear stain is shown at the bottom right. Co-localization of K_V7.2 or K_V7.3 with the α-smooth muscle actin-FITC antibody is indicated by the yellow color in the merged images, respectively. Inclusion of competing peptides for either K_V7.2 (**D**) or K_V7.3 (**E**) channels resulted in loss of specific staining. Data for all experiments were confirmed using DSM tissues from at least 3 guinea pigs. Images were acquired with a Zeiss LSM 700 confocal microscope using a 63x oil objective.

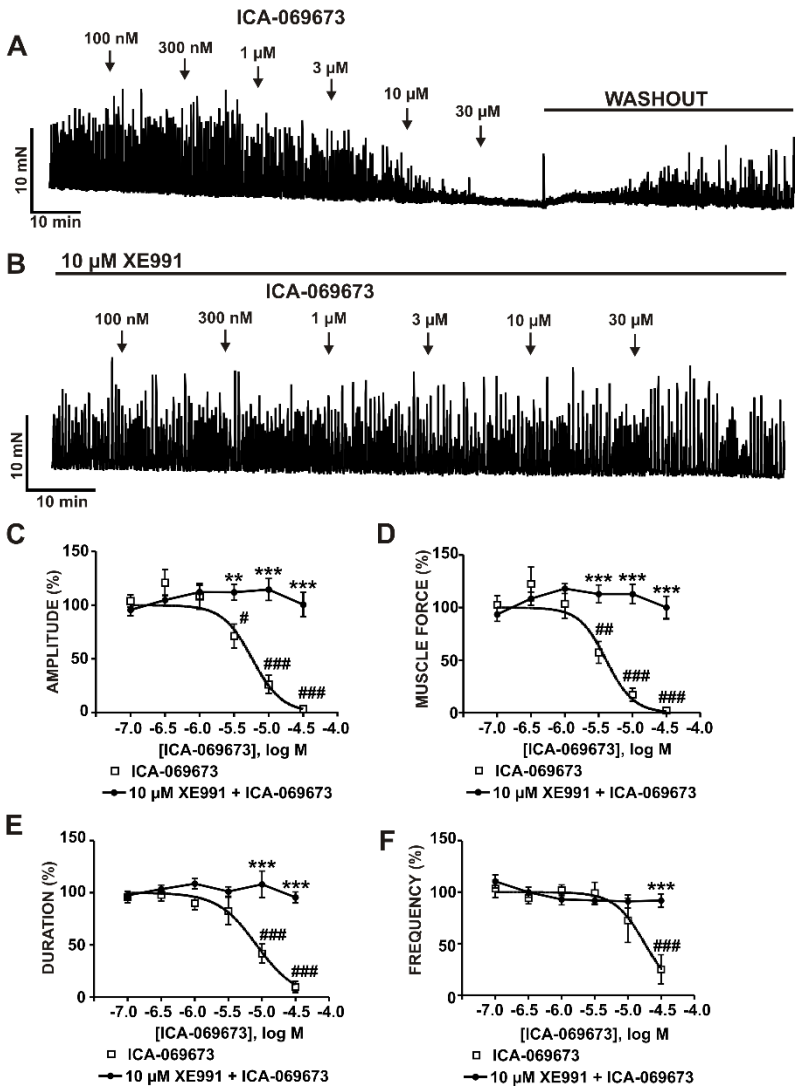

Figure 3.2. ICA-069673 inhibits spontaneous phasic contractions in DSM isolated strips. A) An original isometric DSM tension recording illustrating the inhibition of spontaneous phasic contractions by ICA-069673 (100 nM-30 µM) in a DSM isolated strip. The DSM contractions recovered upon washout of ICA-069673. **B**) An original isometric DSM tension recording illustrating that blocking K_V7 channels with its selective inhibitor XE991 (10 µM) abolished the inhibitory effects of ICA-069673 (100 nM-30 µM) on DSM spontaneous phasic contractions. **C-F**) Cumulative concentration-response curves for ICA-069673 on DSM phasic contraction amplitude, muscle force, duration, and frequency in the absence or presence of 10 µM XE991 (see text for potency and maximum efficacy values). #P<0.05, ##P<0.01, and ###P<0.001 represent statistically significant effects of ICA-069673 on spontaneous phasic contractions in the absence of XE991 in comparison to the control level (i.e. 100%) prior to the addition of ICA-069673 (n=11, N=7). *P<0.05, **P<0.01, and ***P<0.001 represent statistically significant differences between the effects of ICA-069673 in the absence versus presence of XE991 (n=12, N=6).

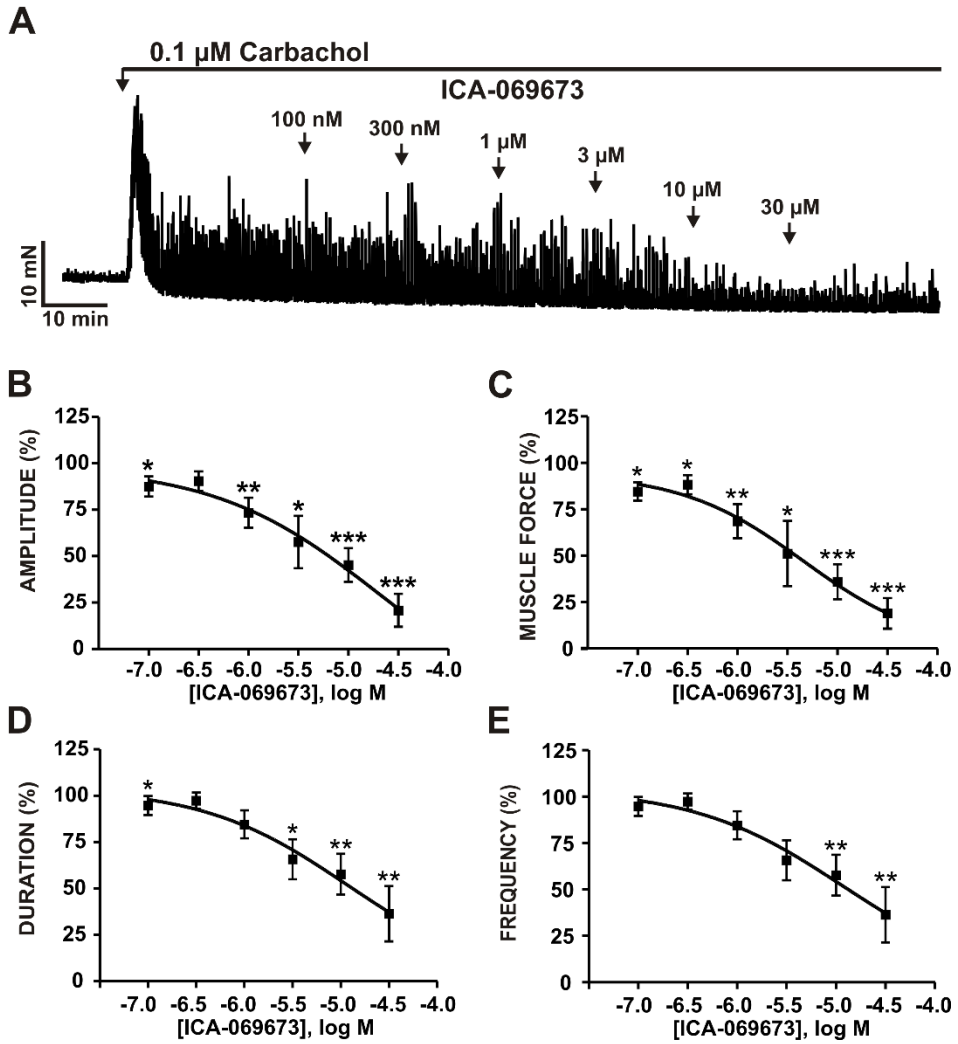

Figure 3.3. ICA-069673 decreases carbachol-induced phasic contractions in DSM isolated strips. A) An original isometric DSM tension recording of 0.1 µM carbachol-induced phasic contractions in a DSM isolated strip illustrating the concentration-dependent inhibitory effects of ICA-069673 (100 nM-30 µM). **B-E)** Cumulative concentration-response curves for ICA-069673 (100 nM–30 µM) on DSM phasic contraction amplitude **(B)**, muscle force **(C)**, phasic contraction duration **(D)**, and phasic contraction frequency **(E)** (n=10, N=7; *P<0.05, **P<0.01, and ***P<0.001); see text for potency and maximum efficacy values.

of the control, respectively (n=9, N=9; P<0.05; **Figure 3.6**). Next, EFS-induced contractions were stimulated over a range of frequencies (3.5-50 Hz) in the absence or presence of either 3 or 10 µM ICA-069673, respectively. ICA-069673 (3 or 10 µM) significantly attenuated the amplitude of EFS-induced contractions stimulated at EFS

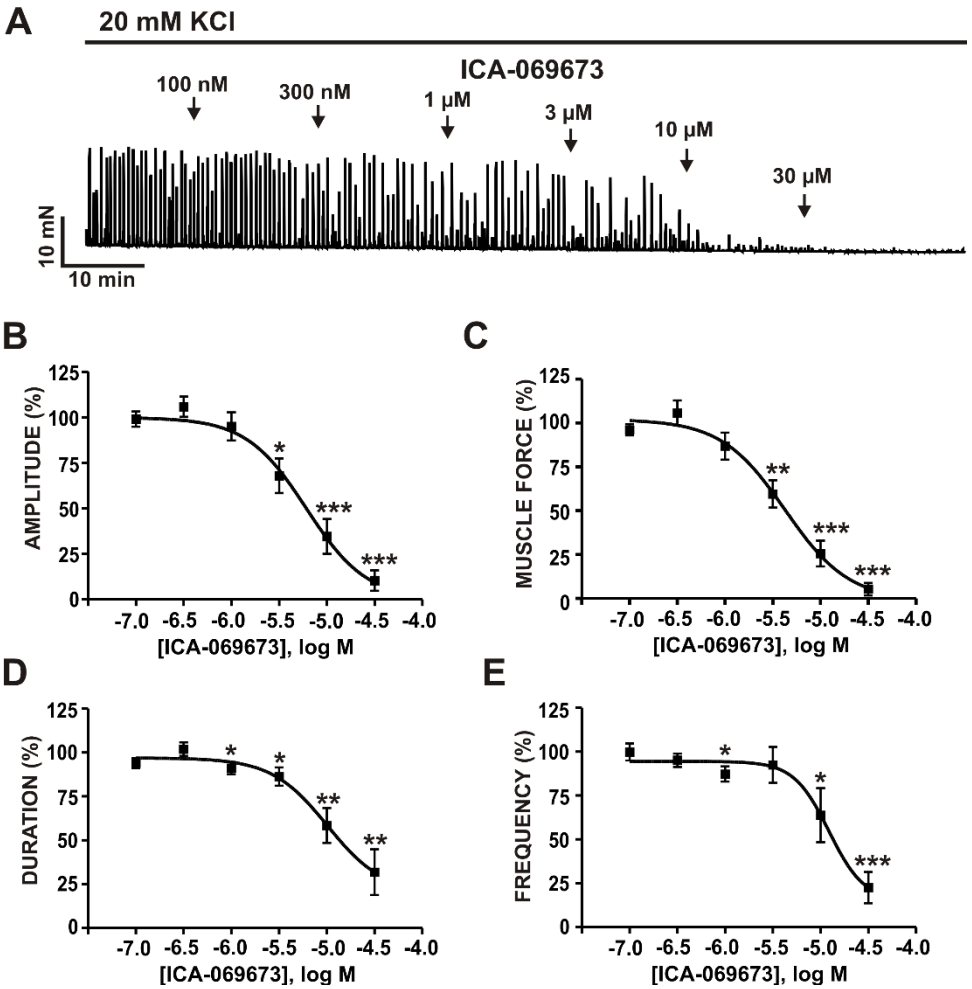

Figure 3.4. ICA-069673 decreases 20 mM KCl-induced phasic contractions in DSM isolated strips. A) An original isometric DSM tension recording illustrating the concentration-dependent inhibitory effects of ICA-069673 (100 nM-30 µM) on DSM phasic contractions induced by 20 mM KCl. **B-E)** Cumulative concentration-response curves for the effects of ICA-069673 on DSM phasic contraction amplitude **(B)**, muscle force **(C)**, phasic contraction duration **(D)**, and phasic contraction frequency **(E)** (n=7, N=7; *P<0.05, **P<0.01, and ***P<0.001); see text for potency and maximum efficacy values.

frequencies from 7.5-50 Hz (n=8-18, N=4-10; P<0.05; **Figure 3.7**). Collectively, these data support the concept that $K_V7.2$- and $K_V7.3$-containing channels are critical regulators of nerve-evoked DSM contractions. **The Kv7.2/Kv7.3 chnanel activator ICA-069673 decreases the global intracellular Ca^{2+} levels in freshly-isolated DSM cells.** Next, we sought to determine the effects of ICA-069673 on global intracellular Ca^{2+} levels in DSM

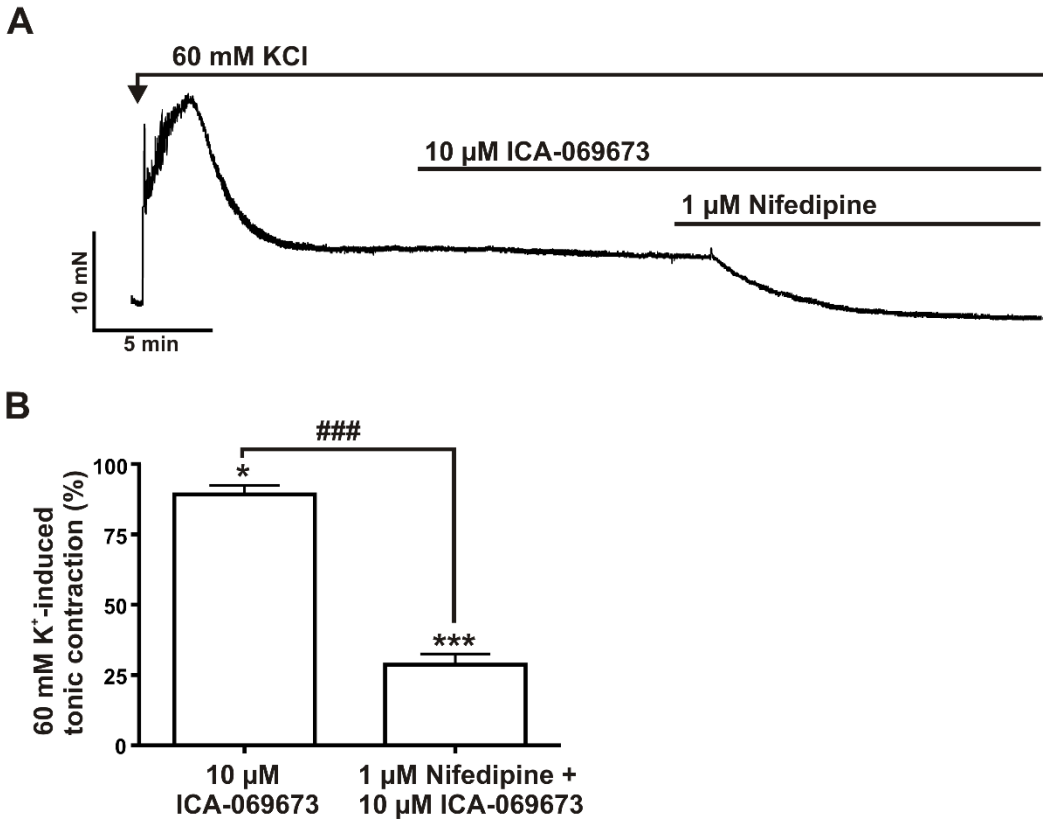

Figure 3.5. Differential effects of ICA-069673 and nifedipine on 60 mM KCl depolarization-induced tonic contraction in DSM isolated strips. A) An original isometric DSM tension recording illustrating the effects of 10 µM ICA-069673 and 1 µM nifedipine on a depolarization-induced DSM tonic contraction caused by 60 mM KCl in a DSM isolated strip. **B)** Summarized data demonstrating the inhibitory effect of ICA-069673 (10 µM) and nifedipine (1 µM) on DSM tonic contraction induced by 60 mM KCl (n=8-9, N=4; *P<0.05 and n=6-7, N=3; ***P<0.0001, respectively. $^{###}$P<0.0001 represents a statistically significant difference for the comparison of ICA-069673 and nifedpine.

single cells by measuring the ratio of fura-2 AM fluorescent emission at 510 nm with excitation at 340 and 380 nm. For the control, the average emitted intensity (F_{340}/F_{380}) prior to ICA-069673 application was 0.470±0.006 (n=11, N=5). At 10 µM ICA-069673, there was a significant decrease in the F_{340}/F_{380} ratio to 0.450±0.006 (n=11, N=5; P<0.05; **Figure 3.8**). To elucidate the mechanism by which ICA-069673 regulates global intracellular Ca^{2+} concentrations, we studied the effects of ICA-069673 (10 µM) in the presence or absence of the L-type Ca_V channel blocker nifedipine (1 µM). In the presence of 1 µM nifedipine, ICA-069673 (10 µM) had no significant effect on intracellular Ca^{2+} levels, with the average

F_{340}/F_{380} ratio being 0.470±0.008 compared to the control value of 0.480±0.005 (n=11, N=5; P>0.05; **Figure 3.8**). These results demonstrate that in guinea pig DSM cells, ICA-069673 decreases global intracellular Ca^{2+} concentrations by an indirect mechanism involving inhibition of Ca^{2+} influx through L-type Ca_V channels, probably due to membrane hyperpolarization.

ICA-069673 hyperpolarizes the resting membrane potential and inhibits spontaneous action potentials in freshly-isolated DSM cells. To determine the regulatory roles of $K_V7.2/K_V7.3$ channels on the DSM cell membrane potential, we employed the $K_V7.2/K_V7.3$ channel activator ICA-069673 and the perforated whole cell patch-clamp technique in current-clamp mode. The effect of ICA-069673 was examined in 7 DSM cells (N=6), which had mean cell capacitance of 43.4±4.3 pF and membrane potential of -16.8±2.8 mV. Two of these seven DSM cells displayed distinguishable spontaneous action potentials. These spontaneous action potentials were abolished by ICA-069673 concurrent with membrane hyperpolarization (**Figure 3.9**). In all DSM cells, ICA-069673 hyperpolarized the DSM cell membrane potential by 8.3±2.7 mV (n=7, N=6; P<0.05; **Figure 3.9**). The ICA-069673-mediated hyperpolarizing effects on the DSM cell membrane potential were fully reversible upon washout (**Figure 3.9**). We then examined the effects of the K_V7 channel inhibitor XE991. As illustrated by the original recording in **Figure 3.9** and summarized data in **Figure 3.9**, XE991 (10 μM) depolarized the DSM cell membrane potential by 4.9±1.4 mV (P<0.05; n=5, N=5). To further investigate the mechanism underlying ICA-069673-induced hyperpolarization, specifically its dependence on K_V7 channel subtypes, the effect of this channel modulator

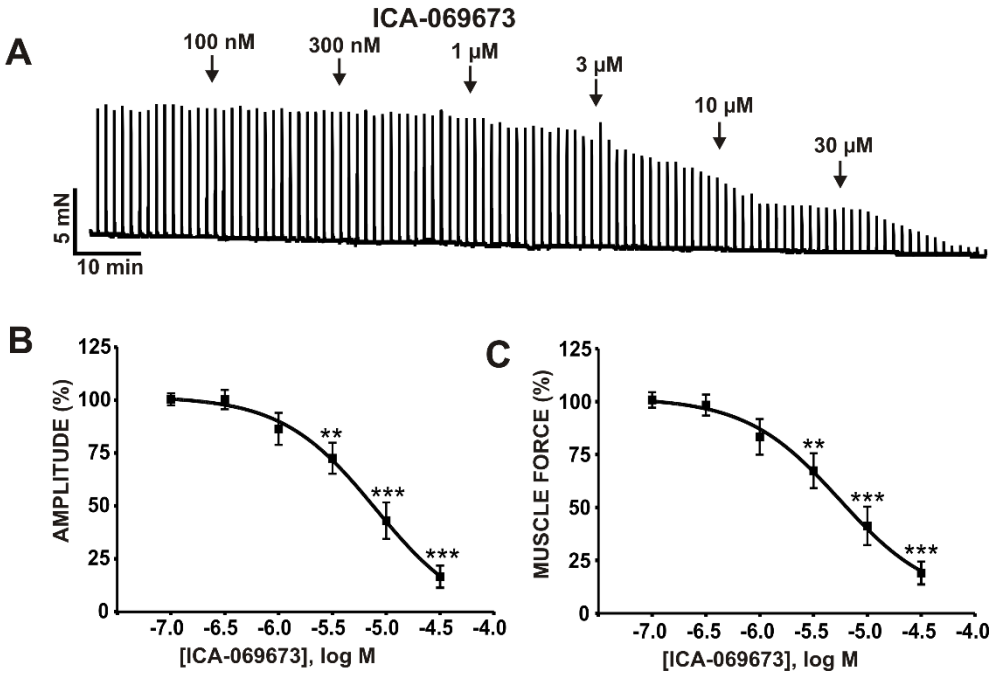

Figure 3.6. ICA-069673 decreases nerve-evoked contractions stimulated by 10 Hz EFS in DSM isolated strips. A) An original isometric DSM tension recording representing the concentration-dependent inhibitory effects of ICA-069673 (100 nM-30 µM) upon nerve-evoked contractions induced by 10 Hz EFS stimulation in a DSM isolated strip. **B)** Cumulative concentration-response curves for the effects of ICA-069673 (100 nM-30 µM) on DSM contraction **(B)** amplitude and **(C)** muscle force integral (n=9, N=9; **P<0.01, and ***P<0.001); see text for potency and maximum efficacy values.

was examined in DSM cells pretreated with XE991 (10 µM). The subsequent addition of ICA-069673 in the continued presence of XE991 did not have a significant hyperpolarizing effect on the membrane potential of DSM cells (n=7, N=5; P>0.05; **Figure 3.9**). There was a statistically significant difference in the effects of ICA-069673 in the absence versus presence of XE991 (n=5-7, N=5-6; P<0.05; **Figure 3.9**). Collectively, these data supports the novel concept that $K_V7.2$- and $K_V7.3$-containing channels are key regulators of DSM cell excitability.

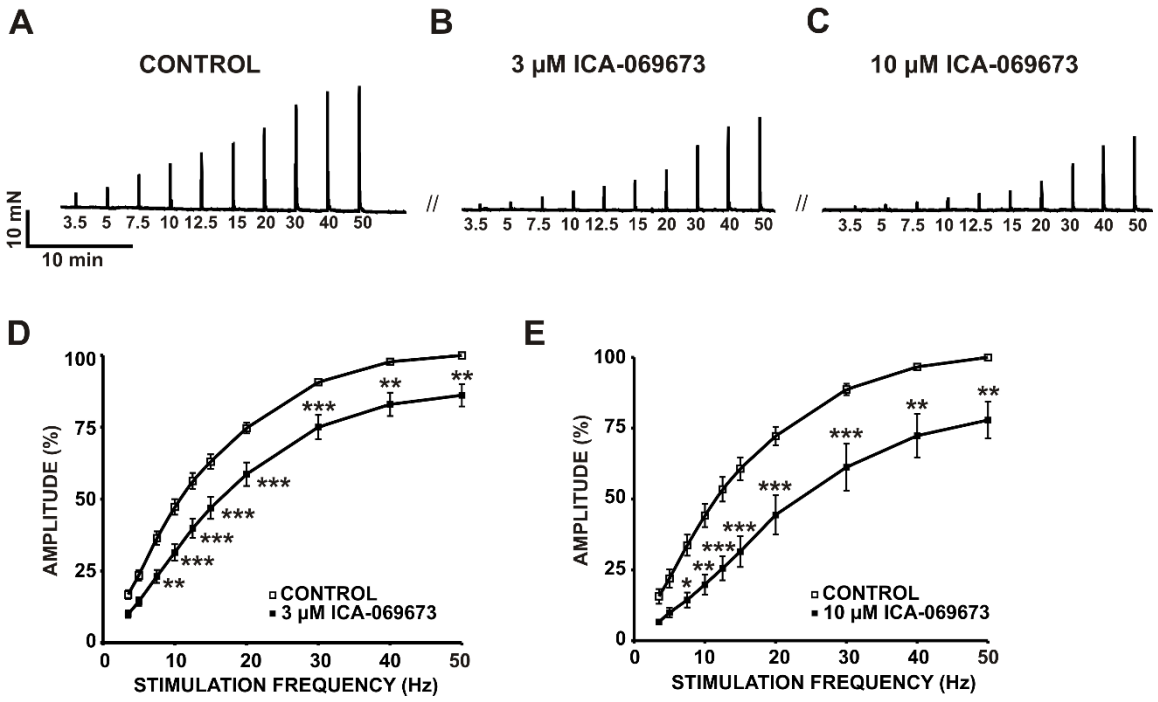

Figure 3.7. ICA-069673 decreases 3.5-50 Hz EFS-induced contractions in DSM isolated strips. A-C) The original isometric DSM tension recordings of 3.5-50 Hz EFS-induced contractions in DSM isolated strips **A)** before (control) and after the addition of **B)** 3 µM ICA-069673 and **C)** 10 µM ICA-069673. **D-E)** Cumulative concentration-response curves demonstrating the effects of **D)** 3 µM ICA-069673 and **E)** 10 µM ICA-069673 on the amplitude of 3.5-50 Hz EFS-induced contractions (n=8-18, N=4-10; *P<0.05, **P<0.01, and ***P<0.001).

DISCUSSION

The present study sought to elucidate the physiological roles of $K_V7.2$- and $K_V7.3$-containing channels in DSM excitability and contractility by targeting their activity with the novel selective $K_V7.2/K_V7.3$ channel activator ICA-069673. This was achieved by applying a multi-level experimental approach at both cellular and tissue levels in DSM. Western blot analysis detected protein expression for $K_V7.2$ and $K_V7.3$ channel subunits in DSM tissue. In isolated DSM cells, immunocytochemical experiments further revealed protein expression for $K_V7.2$ and $K_V7.3$ channel subunits localized within the vicinity of the cell membrane.

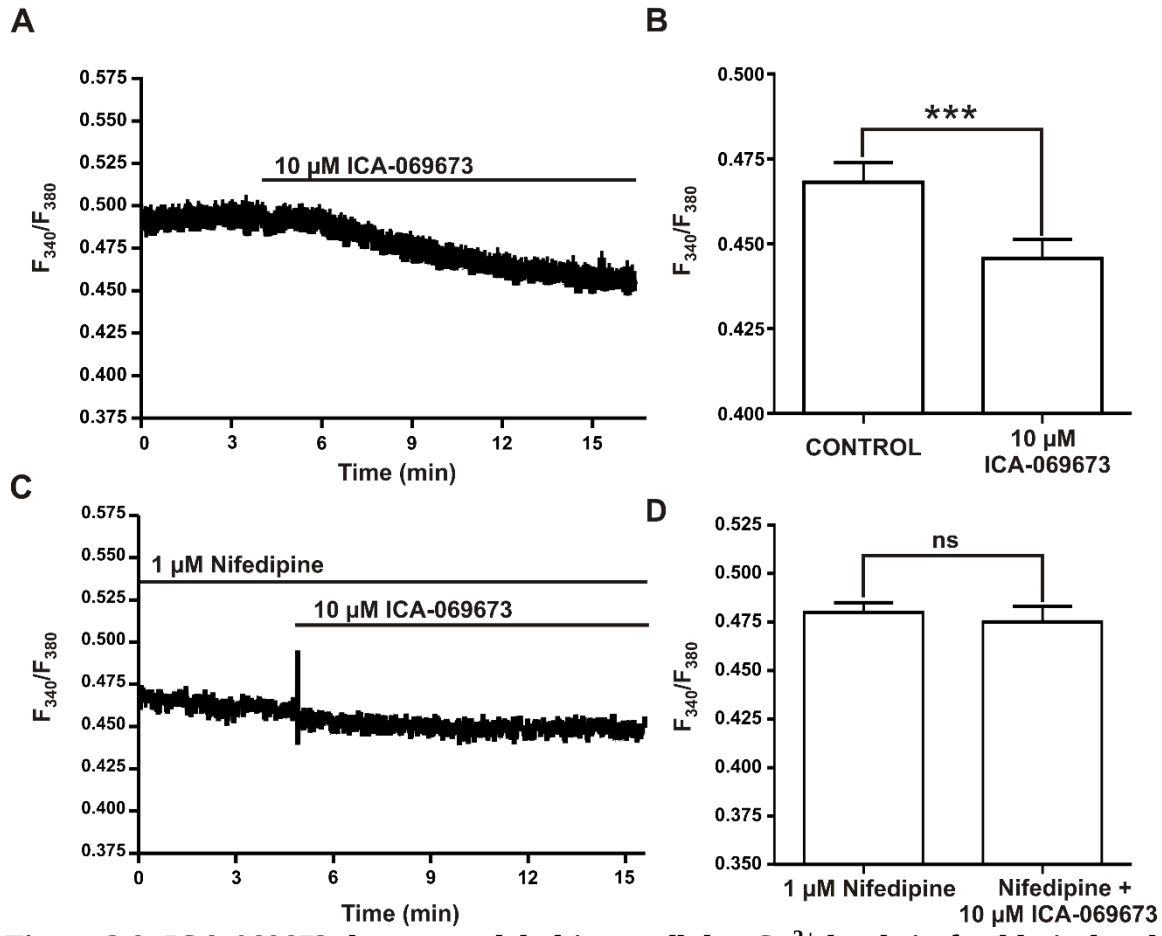

Figure 3.8. ICA-069673 decreases global intracellular Ca^{2+} levels in freshly-isolated DSM cells. A) Original recordings illustrating that ICA-069673 (10 µM) significantly decreased global intracellular Ca^{2+} levels in a freshly-isolated DSM cell. **B)** Summarized data representing the reduction in global intracellular Ca^{2+} levels by 10 µM ICA-069673 (n=11, N=5; *P<0.05). **C)** An original recording representing the lack of effect of ICA-069673 (10 µM) in decreasing global intracellular Ca^{2+} levels in the presence of the L-type Ca_V channel blocker nifedipine (1 µM) in a DSM cell. **D)** Summarized data representing the effects of ICA-069673 (10 µM) on global intracellular Ca^{2+} in the presence of nifedipine (1 µM) (n=10, N=4; P>0.05) in DSM cells. Data are reported as the ratio of fura-2 AM fluorescent emission at 510 nm with excitation at 340 and 380 nm; ns, non-significant.

Pharmacological studies demonstrated that ICA-069673 significantly hyperpolarized the membrane potential, inhibited DSM spontaneous action potentials, and decreased global intracellular Ca^{2+} concentrations of DSM cells. Functional studies on DSM contractility revealed that ICA-069673 inhibits spontaneous, pharmacologically-induced, and nerve-evoked contractions in DSM isolated strips.

The inhibitory effects of ICA-069673 on DSM excitability and contractility were attenuated by the $K_V7.1$-$K_V7.5$ inhibitor XE991, supporting the involvement of K_V7 channel subtypes in the regulation of DSM excitability and contractility. Our combined results suggest a critical role for $K_V7.2$- and $K_V7.3$-containing channels in DSM excitation-contraction coupling.

From all K_V7 channel subunits, mRNA transcripts for $K_V7.1$ and $K_V7.2$ channels are most predominant in guinea pig DSM cells [7]. The expression of K_V7 channels at the protein-level has only been identified in DSM tissue via immunohistochemistry [7, 8], which has the inherent limitation of potentially detecting K_V7 channel expression from neighboring non-DSM cell types such as neurons or interstitial cells in the absence of cell-specific labelling. Thus, as illustrated in **Figure 3.1**, novel immunocytochemical experiments with confocal microscopy reveal the expression of $K_V7.2$- and $K_V7.3$-containing channels in isolated DSM cells, where these channels localize within the vicinity of the cell membrane. Further, Western blot experiments detected protein expression for both $K_V7.2$ and $K_V7.3$ channel subunits in DSM (**Figure 3.1**), consistent with the previous reports by our group and others using immunohistochemistry [7, 8].
K_V7 channel activators and inhibitors such as retigabine and XE991 have provided a useful pharmacological approach for elucidating K_V7 channel roles in urinary bladder function [4, 7-9, 26-28, 34]. However, retigabine and XE991 do not effectively distinguish among $K_V7.2$-$K_V7.5$ and $K_V7.1$-$K_V7.5$ channel subtypes, respectively.

The lack of subtype selectivity of these pharmacological modulators has thus been a substantial limitation for gaining an improved understanding of the K_V7 channel subtypes most critical to DSM function. A novel K_V7 channel activator, ICA-069673, has

demonstrated selectivity for heteromeric $K_V7.2/K_V7.3$ channels and is a pyrimidine analogue of N-(6-chloro-pyridin-3-yl)-3,4-difluoro-benzamide (ICA-27243) [30, 35, 36]. Though less potent than its related analog ICA-27243, ICA-069673 displays greater efficacy and improved selectivity for heteromeric $K_V7.2/K_V7.3$ over $K_V7.1$ channels [30]. In contrast to retigabine, which binds to the pore region (S5-S6) of $K_V7.2$-$K_V7.5$ channels [37], evidence suggests that ICA-069673 is among an emerging novel class of compounds known as "gating modifiers", named so for their ability to bind to the S1-S4 voltage-sensing domain of K_V7 channels [31, 36, 38]. The functional studies on DSM contractility revealed that ICA-069673 effectively inhibited spontaneous phasic contractions in DSM isolated strips in a concentration-dependent manner (**Figure 3.2**). Occurring locally in DSM, spontaneous phasic contractions do not initiate urine voiding; however, these contractile events have been associated with involuntary non-voiding contractions observed in some forms of OAB [11, 12]. The inhibition of DSM contractility was not observed when ICA-069673 was administered in the presence of the K_V7 channel inhibitor XE991, which indicates the inhibitory effects of ICA-069673 on spontaneous phasic contractions were mediated by K_V7 channels (**Figure 3.2**).

Similarly, DSM phasic contractions induced by the muscarinic receptor agonist carbachol (0.1 μM) or through slight membrane depolarization by KCl (20 mM) were significantly inhibited by ICA-069673. Under conditions of high extracellular K^+ (60 mM), which significantly changes the driving force for K^+ and causes sustained membrane depolarization that in turn activates the L-type Ca_V channels, ICA-069673 (10 μM) had a rather modest inhibitory effect on DSM tone (~10% of the maximum relaxation, **Figure 3.5)**. In contrast, the subsequent inhibition of L-type Ca_V channels using nifedipine

decreased DSM tonic contractions by approximately seven -fold in comparison to ICA-069673 alone (**Figure 3.5**).

These results support the concept that ICA-069673 does not directly inhibit L-type Ca_V channels in DSM. These data are consistent with a previous report where ICA-069673 (30 μM) demonstrated no direct effects on L-type Ca_V channels, as well as voltage-gated Na^+ ($Na_v1.5$), hERG, $K_V7.1$, or $GABA_A$ channels at 10 μM [30]. We next examined how ICA-069673 affects nerve-evoked DSM contractions induced by EFS. The results showed that ICA-069673 significantly decreased 10 Hz EFS-induced contractions (**Figure 3.6**) and contractions induced over a large range of EFS frequencies (3.5-50 Hz) (**Figure 3.7**), indicating that $K_V7.2$- and $K_V7.3$-containing channels sensitive to ICA-069673 are essential regulators of urinary bladder nerve-evoked contractions. Qualitatively, the effects of ICA-069673 on DSM contractility were consistent with those reported for retigabine [7]. This similarity suggests the involvement of the same molecular targets by retigabine and ICA-069673, indicating a prominent role for the $K_V7.2$- and $K_V7.3$-containing channels in DSM function.

The contraction of DSM is ultimately triggered in response to a rise in the intracellular Ca^{2+} concentration [1]. Therefore, we sought to determine the effects of ICA-069673 on global intracellular Ca^{2+} levels and to elucidate the role of the $K_V7.2/K_V7.3$ channels in controlling DSM cell Ca^{2+} signaling by conducting ratiometric fluorescence Ca^{2+} imaging on isolated DSM cells. ICA-069673 (10 μM) significantly decreased global intracellular Ca^{2+} levels in DSM cells (**Figure 3.8**), consistent with the inhibitory effects of ICA-069673 on DSM contractility. The reduction of intracellular Ca^{2+} concentrations by ICA-069673 is in agreement with the opposite phenomenon where the K_V7 channel

inhibitor XE991 increased the frequency of Ca^{2+} oscillations in DSM tissue [8]. To further assess the interactions of the $K_V7.2/K_V7.3$ channels with the L-type Ca_V channels, we investigated the effects of ICA-069673 in the presence of the L-type Ca_V channel blocker nifedipine (1 μM). The results showed that when L-type Ca_V channels were inhibited by nifedipine, ICA-069673 had no effect on global intracellular Ca^{2+} levels (**Figure 3.8**). These observations support the concept that in isolated DSM cells, ICA-069673 reduces global intracellular Ca^{2+} levels by inhibiting L-type Ca_V channels indirectly through activation of $K_V7.2$- and $K_V7.3$-containing channels and associated membrane hyperpolarization.

Our group was the first to record spontaneous action potentials in freshly-isolated DSM cells and to report the effects of retigabine on the action potentials using the perforated patch-clamp technique in current-clamp mode [7]. The current study revealed that ICA-069673 (10 μM) hyperpolarized the membrane potential and inhibited spontaneous action potentials in isolated DSM cells (**Figure 3.9**). The hyperpolarizing effects of ICA-069673 on the DSM cell membrane potential were comparable to that of retigabine [7]. ICA-069673-mediated hyperpolarization was blocked when the K_V7 channels were inhibited by XE991 (**Figure 3.9**). XE991 alone induced depolarization as measured with the perforated patch-clamp technique (**Figure 3.9)** consistent with a previous finding using the conventional whole cell patch-clamp technique [8]. The combined results from our patch-clamp studies indicate a key role for $K_V7.2$- and $K_V7.3$-containing channels in regulating spontaneous action potentials and the resting membrane potential of isolated DSM cells.

In conclusion, the current study using the novel $K_V7.2/K_V7.3$ channel activator ICA-069673, provides strong evidence to suggest a critical role for the $K_V7.2$- and $K_V7.3$-containing channels in DSM function at both cellular and tissue levels. Pharmacological activation of $K_V7.2/K_V7.3$ channels with ICA-069673 hyperpolarized the membrane potential and inhibited spontaneous action potentials in freshly-isolated DSM cells preventing Ca^{2+} influx through L-type Ca_V channels to reduce global intracellular Ca^{2+} concentrations, and caused relaxation of DSM isolated strips.

While our study demonstrates important roles for $K_V7.2$- and $K_V7.3$-containing channels in DSM cells and tissue, evidence suggests a prominent role for $K_V7.4$ and $K_V7.5$ channels in non-DSM human smooth muscle tissues [22, 39, 40]. Therefore, it is important for future studies to investigate the expression and function of K_V7 channels in human DSM at both the whole tissue and single-cell levels, which is critical for further evaluating their therapeutic potential as novel targets for the treatment of OAB.

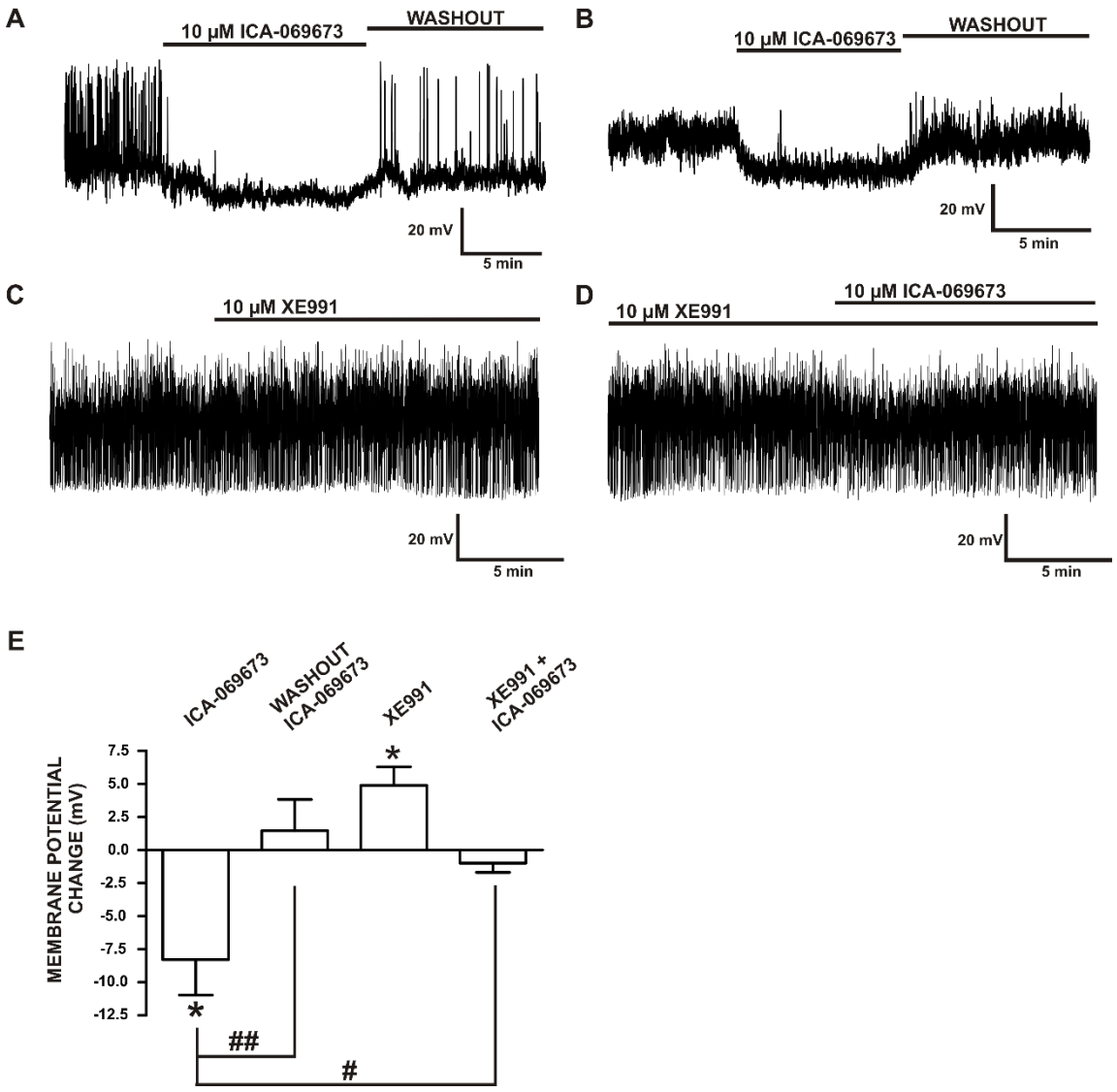

Figure 3.9. ICA-069673 hyperpolarizes the resting membrane potential and inhibits spontaneous action potentials in freshly-isolated DSM cells. A) An original membrane potential recording in current-clamp mode of a DSM cell exhibiting spontaneous action potentials. ICA-069673 (10 µM) hyperpolarized the DSM cell membrane potential and further abolished the spontaneous action potentials in a manner reversible upon washout. **B)** An original membrane potential recording of a DSM cell that does not exhibit spontaneous action potentials. ICA-069673 (10 µM) hyperpolarized the membrane potential, an effect which was recovered upon washout. **C)** An original membrane potential recording illustrating that the K_V7 channel inhibitor XE991 (10 µM) depolarized the DSM cell membrane potential. **D)** A continuation of the recording in **(C)** illustrating that in the presence of XE991 (10 µM), the hyperpolarizing effects of ICA-069673 (10 µM) on the DSM cell membrane potential are attenuated. **E)** Summarized data for the effects of ICA-069673 (10 µM), washout of ICA-069673, XE991 (10 µM), and ICA-069673 (10 µM) in the presence of XE991 (10 µM) on the membrane potential. The Y-axis represents the change in the membrane potential, either depolarization (+) or hyperpolarization (-). With the exception of when ICA-069673 was applied in the presence of XE991, the control

period was in the absence of any pharmacological treatment. When determining the effects of ICA-069673 in the presence of XE991, the control was the 5-min period of stable recording before the addition of ICA-069673 (i.e. in the presence of XE991 only). * indicates statistical difference of $P<0.05$ versus the control for the treatments shown; # $P<0.05$ and ## $P<0.01$ indicate statistically significant differences for the comparisons shown. Each data-point in **(E)** is n=5-7, N=5-6.

Table 3.1. IC_{50} and maximal efficacy values for the effects of ICA-069673 on spontaneous phasic, pharmacologically-induced, and 10 Hz EFS-induced contractions in guinea pig DSM isolated strips. IC_{50}: Mean (95% confidence interval), Maximal efficacy: Mean±SEM. n/a, not applicable. *Maximum efficacy is normalized to the control on a scale from 100% (no relaxation) to 0% (full relaxation).

Condition	Spontaneous Phasic Contractions	CCh (0.1 μM)-induced Contractions	KCl (20 mM)-induced Contractions	10-Hz EFS-induced Contractions
Amplitude	5.60 (3.85-8.15) 3.34 ± 1.85%	5.52 (2.99-10.21) 20.82 ± 8.93%	4.77 (3.42-6.66) 5.33 ± 3.86%	7.51 (5.47-10.29) 16.58 ± 5.23%
Muscle Force	3.96 (2.69-5.85) 2.24 ± 1.42%	3.63 (1.87-7.08) 18.93 ± 8.20%	3.68 (2.76-4.92) 1.44 ± 0.93%	6.81 (4.69-9.86) 19.07 ± 5.40%
Muscle Tone	11.76 (5.26-26.26) 41.94 ±11.39%	N/A	18.30 (7.27-46.09) 46.52 ± 9.74%	N/A
Duration	8.0 (5.72-11.19) 9.83 ± 5.18%	13.33 (6.30-28.20) 36.44 ± 14.90%	11.89 (8.13-17.41) 21.97 ± 13.30%	7.31 (5.18-10.32) 85.24 ± 14.59%
Frequency	17.41 (10.92-27.77) 25.18 ± 14.13%	29.5 (17.15-50.76) 46.54 ± 18.16%	13.05 (9.22-18.45) 14.12 ± 8.16%	N/A

CHAPTER 4

[7]K_V7 CHANNEL PHARMACOLOGICAL ACTIVATION WITH THE NOVEL ACTIVATOR ML213: ROLE FOR HETEROMERIC $K_V7.4/K_V7.5$ CHANNELS IN GUINEA PIG DETRUSOR SMOOTH MUSCLE FUNCTION

ABSTRACT

Voltage-gated K_V7 channels ($K_V7.1$-$K_V7.5$) are important regulators of the cell membrane potential in detrusor smooth muscle (DSM) of the urinary bladder. This study sought to further the current knowledge of K_V7 channel function at the molecular, cellular, and tissue levels in combination with pharmacological tools. We used isometric DSM tension recordings, ratiometric fluorescence Ca^{2+} imaging, amphotericin-B perforated patch-clamp electrophysiology, and *in situ* proximity ligation assay (PLA) in combination with the novel compound N-(2,4,6-Trimethylphenyl)-bicyclo[2.2.1]heptane-2-carboxamide (ML213), an activator of $K_V7.2$, $K_V7.4$ and $K_V7.5$ channels, to examine their physiological roles in guinea pig DSM function. ML213 caused a concentration-dependent (0.1-30 μM) inhibition of spontaneous phasic contractions in DSM isolated strips; effects blocked by the K_V7 channel inhibitor XE991 (10 μM). ML213 (0.1-30 μM) also reduced pharmacologically-induced and nerve-evoked contractions in DSM strips. Consistently, ML213 (10 μM) decreased global intracellular Ca^{2+} concentrations in fura-2 loaded DSM isolated strips. Perforated patch-clamp electrophysiology revealed ML213 (10 μM) caused an increase in the amplitude of whole cell K_V7 currents. Further, in current-clamp mode of

[7] Provence A, Angoli D, Petkov GV. K_V7 Channel Pharmacological Activation with the Novel Activator ML213: Role for Heteromeric $K_V7.4/K_V7.5$ Channels in Guinea Pig Detrusor Smooth Muscle Function. *J Pharmacol Exp Ther*. 2017 Oct 30. pii: jpet.117.243162.

the perforated patch-clamp, ML213 hyperpolarized DSM cell membrane potential in a manner reversible by washout or XE991 (10 μM), consistent with ML213 activation of K_V7 channel currents. Pre-application of XE991 (10 μM) not only depolarized the DSM cells, but also blocked ML213-induced hyperpolarization, confirming ML213 selectivity for K_V7 channel subtypes. *In situ* PLA revealed co-localization and expression of heteromeric $K_V7.4/K_V7.5$ channels in DSM isolated cells. These combined results suggest that ML213-sensitive $K_V7.4$-and $K_V7.5$-containing channels are essential regulators of DSM excitability and contractility.

INTRODUCTION

Voltage-gated K_V7 channels ($K_V7.1$-$K_V7.5$), encoded by *KCNQ* genes (*KCNQ1-KCNQ5*), are critically involved in establishing and maintaining the cell membrane potential of many excitable cells and tissue types [17, 20-22, 24, 40, 41]. In addition, emerging new evidence points to potential physiological roles for the K_V7 channels in detrusor smooth muscle (DSM), the main muscular component of the urinary bladder [7-9, 26, 28, 34, 40, 42, 43].

Recent studies from our laboratory and others show that K_V7 channels serve key functional roles in regulating DSM function in rats [28, 34], guinea pigs [7, 8, 42], pigs [28], and humans [9, 44]. K_V7 channel activation leads to hyperpolarization of the membrane potential thereby decreasing Ca^{2+}-influx through L-type voltage-gated Ca^{2+} channels, which precludes Ca^{2+}-dependent activation of myosin light chain kinase necessary for initiation of DSM contractility [4, 40]. K_V7 channels were initially termed "M channels" as pioneering studies in frog sympathetic neurons demonstrated the suppression of K_V7 channel currents in response to $G_{q/11}$-coupled muscarinic acetylcholine

receptor (mAChR) activation [45]. However, whether mAChRs are involved in the regulation of K_V7 channel activity in DSM is not known.

K_V7 channel pore-forming α-subunits ($K_V7.1$-$K_V7.5$) have been shown to form both homo- and heteromeric channel conformations in experimental cell lines and native biological systems, which significantly expands the molecular and functional diversity of the K_V7 channel family [15, 16]. Further, K_V7 channel expression and function have also been shown to follow a certain level of subtype- and tissue-specificity. For example, $K_V7.1$ channels have established roles in the termination of the cardiac action potential [46], heteromeric $K_V7.2$/$K_V7.3$ channels underlie the neuronal "M-current" [47], and homo- or heteromeric combinations of $K_V7.4$ and $K_V7.5$ channel subtypes appear most critical in smooth muscle function [48]. Understandably, the development of novel K_V7 channel pharmacological modulators with improved selectivity to distinguish among individual K_V7 channel subtypes, is a highly sought endeavor. Indeed, several K_V7 channel pharmacological modulators have emerged in recent years displaying improved selectivity for individual K_V7 channel subtypes, including the $K_V7.2$/$K_V7.3$ channel activator ICA-069673, a potent inhibitor of DSM excitability and contractility [42].

The compound N-(2,4,6-Trimethylphenyl)-bicyclo[2.2.1]heptane-2-carboxamide (ML213) is a novel K_V7 channel activator initially characterized as being selective for $K_V7.2$ and $K_V7.4$ channel subtypes displaying ~80-fold selectivity over other K_V7 channels [49, 50], as well as greater potency than other Kv7 activators such as retigabine and BMS204352 [23]. Subsequent *in vitro* pharmacological and electrophysiological studies in A7r5 vascular smooth muscle cells have reported ML213 as a potent activator of homomeric $K_V7.4$ and $K_V7.5$ channels and heteromeric $K_V7.4$/$K_V7.5$ channels [31].

ML213 is currently the only known K_V7 channel activator with this unique pharmacological selectivity profile. Nonetheless, studies seeking to identify whether heteromeric K_V7 channels, specifically heteromeric $K_V7.4/K_V7.5$ channels, are expressed in DSM are currently absent. To identify the potential ML213-sensitive K_V7 channel conformations expressed at the cellular level in DSM would greatly enhance our understanding of ML213 pharmacological effects on DSM function, while expanding our knowledge of the physiological roles of K_V7 channel subtypes in the urinary bladder.

Here, we used the novel K_V7 channel activator ML213 to reveal insights into the subtype-specific K_V7 channel functional roles in DSM excitability and contractility. This was achieved by a multidisciplinary experimental approach using isometric DSM tension recordings, ratiometric fluorescence Ca^{2+} imaging, and amphotericin-B perforated patch-clamp electrophysiology. Further, *in situ* proximity ligation assay (PLA) was conducted to elucidate whether $K_V7.4$ and $K_V7.5$ channels, key pharmacological targets of ML213, co-localize to form heteromeric channel complexes in DSM cells.

MATERIALS AND METHODS

Ethical approval for animal use. Protocols for the use of experimental animals in the current study are consistent with the NIH guidelines for the care and use of experimental animals and were reviewed and approved by the Institutional Animal Care and Use Committee (IACUC) of the University of South Carolina, protocols #2186-100859-072114 and #2321-101157-092116.

Animal housing, euthanization, and DSM tissue acquisition. 41 adult male Hartley-Albino guinea pigs (Charles River Laboratories, Raleigh, NC, USA), aged 3-12 months and weighing 341-1,191 g (average 902±10 g), were utilized for this study. Animals were

housed in the Animal Resource Facilities at the University of South Carolina where they had free access to food and water and were exposed to 12 h light/dark cycles at room temperature (22-23 ºC). Animals were euthanized via CO_2 inhalation using a SMARTBOX™ Automated CO_2 Delivery System (Euthanex Corp, Palmer, PA, USA), followed by thoracotomy. The urinary bladder was then removed by an incision superior to the bladder neck. Following dissection, the urinary bladder is cut open via a longitudinal incision originating from the urethral orifice. This allows the bladder to be opened and pinned down flat to the base of a Sylgard-coated Petri dish. Under a dissection microscope, microscissors in combination with forceps are used to remove not only the urothelium, but the entire mucosal layer and lamina propria from the detrusor.

DSM cell isolation and collection. DSM single cells were freshly isolated using a combination of papain and collagenase as previously described [51]. DSM cells were used for electrophysiological experiments or *in situ* PLA within 12 h after isolation. Intact DSM strips with urothelium removed were used for single cell isolation, isometric DSM tension recordings, and ratiometric fluorescence Ca^{2+} imaging.

Isometric DSM tension recordings. Isometric DSM tension recordings were conducted as previously described on isolated DSM strips void of urothelium [51]. For experiments on spontaneous phasic, carbachol (CCh)-induced, and KCl-induced contractions, the DSM isolated strips were pretreated with the neuronal voltage-gated Na^+ channel blocker tetrodotoxin (TTX, 1 µM) before the concentration-response effects of ML213 (0.1-30 µM) were assessed. Electrical field stimulation (EFS)-induced DSM contractions were stimulated with a PHM-152I programmable stimulator (Med Associates, Inc., Georgia, VT, USA) in the absence of TTX. Ten or twenty Hz EFS frequency, respectively, was

delivered at 1 min intervals and ML213 (0.1-30 µM) was administered once a stable baseline and contraction amplitude was achieved. In a separate protocol, EFS-induced DSM contractions were stimulated at 3 min intervals over a wide range of frequencies (0.5, 2.0, 3.5, 5, 7.5, 10, 12.5, 15, 20, 30, 40, 50 Hz) in the absence (control) and then in the presence of ML213 (1 or 3 µM). The inhibitory effects of ML213 were normalized to the control (taken to be 100%) and expressed as percentages, with 100% indicated no effect and 0% indicated complete DSM relaxation.

Ratiometric fluorescence Ca^{2+} imaging. Global intracellular Ca^{2+} concentrations of isolated DSM strips were measured using the ratiometric fluorescence Ca^{2+} probe fura-2 AM as previously described [32, 42].

Perforated patch-clamp electrophysiology. K_V7 currents were recorded using the amphotericin-B perforated patch-clamp technique in voltage-clamp mode. At a holding potential of -10 mV (corrected for junction potential), K_V7 currents were recorded by applying 500 ms voltage steps at 10 mV intervals from voltages ranging -80 mV to +40 mV. To effectively isolate K_V7 currents, recordings were made in the presence of the selective large conductance voltage- and Ca^{2+}-activated K^+ (BK) channel inhibitor paxilline (1 µM) and $GdCl_3$ (50 µM), an inhibitor of non-selective cation channels and L-type voltage-gated Ca^{2+} channels [17, 52]. The amphotericin-B perforated patch-clamp technique in current-clamp mode (*I=0*) was used to record the DSM cell membrane potential as previously described [7, 42].

***In situ* Proximity Ligation Assay (PLA).** *In situ* PLA was performed on freshly-isolated DSM cells using the Duolink® *in Situ* orange starter kit goat/rabbit (Cat. No: DUO92106, Sigma-Aldrich, St. Louis, MO) according to the manufacturer's instructions. DSM cells

underwent fixation in 2% paraformaldehyde (10 min, 37°C) followed by two 15-min washes in phosphate buffered saline. DSM cells were then blocked in Duolink blocking solution (30 min, 37°C). Subsequently, DSM cells were incubated with the anti-rabbit $K_V7.4$ (Santa Cruz Biotechnology, Dallas, TX; Cat. No.: sc-50417) and anti-goat $K_V7.5$ (Cat. No.: sc-18048) antibodies or with the control anti-goat inositol triphosphate receptor (IP_3R) antibody (Cat. No.: sc-28614), respectively, in Duolink antibody diluent solution overnight at 4°C, followed by 2x5 min washes in Duolink 1x wash buffer A solution. DSM cells were then incubated with the Duolink PLA probe anti-rabbit MINUS and anti-goat PLUS oligonucleotide-conjugated secondary antibodies (1 h, 37°C), followed by 2x5 min washes in Duolink 1x wash buffer A solution. DSM cells were then incubated in ligase-ligation solution (30 min, 37°C), which hybridizes the two PLA MINUS and PLUS probes when in close proximity (<40 nm). Following ligation, DSM cells were washed 2x2 min in Duolink 1x wash buffer A solution. Finally, DSM cells were incubated in amplification-polymerase solution (100 min, 37°C) containing nucleotides and fluorescently-labelled oligonucleotides. The oligonucleotide arm of one PLA probe is a primer for rolling-circle amplification (RCA). The fluorescently-labeled oligonucleotides hybridize to the RCA product thus permitting detection. Following amplification, DSM cells were washed 2x10 min in 1x wash buffer B and then a 1 min wash in 0.01x wash buffer B. Slides were then mounted using minimal volume of Duolink *in situ* mounting medium with 4',6-diamidino-2-phenylindole, dihydrochloride (DAPI). PLA signals (Duolink *In Situ* Detection Reagents Orange ($\lambda_{excitation/emission}$=554/576 nm)) were detected using laser scanning LSM 700 confocal microscope (Carl Zeiss, Germany) with a 63x oil immersion objective.

Solutions and drugs. Nominally Ca^{2+}-free dissection solution contained the following (in mM): 80 monosodium glutamate; 55 NaCl; 6 KCl; 10 glucose; 10 4-(2-hydroxyethyl) piperazine-1-ethanesulfonic acid (HEPES); 2 $MgCl_2$; NaOH was used to attain pH 7.3. Ca^{2+}-containing physiological saline solution contained the following (in mM): 119 NaCl; 4.7 KCl; 24 $NaHCO_3$; 1.2 KH_2PO_4; 2.5 $CaCl_2$; 1.2 $MgSO_4$; 11 glucose; that was aerated with 95% O_2/5% CO_2 to attain pH 7.4. Physiological bath solution utilized for patch-clamp experiments was composed of the following (in mM): 134 NaCl; 6 KCl; 1 $MgCl_2$; 2 $CaCl_2$; 10 glucose; 10 HEPES; and NaOH was used to obtain pH 7.4. The patch-pipette solution contained (in mM): 110 potassium aspartate; 30 KCl; 10 NaCl; 1 $MgCl_2$; 10 HEPES; 0.05 ethylene glycol-bis(2-aminoethylether)-N,N,N',N'-tetraacetic acid (EGTA); NaOH was used to adjust the pH to 7.2. Amphotericin-B stock solution was prepared daily in dimethyl sulfoxide (DMSO) and was included in the pipette solution (200-300 μg/ml) before the experiment and was replaced every 1-2 h. ML213, TTX citrate, and XE991 were purchased from Tocris Bioscience (Minneapolis, MN). Fura-2 AM was purchased from Life Technologies (Cat No.: F1221, Carlsbad, CA). ML213 and Fura-2 AM were dissolved in DMSO, while XE991 and TTX citrate were dissolved in double-distilled water. All other chemicals were obtained from Fisher Scientific (Waltham, MA), Sigma-Aldrich, or Worthington Biochemical Corp. (Lakewood, NJ).

Data Analysis and Statistics. Isometric DSM tension recording experiments for spontaneous phasic, pharmacologically-induced, and nerve-evoked contractions were conducted and analyzed as previously described [7, 42, 51]. Perforated whole cell patch-clamp experiments were performed and analyzed using pCLAMP 10.3. Where specified in the summarized data, “n” represents the number of freshly-isolated DSM strips or cells,

and "N" represents the number of guinea pigs. Statistical analyses were based on the number of DSM cells or strips, respectively (i.e. "n"). For spontaneous contraction experiments, statistical analysis for the comparison of ML213 in the absence or presence of XE991, two-way ANOVA test was performed followed by Bonferroni post-hoc test. Paired Student's t-tests were used for the remaining statistical analyses. Summarized data are reported as means±SEM. P values <0.05 were considered statistically significant. Corel Draw Graphic Suite X3 software (Corel Co., Mountain View, CA) and GraphPad Prism 4.03 software (La Jolla, CA) was used for data illustration.

RESULTS

ML213 decreased spontaneous phasic contractions in DSM isolated strips. To explore the physiological effects of K_V7 channel pharmacological activation with ML213 on spontaneous phasic contractions, we conducted isometric DSM tension recordings on DSM isolated strips. ML213 (0.1-30 μM) caused a concentration-dependent inhibition of spontaneous phasic contractions in DSM isolated strips (n=6, N=6; P<0.05; **Fig. 4.1**). Pretreatment of DSM isolated strips with the K_V7 channel inhibitor XE991 (10 μM) abolished ML213 (0.1-30 μM)-induced inhibition of spontaneous phasic contractions, confirming selectivity for K_V7 channels (n=6 N=6; P<0.05; **Fig. 4.1**). IC_{50} and maximal efficacy values for ML213 on spontaneous phasic contractions are reported in **Table 4.1**.

ML213 decreased KCl-induced contractions in DSM isolated strips. Next, we elucidated the effects of ML213 (0.1-30 μM) on DSM contractions induced by mild membrane depolarization using 20 mM KCl. In the presence of 20 mM KCl, ML213 (0.1-30 μM) caused a concentration-dependent inhibition of DSM contractions and exhibited a decrease in potency in comparison to ML213 inhibitory effects on spontaneous phasic

contractions (see **Table 4.1**) (n=7, N=7; P<0.05; **Fig. 4.2**). To further explore the role of K^+ conductance in ML213-induced inhibition of DSM contractions and the potential direct interaction with L-type voltage-gated Ca^{2+} channels, we tested the effects of ML213 (10 μM) on tonic DSM contractions stimulated by high 60 mM KCl. Here, ML213 (10 μM) decreased 60 mM KCl-induced muscle tone to only 74±3.5% of the control (n=8, N=4; P<0.01; **Fig. 4.4**). Subsequent application of the L-type voltage-gated Ca^{2+} channel inhibitor nifedipine, however, caused an inhibitory effect significantly greater in comparison to ML213, decreasing DSM tone to 39.7±6.4% of the control (n=8, N=4; P<0.001; **Fig. 4.4**). The difference between the inhibitory effects of ML213 (10 μM) and nifedipine on tonic DSM contraction were statistically significant (n=8, N=4; P<0.001; **Fig. 4.4**). These data suggest ML213 does not directly inhibit L-type voltage-gated Ca^{2+} channel activity in DSM.

Carbachol attenuated ML213-induced inhibition of DSM contractions in a concentration-dependent manner. We next sought to determine the potential involvement of muscarinic acetylcholine receptor (mAChR) signaling in ML213-induced inhibition of DSM contractility. This was achieved by examining the inhibitory effects of ML213 (0.1-30 μM) on DSM contractions stimulated by the mAChR agonist CCh (0.1 or 1 μM). ML213 (0.1-30 μM) caused a concentration-dependent inhibition of both 0.1 μM and 1 μM CCh (n=6, N=6 for both; P<0.05; **Fig. 4.3**). However, in comparison to 0.1 μM, mAChR stimulation with 1 μM CCh markedly reduced the potency of ML213 on DSM contraction amplitude and muscle force (see **Table 4.1**). .IC_{50} and maximal efficacy values for ML213 on 0.1 μM and 1 μM CCh-induced DSM contractions are reported in **Table 4.1**.

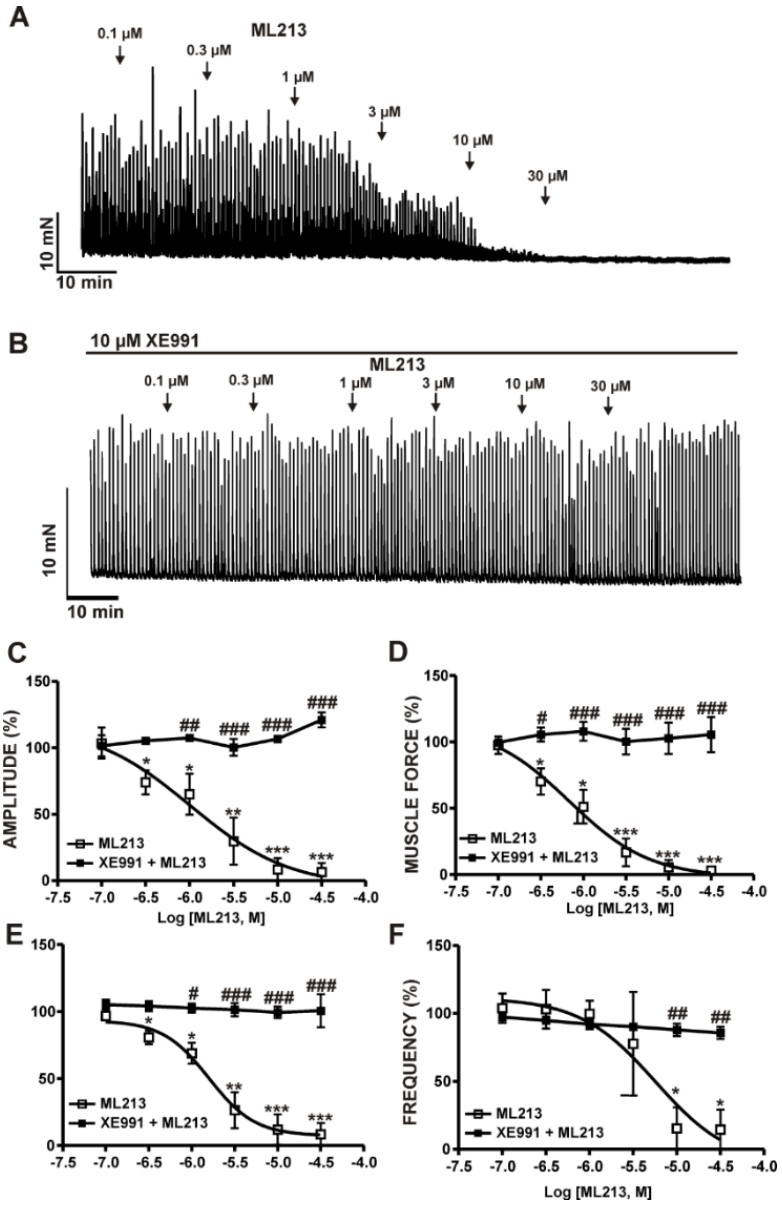

Figure 4.1. K_V7 channel pharmacological activation with ML213 leads to an inhibition of spontaneous phasic contractions in DSM isolated strips. A) A representative isometric DSM tension recording demonstrating that ML213 (0.1-30 µM) inhibited spontaneous phasic contractions in a DSM isolated strip. **B**) A representative isometric DSM tension recording illustrating the K_V7 channel inhibitor XE991 (10 µM) abolished the inhibitory effects of ML213 (0.1-30 µM) on DSM spontaneous phasic contractions. **C-F)** Cumulative concentration-response curves for ML213 on DSM phasic contraction: **C)** amplitude, **D)** muscle force, **E)** duration and **F)** frequency in the absence and presence of the K_V7 channel inhibitor XE991 (n=6, N=6; *P<0.05, **P<0.01, and ***P<0.001). $^{\#}$P<0.05, $^{\#\#}$P<0.01, and $^{\#\#\#}$P<0.001 indicate statistical significance in the effects of ML213 on spontaneous phasic contractions in the absence (control) versus presence of XE991 (n=6, N=6). See **Table 4.1** for potency and maximum efficacy values.

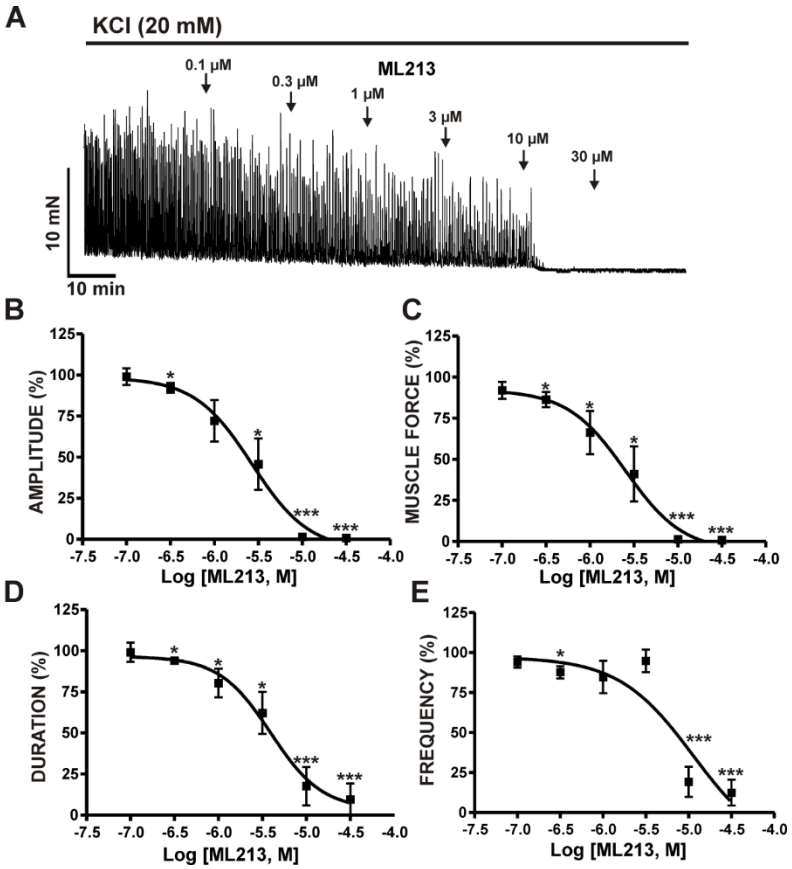

Figure 4.2. Kv7 channel pharmacological activation with ML213 leads to an inhibition of 20 mM KCl-induced phasic contractions in DSM isolated strips. A) A representative isometric DSM tension recording demonstrating the concentration-dependent inhibition of 20 mM KCl-induced DSM phasic contractions by ML213 (0.1-30 µM). **B-E)** Cumulative concentration-response curves for the inhibitory effects of ML213 on DSM phasic contraction: **B)** amplitude, **C)** muscle force, **D)** duration and **E)** frequency (n=7, N=7; *P<0.05 and ***P<0.001). See **Table 4.1** for potency and maximum efficacy values.

ML213 decreased nerve-evoked contractions in DSM isolated strips. To further explore potential roles for mAChRs in ML213-induced inhibition of DSM contractions, ML213 (0.1-30 µM) inhibitory effects were examined on nerve-evoked contractions stimulated by either 10 Hz or 20 Hz EFS. ML213 (0.1-30 µM) caused a concentration-dependent inhibition of EFS-induced contractions stimulated continuously at both 10 and 20 Hz EFS frequencies (n=7, N=6 for 10 Hz; n=6, N=6 for 20 Hz; **Fig. 4.5**).

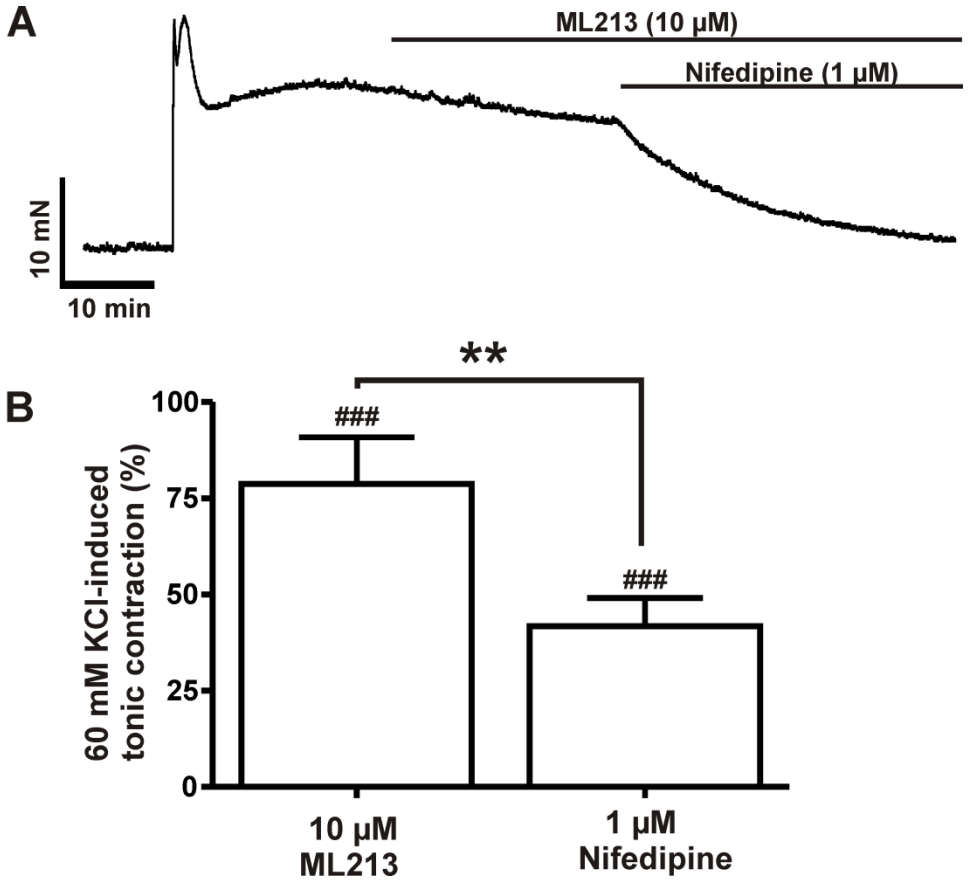

Figure 4.3. Differential inhibitory effects of ML213 and nifedipine on 60 mM KCl-induced tonic contractions in DSM isolated strips. A) A representative isometric DSM tension recording demonstrating the differential effects of 10 µM ML213 and 1 µM nifedipine upon a depolarization-induced DSM tonic contraction caused by 60 mM KCl in a DSM isolated strips. **B)** Summarized data demonstrating the differential inhibitory effects of ML213 (10 µM) and nifedipine (1 µM) on DSM 60 mM KCl-induced tonic contraction (n=8, N=4; $^{\#\#}P<0.01$ vs. control, and $^{**}P<0.001$ ML213 vs. nifedipine, respectively).

IC_{50} and maximal efficacy values for ML213 on 10 Hz and 20 Hz EFS-induced contractions are reported in **Table 4.1.** In comparison to 10 Hz EFS, the potency of ML213 on 20 Hz EFS-induced contractions was reduced by more than two-fold (see **Table 4.1**). Next, ML213 (1 or 3 µM) inhibitory effects were examined on contractions induced over a range of EFS frequencies (0.5-50 Hz). ML213 (1 or 3 µM) decreased the amplitude of 10-50 Hz EFS-induced contractions (n=6, N=6; $P<0.05$; **Fig. 4.6**).

ML213 decreased global intracellular Ca^{2+} concentrations in DSM isolated strips. We next aimed to assess the effects of ML213 on global intracellular Ca^{2+} concentrations of isolated DSM strips loaded with fura-2. This was achieved using the ratiometric fluorescence Ca^{2+} indicator fura-2 AM and measuring the emission at 510 nm with excitation at 340 and 380 nm. Under control conditions in the absence of ML213, the mean intensity (F_{340}/F_{380}) was 0.84±0.05 (n=7, N=6) and in the presence of ML213 (10 μM) the mean F_{340}/F_{380} ratio was decreased to 0.77±0.05 (n=7, N=6; P<0.05; **Fig. 4.7**). These results suggest K_V7 channel pharmacological activation with ML213 critically regulates global intracellular Ca^{2+} concentrations in DSM isolated strips and thus DSM contractility.
ML213 decreased global intracellular Ca^{2+} concentrations in DSM isolated strips. We next aimed to assess the effects of ML213 on global intracellular Ca^{2+} concentrations of isolated DSM strips loaded with fura-2. This was achieved using the ratiometric fluorescence Ca^{2+} indicator fura-2 AM and measuring the emission at 510 nm with excitation at 340 and 380 nm. Under control conditions in the absence of ML213, the mean intensity (F_{340}/F_{380}) was 0.84±0.05 (n=7, N=6) and in the presence of ML213 (10 μM) the mean F_{340}/F_{380} ratio was decreased to 0.77±0.05 (n=7, N=6; P<0.05; **Fig. 4.7**). These results suggest K_V7 channel pharmacological activation with ML213 critically regulates global intracellular Ca^{2+} concentrations in DSM isolated strips and thus DSM contractility.
ML213 enhanced the amplitude of whole cell K_V7 currents in freshly-isolated DSM cells. We next sought to examine the pharmacological effects of ML213 on whole cell K_V7 currents using the perforated patch-clamp technique in voltage-clamp mode. In the first series of experiments, K_V7 currents were recorded at a holding potential of -10 mV wherein 500 ms voltage steps were applied at 10 mV intervals from -80 mV to +40 mV.

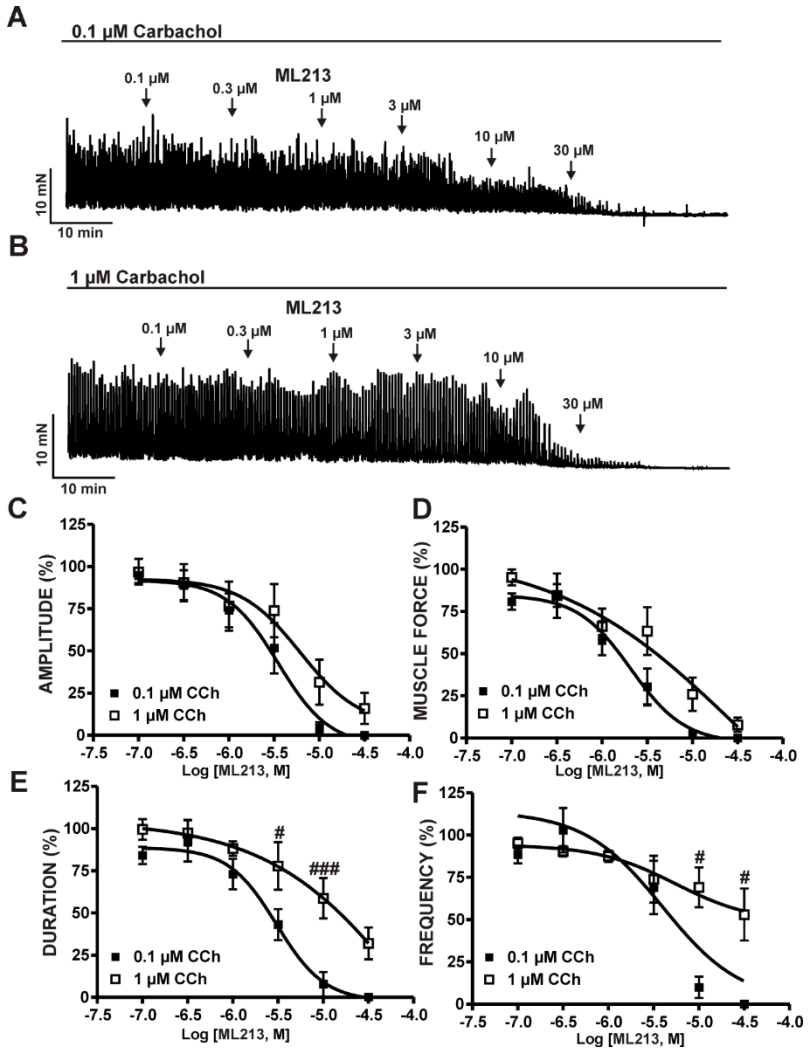

Figure 4.4. K_V7 channel pharmacological activation with ML213 leads to an inhibition of CCh-induced DSM phasic contractions. A) A representative isometric DSM tension recording demonstrating the concentration-dependent inhibition of 0.1 µM CCh-induced phasic contractions in a DSM isolated strip. **B)** A representative isometric DSM tension recording demonstrating the concentration-dependent inhibition of 1 µM CCh-induced phasic contractions in a DSM isolated strip. **C-F)** Cumulative concentration-response curves for ML213 on CCh (0.1 or 1 µM)-induced DSM phasic contraction **C)** amplitude and **D)** muscle force, **E)** duration, and **F)** frequency (n=6, N=6 for both data sets; $^{\#}P<0.05$, $^{\#\#\#}P<0.001$). See **Table 4.1** for potency and maximum efficacy values.

To effectively isolate K_V7 currents, recordings were made in the presence of the selective large-conductance voltage- and Ca^{2+}- activated K^+ (BK) channel inhibitor paxilline (1 µM) and $GdCl_3$ (50 µM), an inhibitor of non-selective cation and L-type voltage-gated Ca^{2+} channels.

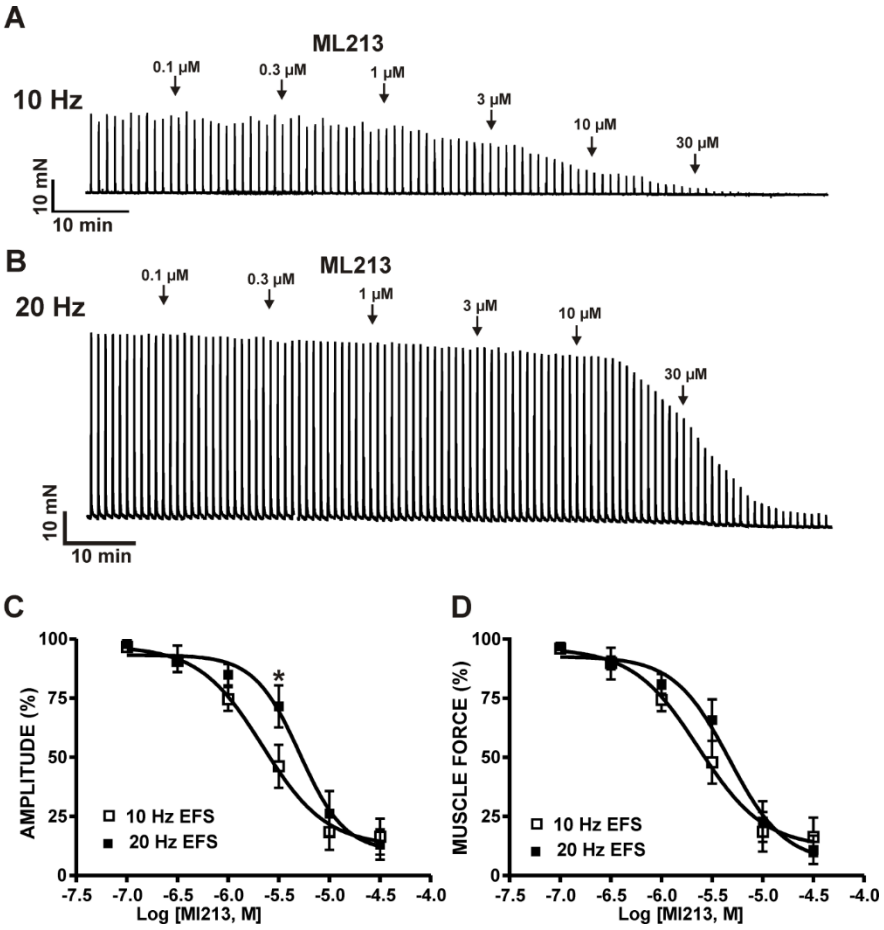

Figure 4.5. K_V7 channel pharmacological activation with ML213 leads to an inhibition of nerve-evoked contractions induced by 10 Hz and 20 Hz EFS in DSM isolated strips. A) A representative isometric DSM tension recording demonstrating the concentration-dependent inhibition of 10 Hz EFS-induced contractions by ML213 (0.1-30 µM) in DSM isolated strips. **B)** A representative isometric DSM tension recording illustrating the concentration-dependent inhibition of 20 Hz EFS-induced contractions by ML213 (0.1-30 µM) in DSM isolated strips. **C-D)** Cumulative concentration-response curves for ML213 on DSM EFS-induced: **C)** contraction amplitude and **D)** muscle force (n=7, N=6 for 10 Hz; n=6, N=6 for 20 Hz; *P<0.05 for 10 vs. 20 Hz). See **Table 4.1** for potency and maximum efficacy values.

Further, the more depolarized holding potential of -10 mV that we used ensures inactivation of other non-K_V7 K^+ channels, such as inward-rectifying K^+ channels [53]. ML213 (10 µM) caused a significant increase in the amplitude of whole cell K_V7 currents at all voltages from -50 to +40 mV (n=7, N=5; P<0.05; **Fig. 4.8**). We further sought to examine the time course for the pharmacological effects of ML213 on K_V7 currents in

DSM cells. This was achieved using a one-step voltage-clamp protocol with a 5 s duration stimulus applied every 20 s from a -10 mV holding potential to +40 mV. ML213 (10 µM)

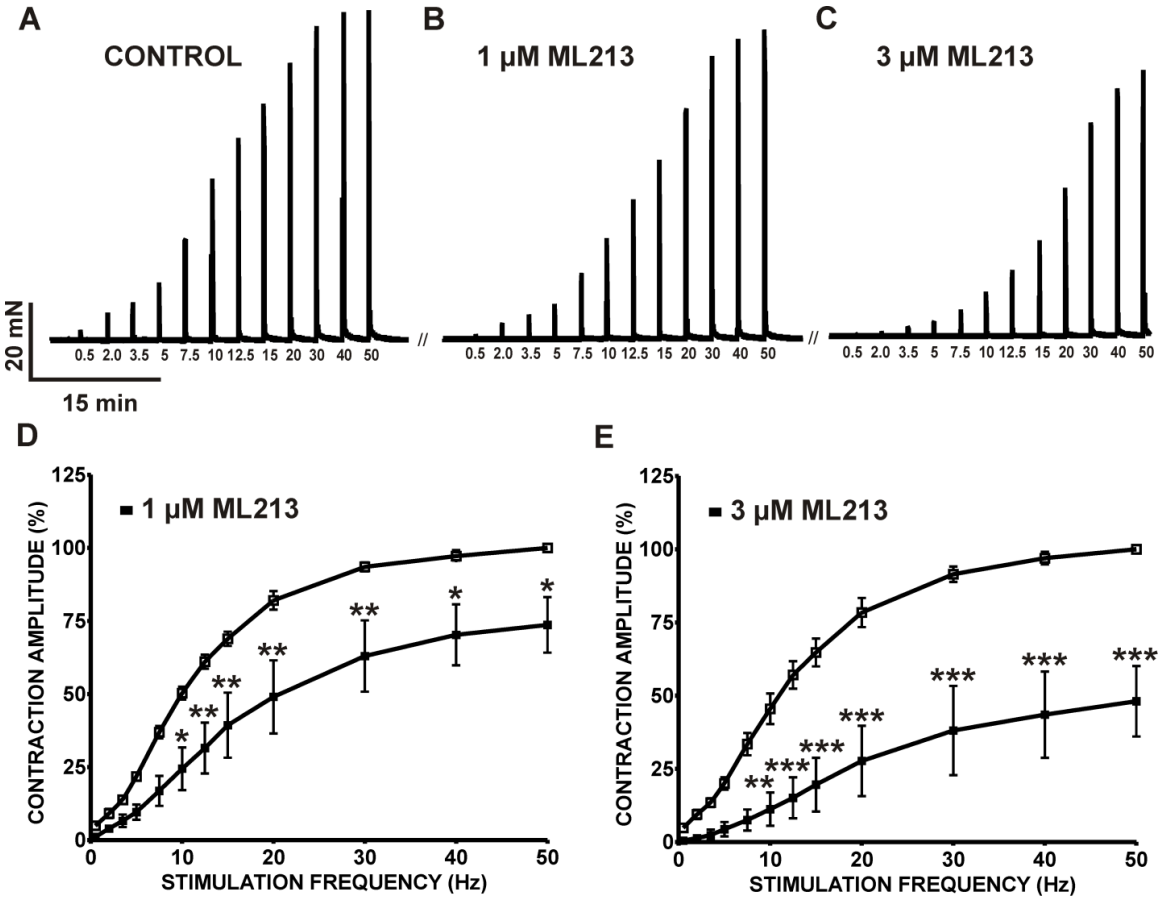

Figure 4.6. ML213 decreases 0.5-50 Hz EFS-induced contractions in DSM isolated strips. A-C) The original isometric DSM tension recordings of 0.5-50 Hz EFS-induced contractions in DSM isolated strips **A)** before (control), and after the addition of **B)** 1 µM ML213, and **C)** 3 µM ML213. **D-E)** Cumulative frequency-response curves demonstrating the inhibitory effects of **D)** 1 µM ML213 and **E)** 3 µM ML213 on the amplitude of 0.5-50 Hz EFS-induced contractions in DSM isolated strips (n=6, N=6 for both data sets; *P<0.05, **P<0.01, and ***P<0.001).

caused a significant increase in the whole cell K_V7 current amplitude by 106.7±54.95% and 48.4±21.33%, respectively, in comparison to the control (n=8, N=5, P<0.05; **Fig. 4.9**).

ML213 hyperpolarizes the resting membrane potential in freshly-isolated DSM cells. Using the perforated whole cell patch-clamp technique in current-clamp mode, we next sought to determine the physiological role of ML213-sensitive K_V7 channels in regulating

the DSM cell membrane potential. ML213-induced inhibitory effects were examined in 6 DSM isolated cells from 6 different animals, which had an average resting membrane potential of -22±4.2 mV. ML213 hyperpolarized the DSM cell membrane potential from the control value of -22±4.2 mV to -42.6±4.2 mV (n=6, N=6; P<0.05; **Fig. 4.10**). ML213-induced DSM cell membrane hyperpolarization was fully reversible by washout of ML213 (**Fig. 4.10**). On the contrary, XE991 (10 μM) depolarized the DSM cell membrane potential from -29.8±4.3 to -18.7±2.7 and blocked ML213 (10 μM) hyperpolarization at -20.6±2.8 (n=8, N=4; P<0.05; **Fig. 4.10**), confirming ML213 selectivity for the K_V7 channels. XE991 (10 μM) was also effective in reversing the hyperpolarizing effects of ML213 from -39.2±9.2 to -23.2±5.5 (control was -26.6±7.2) (n=7, N=6; P<0.05; **Fig. 4.11**). These combined results suggest key involvement for ML213-sensitive $K_V7.2$, $K_V7.4$, and $K_V7.5$ channels in regulating the DSM cell membrane potential.

$K_V7.4$ and $K_V7.5$ channel α-subunits assemble to form heteromeric $K_V7.4/K_V7.5$ channel subtypes in freshly-isolated DSM cells. Using *in situ* PLA, we sought to determine whether $K_V7.4$ and $K_V7.5$ channels, among the key targets of ML213, form heteromeric channels in freshly-isolated DSM cells. *In situ* PLA demonstrated $K_V7.4$ and $K_V7.5$ channel subunits associate to form heteromeric $K_V7.4/K_V7.5$ channels in isolated DSM cells. As shown in **Figure 4.12**, *in situ* PLA experiments demonstrated the co-localization of $K_V7.4$ and $K_V7.5$, channel α-subunits within 40 nm and within the vicinity of the DSM cell membrane. Primary antibodies against the IP_3R, which would not be expected to co-localize with members of the K_V7 channel family, were used as a negative control. Co-incubation of the $K_V7.4$ channel primary antibody with the primary antibody of the IP_3Rs yielded no PLA fluorescent signal (**Fig. 4.12**). These combined results suggest

that $K_V7.4$ and $K_V7.5$ channel subunits assemble to form heteromeric $K_V7.4/K_V7.5$ channel subtypes in DSM cells.

DISCUSSION

The current study utilized the novel compound ML213, a potent and selective activator of $K_V7.2$, $K_V7.4$, and $K_V7.5$-containing channels, to elucidate their physiological roles in DSM excitability and contractility. ML213 inhibited spontaneous, pharmacologically-induced, and nerve-evoked DSM contractions and decreased global intracellular Ca^{2+} concentrations in DSM strips. ML213 enhanced whole cell K_V7 currents and hyperpolarized the resting membrane potential of freshly-isolated DSM cells. *In situ* PLA studies further revealed the expression of heteromeric $K_V7.4/K_V7.5$ channels within the vicinity of the DSM cell membrane, which are key pharmacological targets of ML213. Previous studies on guinea pig, including those from our group, have demonstrated a role for K_V7 channels in DSM function through the use of K_V7 channel pharmacological modulators [7, 8, 42]. ML213 promoted concentration-dependent inhibition of spontaneous phasic contractions with IC_{50} values of 1.1 and 0.7 μM, respectively (**Fig. 4.1** and **Table 4.1**). Consistently, the inhibitory effects of ML213 on DSM contractile activity in our study are consistent with previous reports in human and pig DSM [9, 28, 44]. Based on our data, ML213 displays greater potency in comparison to retigabine, the $K_V7.1$ channel activator L-364373, and the $K_V7.2/K_V7.3$ channel activator ICA-069673 for inhibiting DSM spontaneous phasic contraction amplitude and muscle force [7, 8, 42]. ICA-069673 and ML213 have each been demonstrated to potently activate homomeric $K_V7.4$ channels, however, the key distinction between these two compounds was the ability for ML213 to potently activate homomeric $K_V7.5$ and heteromeric $K_V7.4/K_V7.5$ channels [31].

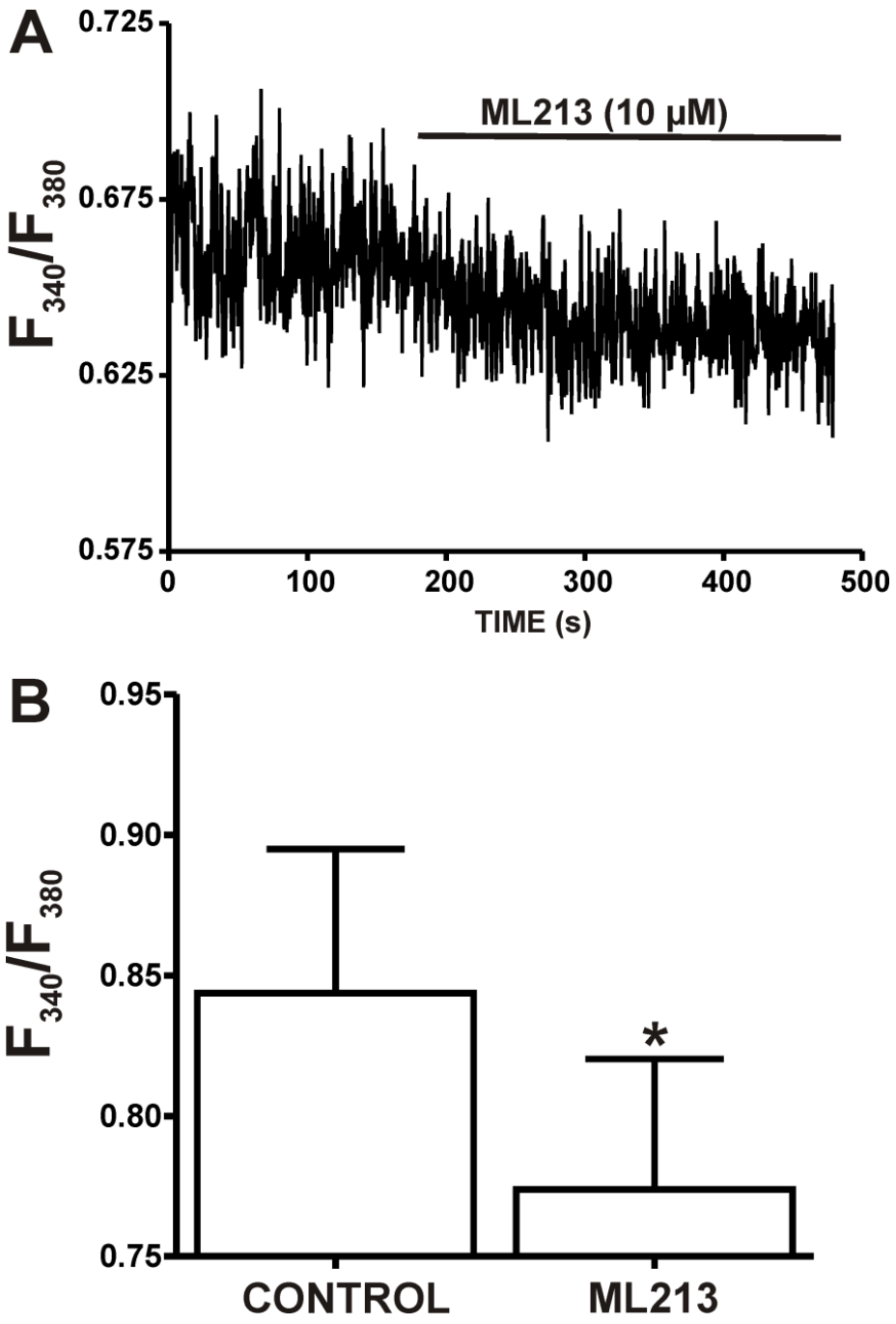

Figure 4.7. ML213 decreases global intracellular Ca^{2+} concentrations in DSM isolated strips. A) Original recordings illustrating that ML213 (10 µM) significantly decreased global intracellular Ca^{2+} levels in a fura 2-loaded DSM strip. **B)** Summarized data representing the reduction in global Ca^{2+} levels by 10 µM ML213 in DSM isolated strips (n=7, N=6; *P<0.05).

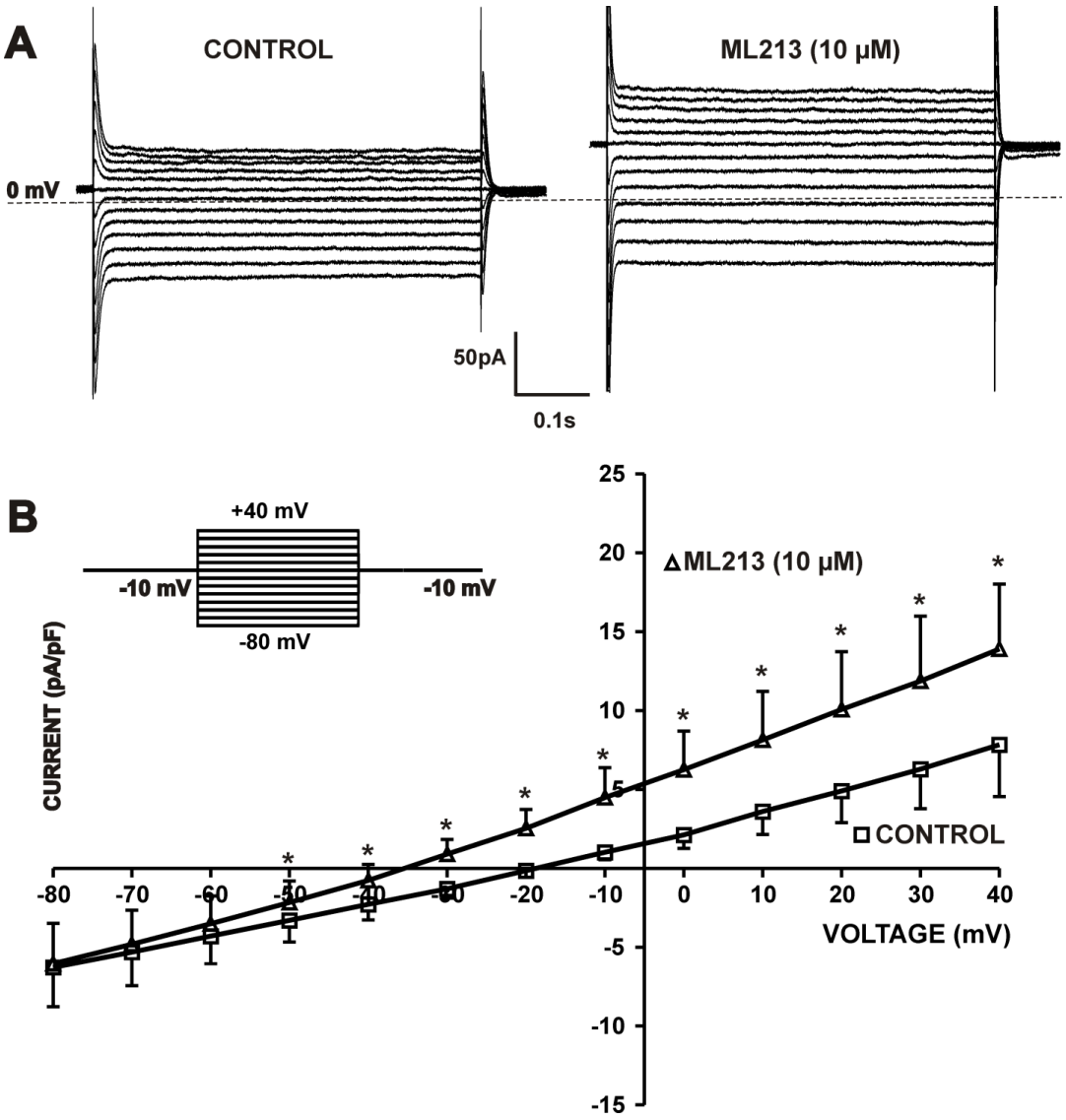

Figure 4.8. ML213 (10 µM) enhanced whole cell K_V7 currents in freshly-isolated DSM cells. A) Representative whole cell patch-clamp recordings illustrating the potentiation of K_V7 currents induced by the introduction of ML213 in the bath external solution. Paxilline (1 µM) and $GdCl_3$ (50 µM) were present in the solution. **B)** Current-voltage relationships obtained in the absence (control) or presence of 10 µM ML213 in a whole cell voltage-clamp recording. The two curves represent the current–voltage relationship expressed as normalized current in the absence or presence of 10 µM ML213 (n=7, N=5, *P<0.05). **Top left insert:** 500 ms voltage-step protocol from -80 to +40 mV with holding potential at -10 mV.

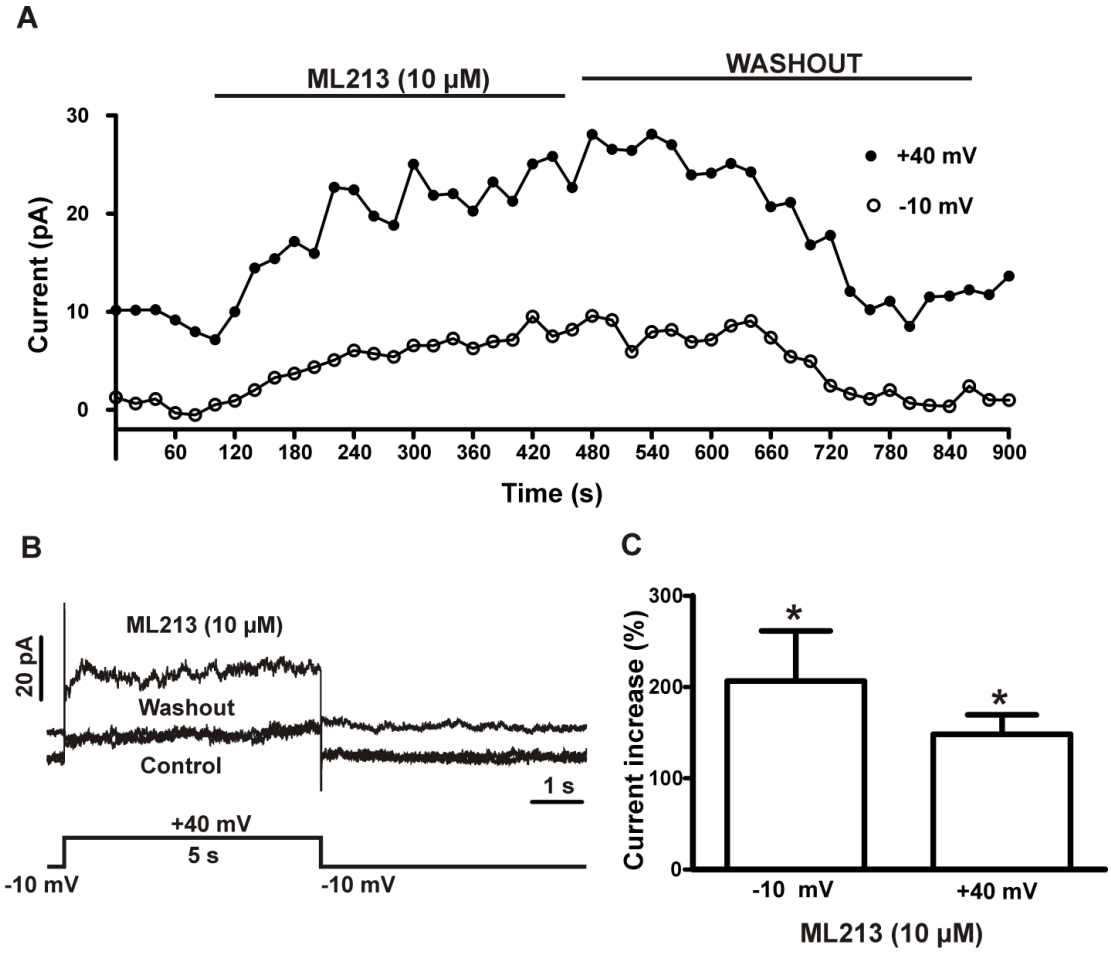

Figure 4.9. Time course of ML213-induced activation of K_V7 channel currents in freshly-isolated DSM cells. A) Effects of ML213 on K_V7 currents recorded using a one-step voltage-clamp protocol with a 5 s duration stimulus applied every 20 s from a -10 mV holding potential to +40 mV. **B)** Representative traces (and voltage step used) of the experiment plotted in **A)** for the control, ML213 (10 µM) and washout of ML213. **C)** Summary data for the percentage of K_V7 currents in the presence of ML213 compared to control at -10 and +40 mV respectively (n=8, N=5, *P<0.05). Summarized data illustrate the average of 4 to 6 points of each steady-state current.

The greater capacity and potency for ML213 to inhibit spontaneous phasic, pharmacologically-induced, and EFS-induced DSM contractions (**Figs. 4.1-4.6**) in comparison to ICA-069673 [42], potentially implicates key involvement of $K_V7.4$ or $K_V7.5$-containing channels in DSM function. Similar observations were reported by studies using ML213 in rodent mesenteric arteries, where the $K_V7.4$ channels subtypes are predominately expressed [23]

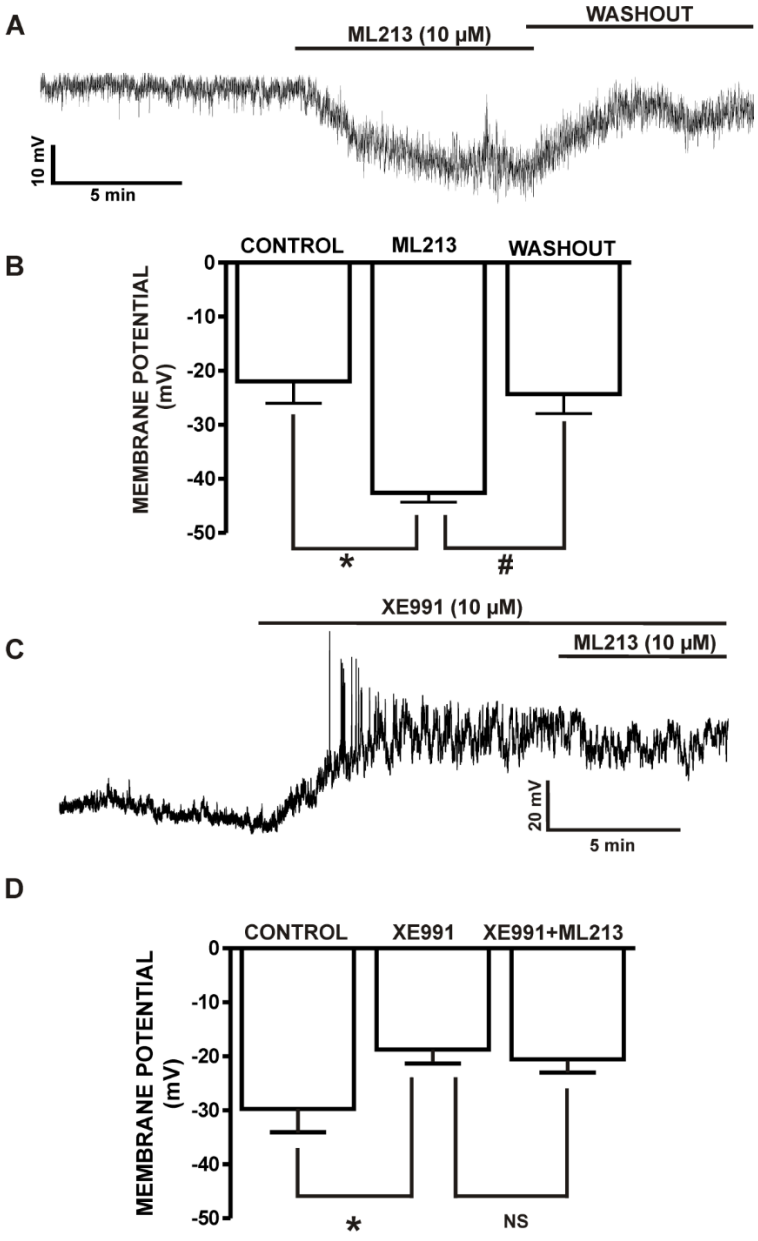

Figure 4.10. ML213 hyperpolarizes the resting membrane potential in freshly-isolated DSM cells. A) A representative membrane potential recording in current-clamp mode illustrating that ML213 (10 µM) hyperpolarized the DSM cell membrane potential in a freshly-isolated DSM cell and that this effect was reversible by washout. **B)** Summarized data for the hyperpolarizing effects of ML213 (10 µM) on the DSM cell membrane potential (n=6, N=6; *P<0.05). **C)** A representative membrane potential recording in current-clamp mode demonstrating that XE991 (10 µM) depolarized the DSM cell membrane potential and blocked ML213 (10 µM) hyperpolarization in a freshly-isolated DSM cell (**D)** Summarized data for XE991 (10 µM)-induced depolarization in freshly-isolated DSM cells and the lack of ML213 (10 µM) hyperpolarizing effects in the presence of 10 µM XE991 (n=8, N=4; *P<0.05).

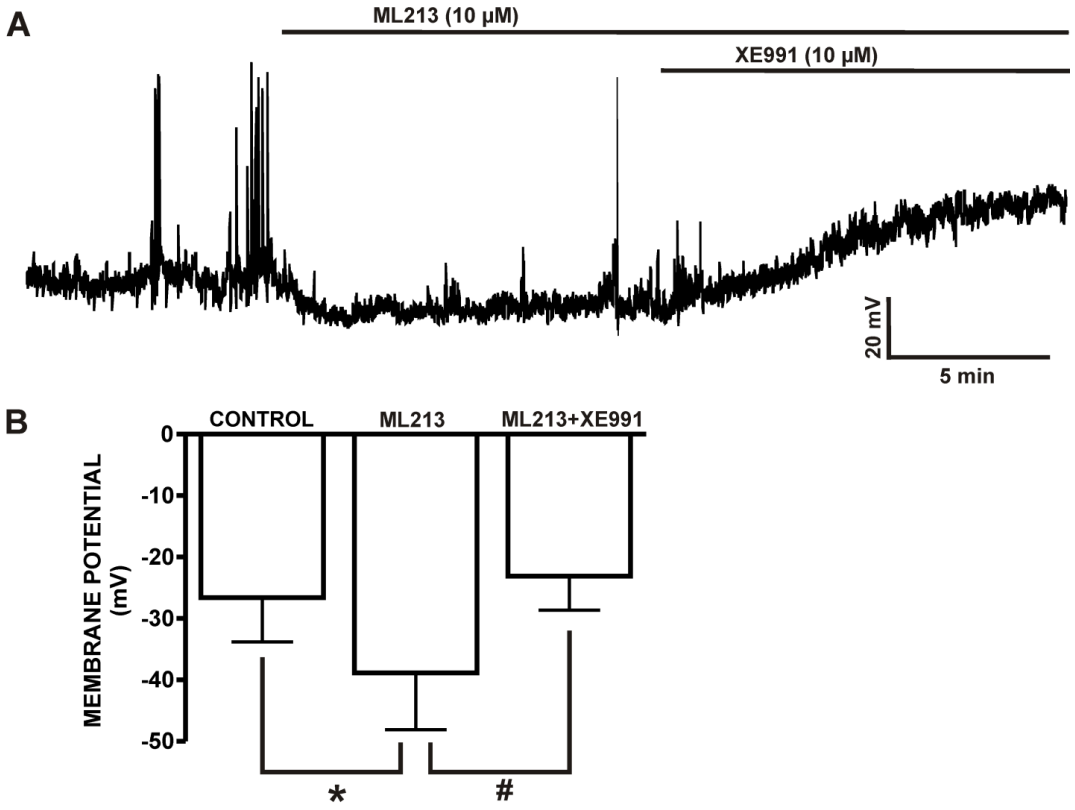

Figure 4.11. ML213-induced hyperpolarization is reversed by K_V7 channel inhibition with XE991. A) A representative current-clamp recording from a freshly-isolated DSM cell illustrating hyperpolarization of the DSM cell membrane potential by ML213 (10 µM) and that the ML213-induced hyperpolarization is reversed by the K_V7 channel inhibitor XE991 (10 µM). **B)** Summary data for the hyperpolarizing effects of ML213 (10 µM) on the DSM cell membrane potential (n=7, N=5, *P<0.05, effects reversible by 10 µM XE991 (n=7, N=5, $^{\#}$P<0.05). NS-non-significant.

The ability of ML213 to inhibit DSM contractions was decreased in a concentration-dependent manner by the mAChR agonist CCh (**Fig. 4.4**). Consistently, ML213 exhibited a reduced potency on 20 Hz EFS-induced DSM contractions in comparison to 10 Hz (**Fig. 4.5**). ML213 inhibitory effects on CCh and EFS-induced DSM contractions are consistent with previous reports in pigs and humans [9, 28]. These results suggest that cellular pathways leading to the activation K_V7 channels may potentially function in opposition to mAChR signaling. However, confirming the existence of functional link between K_V7 channels and mAChRs in DSM will require additional future studies involving extensive pharmacological and electrophysiological approaches.

Parasympathetic nerves release ACh and ATP which act on mAChRs and purinergic receptors, respectively, to trigger bladder contraction during micturition [1, 2, 54]. ACh-induced activation of mAChRs constitutes the primary mechanism initiating bladder contractions during micturition [1]. EFS evokes ACh release from parasympathetic nerve terminals, which leads to depolarization of the DSM cell membrane potential and associated DSM contractions [3]. While mAChR regulation of K_V7 channel activity is consistent with early studies in neurons [45], whether a similar regulatory mechanism exists in DSM remains unknown. A recent study in airway smooth muscle reported that, unlike neuronal K_V7 channels [55], mAChR activation by CCh did not exhibit significant inhibitory effects on K_V7 currents [41]. Thus, K_V7 channel activation in DSM may act in opposition to mAChRs through an indirect mechanism, for example, activation of L-type voltage-gated Ca^{2+} channels. Nonetheless, regulation of K_V7 channels by mAChRs in DSM represents an interesting topic for future investigations. Consistent with ML213 inhibitory effects on DSM contractions, we further observed attenuation of global intracellular Ca^{2+} concentrations by ML213 in DSM strips (**Fig. 4.7**).

For the first time, we report the activation of whole cell K_V7 currents by ML213 in freshly-isolated DSM cells (**Figs. 4.8-9**). The use of a more depolarized holding potential (-10 mV) in our study ensures inactivation of other non-K_V7 K^+ channels, such as inward-rectifying K^+ channels [53]. Also, at -10 mV holding potential, some of the K_V7 channels are open and generate quantifiable currents, which are not contaminated by the presence of non-selective cation currents due to the inclusion of $GdCl_3$. Thus, the stimulatory effects of ML213 on K_V7 currents are evident (**Fig. 4.8**). Our data support the concept that the hyperpolarizing currents following addition of ML213 are a direct result of K_V7 channel

pharmacological activation. In a series of experiments, we used short voltage steps (500 ms) marginally revealing the kinetics of voltage-dependence of activation of the K_V7 channels. Alternatively, using longer voltage-step protocols (5 s) with multiple voltage steps may result in time-dependent rundown after several minutes of recording. Hence, we sought to examine the time course effects of ML213 on K_V7 current activity by performing a one-step 5 s voltage-clamp protocol from a -10 mV holding potential to +40 mV at 20 s intervals (**Fig. 4.9**). This protocol allowed for the recording of K_V7 channel currents without encountering substantial current run-down. The stimulatory effects of ML213 on K_V7 currents were modest, but statistically significant (**Fig. 4.8**). Albeit, it is well-established that small changes in DSM cell excitability can have pronounced effects on DSM contractility [56, 57]. Indeed, we observed very robust ML213 inhibitory effects on DSM contractility (**Figs. 4.1-4.3**).

Overall, the experimental design for our electrophysiological experiments aimed not only to examine K_V7 current activity and its response to pharmacological activation with ML213, but also to mimic a physiological environment characterized by a more depolarized resting membrane potential, which normally occurs under physiological conditions during the action potential. Activation of ML213-sensitive K_V7 channels was further shown to hyperpolarize the DSM cell membrane potential (**Fig. 4.10**), consistent with ML213 inhibitory effects on global intracellular Ca^{2+} concentrations and DSM contractility. K_V7 channel α-subunits are known to form functional homo- and heteromeric channel conformations *in vitro* and *in vivo* [14, 40], with $K_V7.4$, and $K_V7.5$ being prominent in smooth muscle tissues [58].

In vascular myocytes, ML213 has been shown to activate heteromeric $K_V7.4/K_V7.5$ channels in addition to the homomeric channels composed either $K_V7.4$ or $K_V7.5$ channel α-subunits, respectively [31, 49]. In addition to $K_V7.2$ channel expression in guinea pig DSM [7, 8, 42], $K_V7.4$ [8], and $K_V7.5$ [7, 8] channel α-subunits have been identified. However, whether these K_V7 channel subunits, in particular $K_V7.4$ or $K_V7.5$, associate to form functional heteromers in DSM remains unknown. We confirmed the expression of heteromeric $K_V7.4/K_V7.5$ channels in isolated DSM cells using *in situ* PLA. PLA fluorescent signals for $K_V7.4/K_V7.5$ α-subunit co-localization were uniformly detected through the DSM cell periphery, suggesting plasmalemmal expression of heteromeric $K_V7.4/K_V7.5$ channels (**Fig. 4.12**). These findings, which are consistent with studies on rodent vasculature [18] and provide strong evidence confirming heteromeric $K_V7.4/K_V7.5$ channel expression in DSM cells. While heteromeric $K_V7.4/K_V7.5$ channels are potently activated by ML213 pharmacological activation, it has not yet been reported whether heteromeric $K_V7.2/K_V7.3$ channels or other $K_V7.2$-containing channels, are ML213-sensitive. Albeit, the potential activation of $K_V7.2/K_V7.3$ channels, for example, by ML213 would presumably be mediated by the $K_V7.2$ channel subunit as $K_V7.3$ channel subtypes are insensitive to ML213.

In addition, further studies to elucidate the precise stoichiometry of K_V7 channels and their associations with β-regulatory subunits (KCNE1-5) will be required to further understand the potential ML213 targets in DSM. Indeed, a recent study in rodent arterial myocytes demonstrated KCNE4 co-localization with $K_V7.4$ and $K_V7.5$ channels, respectively [59]. Also, co-expression of KCNE4 with $K_V7.4$ channels was found to increase $K_V7.4$ channel expression and current amplitudes [59]. Moreover, a report from

bovine DSM suggests K_V7.4 channel subtypes as the most abundantly expressed; findings consistent with emerging studies in humans demonstrating K_V7.4 mRNA expression as the primary K_V7 channel expressed in DSM [9, 60]. A separate group reported K_V7.5 channel mRNA expression as the most highly expressed K_V7 channel subtype in human DSM [61]. Although ML213 and ICA-069673 activate K_V7.2 channels, their differential selectivity among K_V7.4 and K_V7.5-containing channels demonstrates the capacity for subtype-specific pharmacological targeting.

As our *in situ* PLA experiments provided decisive evidence confirming the expression of heteromeric K_V7.4/K_V7.5 channel subtypes in DSM (**Fig. 4.12**), these channels may be among the key pharmacological targets for ML213. Albeit, homomeric K_V7.4 and K_V7.5 channel subtypes may also be critically involved as a previous report revealed ML213 as equally potent among K_V7.4 and K_V7.5-containing channels [31]. Based on our novel findings regarding K_V7 channel conformations in DSM in conjunction with our recent electrophysiological studies of ML213, our data suggests key roles for K_V7.4- and K_V7.5-containing channels, including K_V7.4/K_V7.5 heteromers, in mediating the effects of ML213 in DSM. The ability to fine-tune K_V7 channel pharmacological modulators to exhibit improved selectivity between K_V7.4, K_V7.5, and K_V7.4/K_V7.5 channels, may represent a substantial breakthrough in the development of novel and efficacious therapeutic modalities for lower urinary tract dysfunction.

In conclusion, our study demonstrates that ML213-sensitive K_V7.4-and K_V7.5-containing channels are essential regulators of DSM excitability and contractility. K_V7 channel activation by the novel activator ML213 leads to the activation of K_V7 currents,

hyperpolarization of the membrane potential, a decrease in global intracellular Ca^{2+} concentration, and the attenuation of DSM contractility.

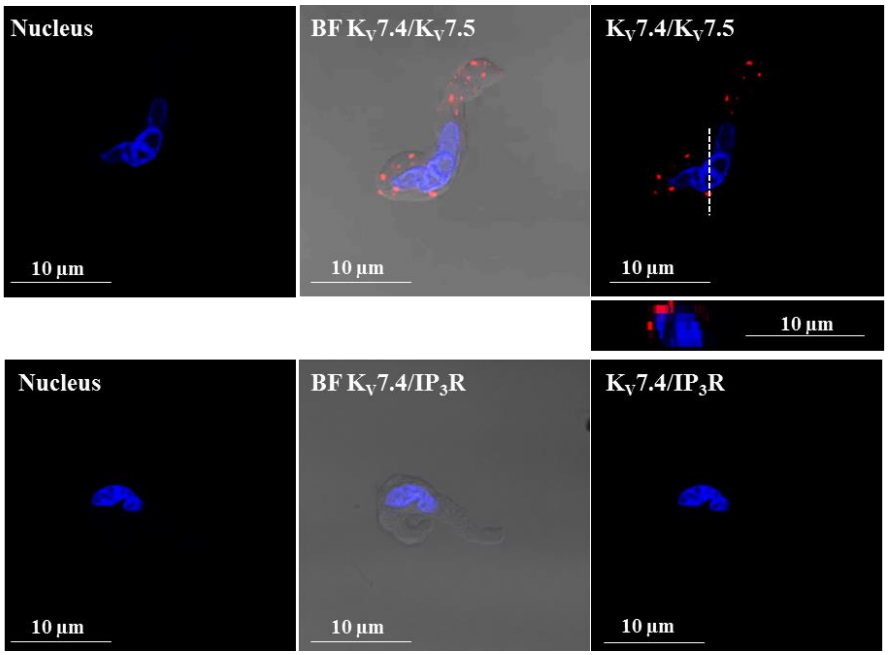

Figure 4.12. PLA shows that Kv7.4/Kv7.5 heteromeric channels are expressed in isolated guinea pig DSM cells. Images of a freshly-isolated DSM cell stained with the combination of anti-K_V7.4 and anti-K_V7.5 channel antibodies (*upper panels*). PLA fluorescent signals are shown in red. No PLA fluorescent signals were observed when the anti-K_V7.4 antibody was co-incubated with the anti-IP_3R antibody (*lower panels*). An orthogonal cross-section image of the DSM cell displaying PLA signals was obtained following z-stack scans collected along the viewing plane indicated by the dashed (- - -) lines and is represented directly below the top right panel. BF, bright field; DAPI, 4′,6-Diamidine-2′-phenylindole dihydrochloride (nuclear staining shown in *blue*).

Table 4.1. IC_{50} and maximal efficacy values for the effects of ML213 DSM Contractions

CONDITION	AMPLITUDE	MUSCLE FORCE	DURATION	FREQUENCY	n/N
Spontaneous Phasic Contractions	1.1 (0.5-2.4) µM; 95.6 ± 4.4%	0.7 (0.2-2.8) µM; 96.8 ± 3.2%	1.6 (0.8-2.9) µM; 91.6 ± 8.41%	3.9 (0.8-20.3) µM; 85.4 ± 14.6%	6/6
KCl (20 mM)-Induced Contractions	2.7 (1.4-5.1) µM; 99.2 ± 0.8%	2.5 (1.2-5.3) µM; 99.1 ± 0.9%	3.9 (1.9-8.2) µM; 90.3 ± 9.7%	n/a; 87.6 ± 8.2%	7/7
CCh (0.1 µM)-Induced Contractions	3.5 (1.9-6.4) µM; 100% inhibition	2.1 (1.1-3.9) µM; 100% inhibition	3.0 (1.8-5.3) µM; 99.7 ± 0.29%	n/a; 100% inhibition	6/6
CCh (1 µM)-Induced Contractions	6.2 (1.2-30.7) µM; 84 ± 9.1%	n/a; 92.1 ± 4.2%	n/a; 68 ± 9.5%	n/a; 47.1 ± 15.4%	6/6
10-Hz EFS-Induced Contractions	2.2 (1.3-3.7) µM; 83.6 ± 7.6%	2.3 (1.3-4.1) µM; 83.9 ± 8.2%	n/a; 32.78 ± 13.5%	n/a	7/6
20-Hz EFS-Induced Contractions	5.1 (3.1-8.2) µM; 86.9 ± 6.4%	4.7 (2.7-8.1) µM; 89.1 ± 6.0%	n/a; 37.46 ± 9.3%	n/a	6/6

CHAPTER 5

PHYSIOLOGICAL ROLES OF VOLTAGE-GATED $K_V7.4/K_V7.5$ CHANNELS IN HUMAN DETRUSOR SMOOTH MUSCLE EXCITABILITY AND CONTRACTILITY

ABSTRACT

Emerging research efforts have established voltage-gated K_V7 channels ($K_V7.1$-$K_V7.5$) as key regulators of detrusor smooth muscle (DSM) function; however, essential information regarding K_V7 channel expression, tetrameric conformations, and physiological roles remain to be explored at cellular and tissue levels in human DSM. We used RT-PCR, , Western blot, immunocytochemistry, *in situ* proximity ligation assays (PLA), ratiometric fluorescence Ca^{2+} imaging, isometric DSM tension recordings, and perforated patch-clamp electrophysiology using freshly-isolated human DSM strips and cells. Human DSM tissues were collected from ## donors undergoing routine open bladder surgeries. RT-PCR detected mRNA transcripts for K_V7 channel subtypes in human DSM tissue and isolated cells. Western blot analysis and immunocytochemistry further demonstrated K_V7 channel protein expression in DSM tissue and isolated cells, respectively. *In situ* PLA experiments identified co-localization of $K_V7.4$ and $K_V7.5$ channel subunits, suggesting expression of heteromeric $K_V7.4/K_V7.5$ channel subtypes in human DSM cells. The K_V7 channel activator, retigabine, decreased global Ca^{2+} concentrations in DSM isolated strips, while the K_V7 channel inhibitor XE991 increased global Ca^{2+} concentrations. Retigabine decreased spontaneous phasic and nerve-evoked contractions in DSM isolated strips, while the K_V7 channel inhibitor XE991 increased

spontaneous phasic and nerve-evoked contractions in DSM isolated strips. Retigabine-induced DSM relaxation was attenuated in the presence of XE991. The $K_V7.2/K_V7.3$ channel activator ICA-069673 and $K_V7.1$ activator L-364,373 also inhibited spontaneous phasic contractions. In voltage-clamp mode of the perforated patch-clamp technique, retigabine (10 μM) caused a significant increase in the amplitude of whole cell K_V7 currents, effects reversible by washout or blocked by XE991. Further, retigabine hyperpolarized the DSM resting membrane potential, while XE991 caused DSM membrane depolarization. This study reveals novel aspects of K_V7 channel function and molecular composition in human DSM cells and tissues, strongly supporting their potential therapeutic utility for treatment of lower urinary tract dysfunction.

INTRODUCTION

DSM contraction and relaxation underlies the two main functions of the urinary bladder: the storage and release of urine. The excitability of DSM is critically regulated by the activity of ion channels, including voltage-gated K_V7 channels ($K_V7.1$-$K_V7.5$) [4]. K_V7 channels have a prominent role in regulating the DSM resting membrane potential.

In contrast to other K^+ channels, such as the large-conductance voltage- and Ca^{2+}-activated K^+ channels, K_V7 channels do not have a significant role in the repolarization phase of action potentials [47, 57]. As the K_V7 channels activate at membrane voltages near -60 mV, below the threshold for L-type voltage-gated Ca^{2+} channel activation, these channels are critically involved in establishing the resting membrane potential [4, 62].

K_V7 channels attain vast heterogeneity as their five pore-forming α-subunits form distinct homo- or hetero-tetrameric complexes [14, 63]. Further, K_V7 channels associate with KCNE-encoded β-regulatory subunits (KCNE1-KCNE5), which may alter K_V7

channel biophysical properties including subcellular localization, pharmacology, and selectivity [14-16, 40, 64]. In neurons, K_V7 channel currents were initially characterized as "M-currents" [65], preceding the determination that $K_V7.2/K_V7.3$ channels were the molecular correlate of this current [66]. Also, early studies in the heart revealed the key role of the $K_V7.1$/KCNE1 channels in the cardiac delayed rectifier K^+ (I_{Ks}) current [46]. Nonetheless, based on the emergence of commercially available K_V7 channel pharmacological modulators, physiological roles for K_V7 channels in other tissues, including smooth muscle, is becoming apparent [14, 21, 40, 64, 67-69].

In DSM, K_V7 channel functional roles, including in studies from our laboratory [7, 42], have recently been identified in the guinea pig [7, 8, 42], pig [28]; and rat (Rode, 2010, 20385123), where the K_V7 channel activator retigabine was shown to have pronounced effects in reducing DSM contractility [34]. This may elude to the increased micturition volume and voiding intervals observed in rats subjected to acute retigabine exposure *in vivo* [26, 28, 34]. More relevant, clinical evidence has proven retigabine to be associated with the increased occurrence of urinary retention [70]. As the mechanism of action of retigabine is via the activation of K_V7 channels, its collateral side effect of urinary retention is a significant observation that should be explored scientifically and in the context of overall urinary bladder function and OAB medicinal treatment.

As important functional roles for K_V7 channels in DSM function has been established in experimental animals, it is of key interest to ascertain the translation implications of these findings to humans. Indeed, the clinical effects of retigabine on urinary bladder function are noteworthy, albeit evidence of K_V7 channel expression and

function in human DSM remains largely unexplored as documented by two similar tissue-level studies in human DSM [9, 44].

In this study, we used RT-PCR, qPCR, Western blot, immunocytochemistry, and *in situ* proximity ligation assays (PLA) to determine the mRNA and protein expression of K_V7 channels and the identify of which K_V7 channel α-subunits assemble to form functional tetramers. Further, we conducted ratiometric fluorescence Ca^{2+} imaging, isometric DSM tension recordings, and perforated patch-clamp electrophysiology in combination with K_V7 channel pharmacological modulators to elucidate their physiological role in regulating human DSM excitability and contractility. This study provides the first molecular, cellular, and tissue-based examination of K_V7 channel expression and function in human DSM, where these channels serve a key role in overall urinary bladder function.

MATERIALS AND METHODS

Ethical Approval. All procedures involving the acquisition of human DSM tissues for the current studies have been reviewed and approved by the Institutional Review Board of the Medical University of South Carolina (protocol number Pro00045232).

DSM cell isolation and collection. Human DSM single cells were freshly isolated using a combination of papain and collagenase as previously described [32]. Human DSM cells were used for electrophysiological experiments, PCR, or *in situ* PLA within 12 h after isolation. Intact human DSM strips with urothelium removed were used for single cell isolation, isometric DSM tension recordings, and ratiometric fluorescence Ca^{2+} imaging.

RT-PCR

RT-PCR experiments were conducted on freshly-isolated human DSM tissues and cells as previously described [32].

Western blot and Immunocytochemistry

Western blot and immunocytochemical experiments on human DSM tissues and freshly-isolated cells, respectively, were conducted as previously described [32].

***In situ* Proximity Ligation Assay.** *In Situ* PLA was performed on freshly-isolated human DSM cells using the Duolink *In Situ* Proximity Ligation Assay kit (Thermo Fisher Scientific, Waltham, MA, USA) according to the manufacturer's instructions. DSM cells underwent fixation in 2% paraformaldehyde (10 min, 37°C) followed by two 15-min washes in PBS. DSM cells were then blocked in Duolink blocking solution (30 min, 37°C). Subsequently, isolated DSM cells were incubated with anti-rabbit K_V7.#/anti-goat K_V7.# antibodies or anti-goat K_V7.#/anti-rabbit K_V7.# antibodies, respectively, in Duolink antibody diluent solution overnight at 4°C, followed by 2 x 5 min washes in Duolink 1x Wash Buffer A solution. DSM cells were then incubated with the Duolink PLA probe anti-rabbit MINUS and anti-goat PLUS oligonucleotide-conjugated secondary antibodies (1 h, 37°C), followed by 2 x 5 min washes in Duolink 1x wash buffer A solution. DSM cells were then incubated in ligase-ligation solution (30 min, 37°C), which hybridizes the two PLA MINUS and PLUS probes when in close proximity (<40 nm). Following ligation, DSM cells were washed 2 x 2 min in Duolink 1x wash buffer A solution. Finally, DSM cells were incubated in amplification-polymerase solution (100 min, 37°C) containing nucleotides and fluorescently-labelled oligonucleotides. The oligonucleotide arm of one PLA probe is a primer for rolling-circle amplification. The fluorescently-labeled

oligonucleotides hybridize to the rolling-circle amplification product thus permitting detection. Following amplification, DSM cells were washed 2 x 10 min in 1x wash buffer B and then a 1 min wash in 0.01x wash buffer B. Slides were then mounted using minimal volume of Duolink *In Situ* mounting medium with 4',6-Diamidino-2-Phenylindole, Dihydrochloride (DAPI). PLA signals (Duolink *In Situ* Detection Reagents Orange ($\lambda_{excitation/emission}$= 554/576 nm)) were detected using a laser scanning LSM 700 confocal microscope (Carl Zeiss, Germany) with a 63x oil immersion objective.

Isometric DSM tension recordings. Isometric DSM tension recordings were conducted as previously described on isolated DSM strips void of urothelium [51]. For experiments on spontaneous phasic contractions, the isolated DSM isolated strips were pretreated tetrodotoxin (TTX, 1 µM), a neuronal voltage-gated Na^+ channel blocker, before the application of K_V7 channel pharmacological modulators. Electric field stimulation (EFS)-induced DSM contractions were stimulated with a PHM-152I programmable stimulator (Med Associates, Inc., Georgia, VT, USA) in the absence of TTX. 0.5-50 Hz EFS-induced contractions were stimulated at 3 min intervals over a wide range of frequencies (0.5, 2.0, 3.5, 5, 7.5, 10, 12.5, 15, 20, 30, 40, 50 Hz) in the absence (control) and then in the presence of either retigabine (10 µM) or XE991 (10 µM).

Ratiometric Fluorescence Ca^{2+} imaging. Global intracellular Ca^{2+} concentrations of isolated human DSM strips were measured using the ratiometric fluorescence Ca^{2+} probe fura-2 AM as previously described [32].

Solutions and drugs. Ca^{2+}-free dissection solution contained the following (in mM): 80 monosodium glutamate; 55 NaCl; 6 KCl; 10 glucose; 10 4-(2-hydroxyethyl) piperazine-1-ethanesulfonic acid (HEPES); 2 $MgCl_2$; NaOH was used to attain pH 7.3. Ca^{2+}-containing

physiological saline solution contained the following (in mM): 119 NaCl; 4.7 KCl; 24 $NaHCO_3$; 1.2 KH_2PO_4; 2.5 $CaCl_2$; 1.2 $MgSO_4$; 11 glucose; that was aerated with 95% O_2/5% CO_2 to attain pH 7.4. Physiological bath solution utilized for patch-clamp experiments was composed of the following (in mM): 134 NaCl; 6 KCl; 1 $MgCl_2$; 2 $CaCl_2$; 10 glucose; 10 HEPES; and NaOH was used to obtain pH 7.4. The patch-pipette solution contained (in mM): 110 potassium aspartate; 30 KCl; 10 NaCl; 1 $MgCl_2$; 10 HEPES; 0.05 ethylene glycol-bis(2-aminoethylether)-N,N,N',N'-tetraacetic acid (EGTA); NaOH was used to adjust the pH to 7.2. Amphotericin-B stock solution was prepared daily in dimethyl sulfoxide (DMSO) and was included in the pipette solution (200-300 μg/ml) before the experiment and was replaced every 1-2 h. ML213, TTX citrate, and XE991 were purchased from Tocris Bioscience (Minneapolis, MN). Fura-2 AM was purchased from Life Technologies (Cat No.: F1221, Carlsbad, CA). ML213 and Fura-2 AM were dissolved in DMSO, while XE991 and TTX citrate were dissolved in double-distilled water. All other chemicals were obtained from Fisher Scientific (Waltham, MA), Sigma-Aldrich, or Worthington Biochemical Corp. (Lakewood, NJ).

RESULTS

K_V7 channel subtypes are expressed at the mRNA level in freshly-isolated human DSM cells and tissues. To elucidate K_V7 channel mRNA expression in human DSM, we began by conducting conventional RT-PCR using human DSM tissues. At the tissue-level in human DSM, we detected mRNA transcripts for all K_V7 channel subtypes except K_V7.2 (**Figure 5.1**). K_V7 channels are known to be expressed in non-DSM tissues including neurons and instersitial cells. Therefore, we sought to clarify K_V7 channel mRNA expression by conducting parallel RT-PCR experiments using RNA isolated specifically

from human DSM single cells. At the cellular level in DSM, we identified transcripts for $K_V7.4$ and $K_V7.5$ subunits.

K_V7 channel subtypes are expressed at the protein-level in human DSM tissues and freshly-isolated cells. To confirm K_V7 channel protein expression in human DSM tissues and freshly-isolated cells, we utilized Western blot analysis and immunocytochemistry with confocal microscopy. As shown in **Figure 5.2**, Western blot data identified protein expression for all K_V7 channel subtypes except $K_V7.2$ in human DSM tissue. Chemiluminescent bands were not observed when $K_V7.1$ and $K_V7.3$-$K_V7.5$ channel antibodies were incubated in the presence of their competing peptides (+CP), respectively. Again, as K_V7 channels are expressed in non-DSM tissues within the detrusor layer, we sought to confirm K_V7 channel protein expression directly in freshly-isolated DSM cells using immunocytochemistry with confocal microscopy (**Figure 5.3**).

$K_V7.4$ and $K_V7.5$ channel α-subunits associate to form heterotetrameric $K_V7.4$/$K_V7.5$ channel subtypes in freshly-isolated DSM cells. K_V7 channel subunits ($K_V7.1$-$K_V7.5$) differentially associate to form functional tetrameric channels with distinct biophysical properties [14]. Using *in situ* PLA, we sought to determine whether $K_V7.4$ and $K_V7.5$ channels, the K_V7 channel subtypes expressed in isolated DSM cells (Figure 1), form heteromeric channels in freshly-isolated DSM cells. *In situ* PLA demonstrated $K_V7.4$ and $K_V7.5$ channel subunits associate to form heteromeric $K_V7.4$/$K_V7.5$ channels in isolated human DSM cells. As shown in **Figure 5.4**, *in situ* PLA experiments demonstrated the co-localization of $K_V7.4$ and $K_V7.5$, channel α-subunits within 40 nm and within the vicinity of the DSM cell membrane. Primary antibodies against the IP_3R, which would not be expected to co-localize with members of the K_V7 channel family, were used as a negative

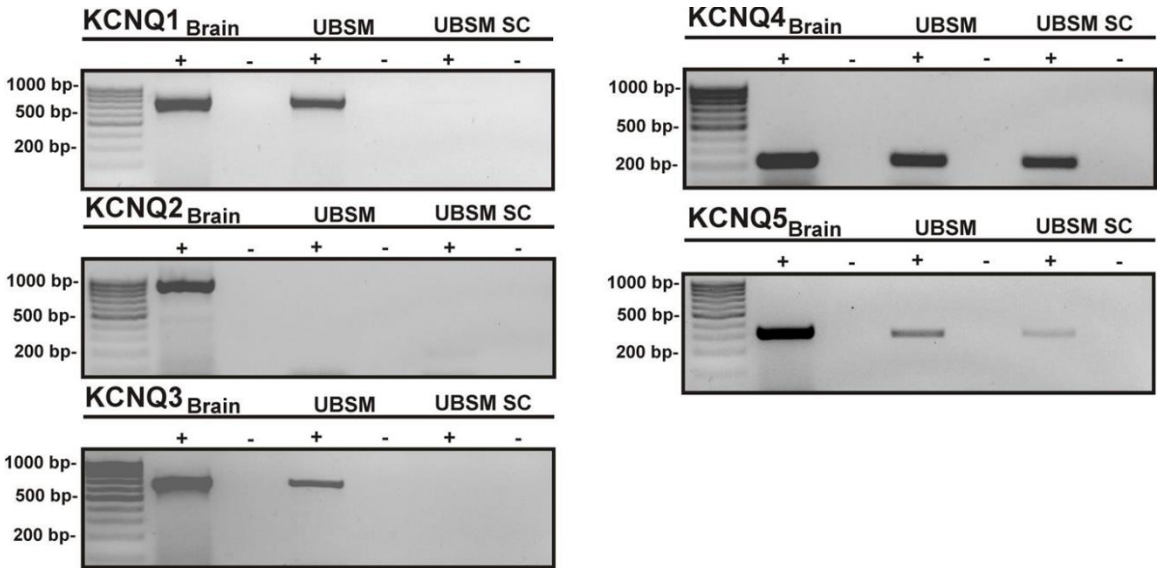

Figure 5.1. K_V7 channels mRNA transcripts are present in freshly-isolated human DSM cells and tissues. K_V7 channel subtype mRNA detection in human DSM whole tissues and freshly-isolated single cells. RT-PCR experiments detected mRNA for all K_V7 channel subtypes except $K_V7.2$ in whole human DSM tissues. Further experiments using freshly-isolated human DSM single cells revealed $K_V7.4$ and $K_V7.5$ channels are the only subtypes present at the mRNA level in human DSM. No bands were observed in the absence of reverse transcriptase (-RT). Results were confirmed in experiments from at least three DSM tissues isolated from 3 different patients.

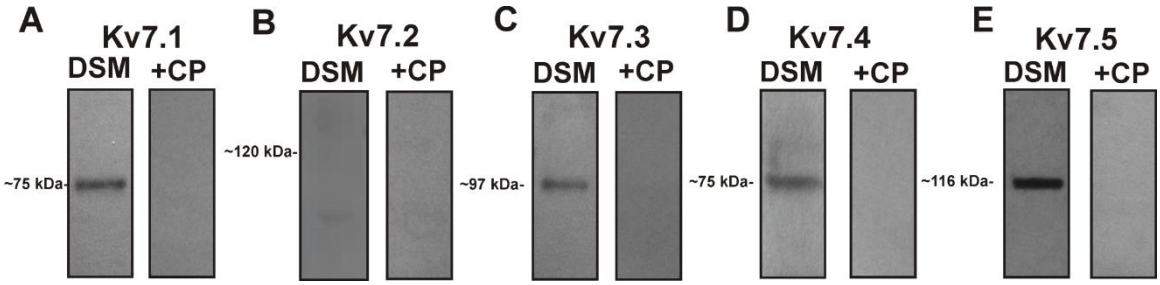

Figure 5.2. Western blot analyses demonstrated protein expression for $K_V7.1$ and $K_V7.4$-$K_V7.5$ channel subtypes in human DSM. Western blot experiments demonstrate protein expression for $K_V7.1$-5 channel subtypes in human DSM. **A)** $K_V7.1$, **B)** no $K_V7.2$, **C)** $K_V7.3$, **D)** $K_V7.4$ and **E)** $K_V7.5$ channel subtypes were detected using K_V7 channel subtype-specific antibodies. Incubation of the K_V7 channel primary antibodies with each respective competing peptide (+CP) eliminated protein detection thereby confirming antibody selectivity. These results were verified in at least three human DSM tissues isolated from 3 different patients.

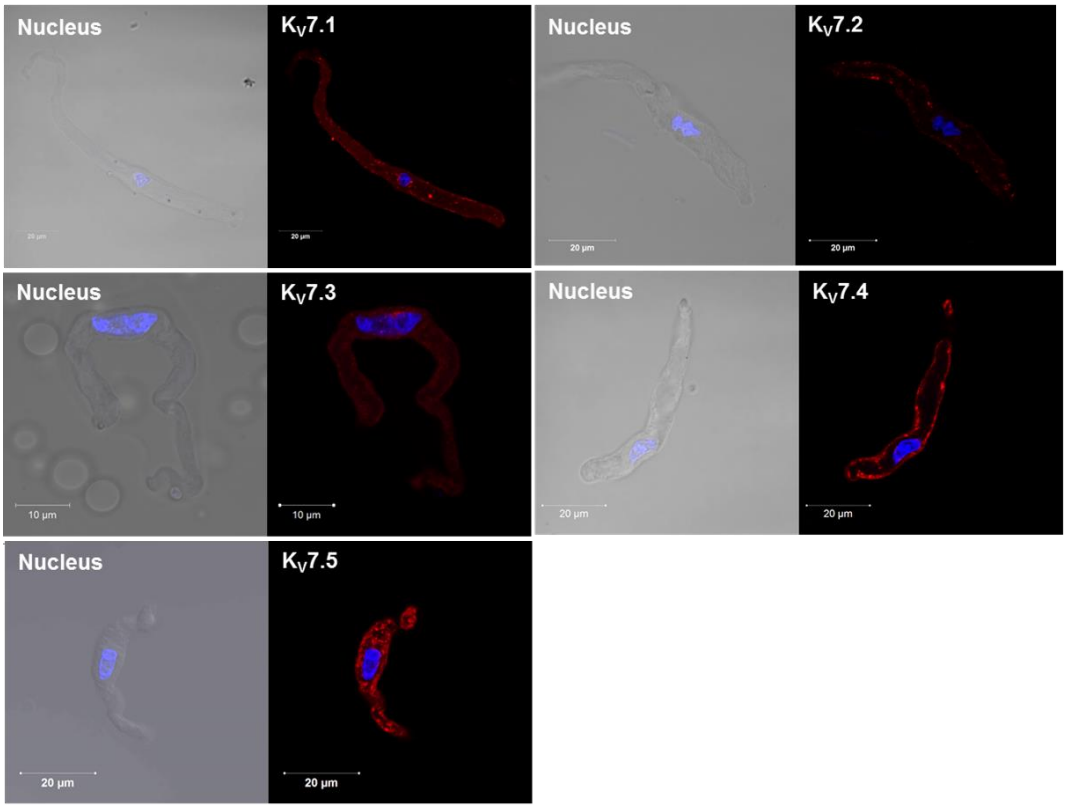

Figure 5.3. K_V7.1 and K_V7.4-K_V7.5 channel subtypes are expressed at the protein level in freshly-isolated human DSM cells. Confocal images from immunocytochemical experiments demonstrate the expression K_V7.1- K_V7.5 (**A-E**) channel subunits in freshly-isolated human DSM cells. Red staining indicates detection of K_V7.1- K_V7.5 channel subunits, respectively. Blue staining indicates the nucleus. The anti-actin, α-smooth muscle probe is shown in green (top right). The overlaid images for K_V7.1- K_V7.5 channels with anti-actin, α-smooth muscle probe and DAPI nuclear stain is shown at the bottom right, respectively. Co-localization of each K_V7channel subtypes with the anti-actin, α-smooth muscle is indicated by the yellow color in the merged images, respectively. Data were confirmed in multiple experiments using DSM tissues from at least 3 guinea pigs. Images were acquired with a Zeiss LSM 700 confocal microscope using a 63X oil objective. control. Co-incubation of the K_V7.4 channel primary antibody with the primary antibody of the IP_3Rs yielded no PLA fluorescent signal (**Fig. 5.4)**. These combined results suggest that K_V7.4 and K_V7.5 channel subunits assemble to form heteromeric K_V7.4/K_V7.5 channel subtypes in DSM cells.

K_V7 channels regulate spontaneous phasic contractions in human DSM isolated strips. To elucidate whether K_V7 channel pharmacological modulation of the K_V7 channels corresponds to functional changes in human DSM contractility, we conducted isometric tension recordings on human DSM isolated strips. As demonstrated by **Fig. 5.5**, K_V7

channel pharmacological activation with retigabine (10 μM) decreased spontaneous phasic contractions in human DSM isolated strips from control (non-OAB) and OAB patients (**n=9, N=5** for Control non-OAB, **Fig. 5.5**; **n=5, N=5** for OAB, **Fig. 5.5**; *P<0.05). There was no statistically significant difference in the inhibitory effects of retigabine on spontaneous phasic contraction parameters in control versus OAB patients. The K_V7 channel inhibitor XE991 (10 uM) increased spontaneous phasic contractions of DSM isolated strips (**n=12, N=7**; *P<0.05; **Figure 5.6, A-B**). In the presence of XE991 (10 uM), retigabine had no significant inhibitory effects on spontaneous phasic contractions (**n=5, N=4**; *P<0.05; **Figure 5.6, C-D**), confirming the selectivity of retigabine for the K_V7 channel subtypes. There was a statistically significant difference between the inhibitory effects of retigabine in the absence versus presence of XE991, confirming the selectivity of retigabine for K_V7 channel subtypes.

K_V7 channels regulate nerve-evoked contractions in human DSM isolated strips. We next aimed to elucidate the role of the K_V7 channels in regulating nerve-evoked contractions in human DSM isolated strips using electrical field stimulation (EFS) contractions induced over a range of EFS frequencies (0.5-50 Hz) in combination with K_V7 channel pharmacological modulators. Retigabine (10 μM) caused a significant decrease in the amplitude of 0.5-50 Hz EFS-induced contractions (n=7, N=4; P<0.05; **Figure 5.7, D-E**). K_V7 channel inhibition with XE991 decreased 0.5-50 Hz EFS-induced contractions (n=6, N=5; P<0.05; **Figure 5.7, A-B**). These results poise the K_V7 channels as important regulators of nerve-evoked contractions in human DSM isolated strips.

OVERALL CONCLUSIONS

This study examined the expression and physiological roles of voltage-gated K_V7 channels in human DSM excitability and contractility. PCR experiments detected mRNA transcripts for $K_V7.1$ and $K_V7.3$-$K_V7.5$ channel subtypes in DSM tissue, with only $K_V7.4$-$K_V7.5$ channel subtypes at the cellular level in human DSM. Western blot analysis confirmed $K_V7.1$ and $K_V7.3$-$K_V7.5$ channel protein expression in human DSM tissues. However, immunocytochemistry revealed only $K_V7.4$ and $K_V7.5$ channel subtype protein expression was present in freshly-isolated human DSM cells. Further, using *in situ* PLA, we confirmed the molecular interaction between $K_V7.4$ and $K_V7.5$ channel α-subunits, suggesting heteromeric $K_V7.4/K_V7.5$ channel subtype expression at the cellular level in human DSM cells. Retigabine decreased spontaneous and nerve-evoked contractions, decreased global Ca^{2+} concentrations, hyperpolarized the DSM cell membrane potential, and enhanced whole cell K_V7 currents in DSM cells. XE991 increased spontaneous and nerve-evoked DSM contractions, increased global Ca^{2+} concentrations, depolarized the DSM cell membrane potential, and blocked retigabine-induced inhibition of DSM contractions.

K_V7 channel expression and functional roles have been emerging in recent years in reports on experimental animals. However, studies of K_V7 channel expression and function in human DSM are currently lacking and represented by only two superficial and tissue-level studies in human DSM [9, 44]. One of these studies reported the detection of mRNA transcripts for all K_V7 channel subtypes except $K_V7.2$ at the tissue level in human DSM [9]. Consistently, a second report in human DSM utilizing qPCR reported K_V7 channel subtype expression in rank order: $K_V7.4>K_V7.5>K_V7.3>K_V7.1$, with minimal or no detection of $K_V7.2$ channel subtypes [44].

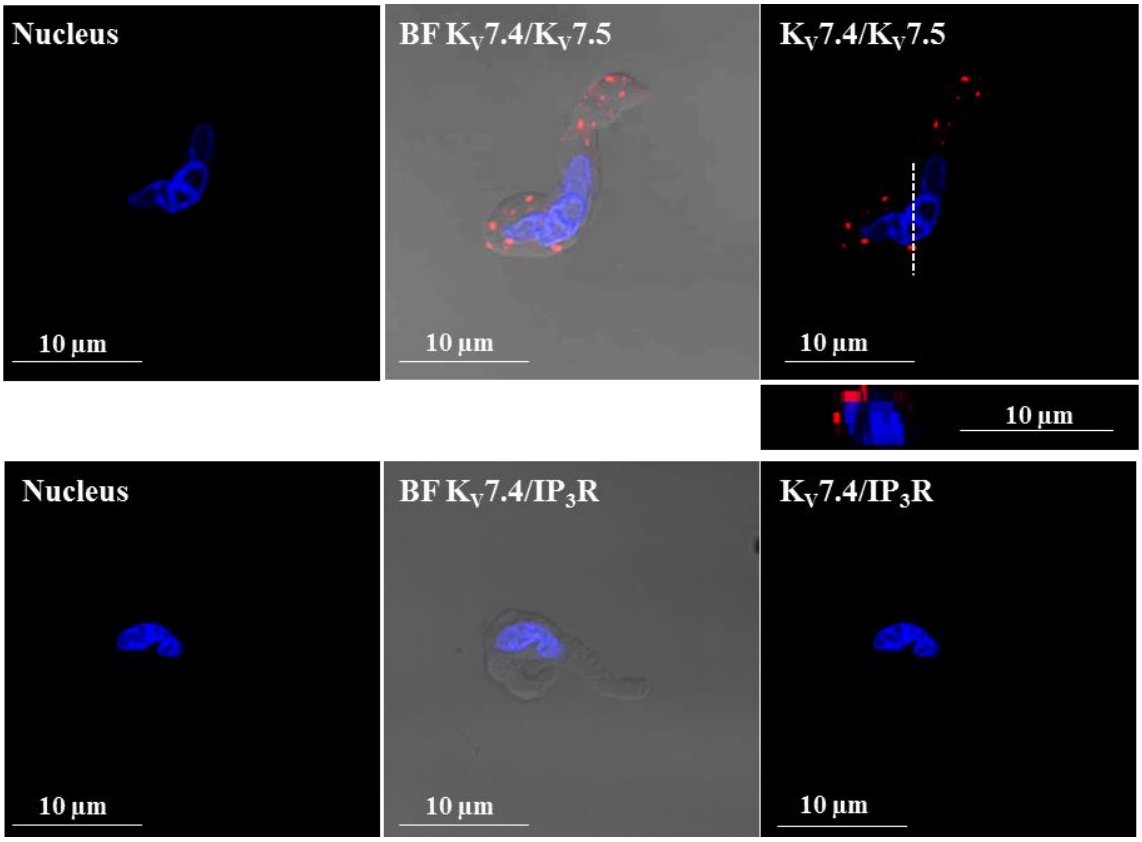

Figure 5.4. *In situ* PLA detection of K_V7.4/K_V7.5 heteromeric channels expressed in isolated guinea pig DSM cells. Images of a freshly-isolated DSM cell stained with the combination of anti-K_V7.4 and anti-K_V7.5 channel antibodies (*upper panels*). PLA fluorescent signals are shown in red. No PLA fluorescent signals were observed when the anti-K_V7.4 antibody was co-incubated with the anti-IP_3R antibody (*lower panels*). An orthogonal cross-section image of the DSM cell displaying PLA signals was obtained following z-stack scans collected along the viewing plane indicated by the dashed (- - -) lines and is represented directly below the top right panel. BF, bright field; DAPI, 4′,6-Diamidine-2′-phenylindole dihydrochloride (nuclear staining shown in *blue*).

Protein expression for K_V7.1, K_V7.4, and K_V7.5 channel subtypes was further reported using Western blot analysis [44]. However, these experiments by Bientinesi *et al.*, which excluded K_V7.3 channel subtypes, did not include appropriate positive or negative controls [44], which raise questions as to the validity of the data. Minimal or no expression of K_V7.2 channel mRNA has also been reported in several non-DSM tissue types across multiple species including the murine and rat airway [20, 71], rat mesenteric arteries [72], human airway smooth muscle [17], and in human arteries [22].

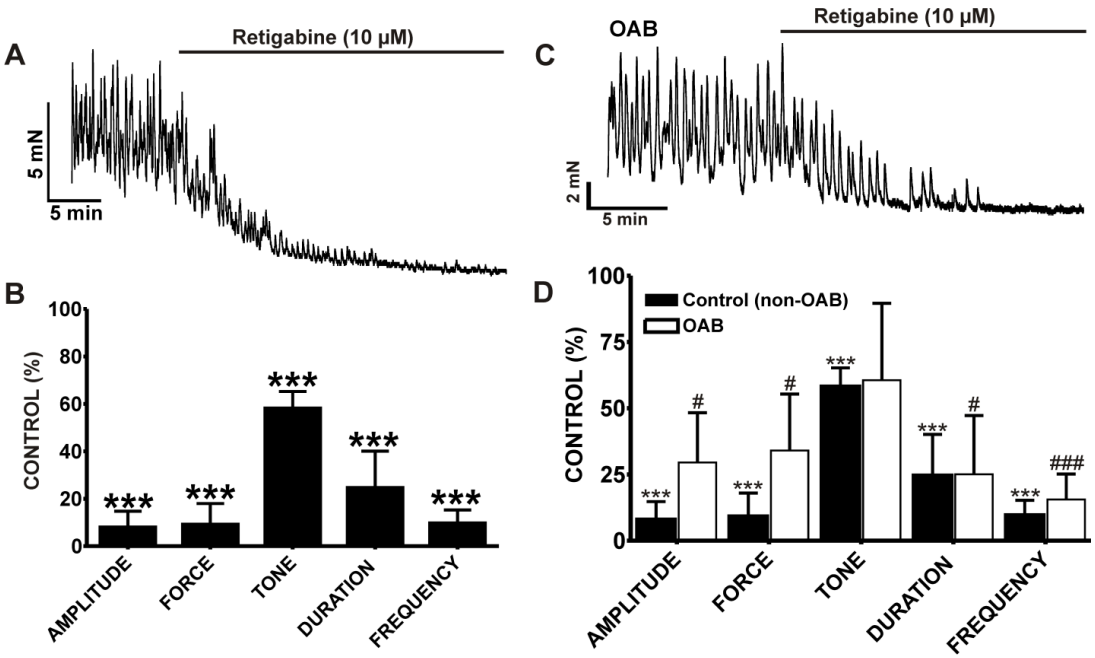

Figure 5.5. Retigabine, a Kv7.2-Kv7.5 channel subtype activator inhibited spontaneous phasic contractions in human DSM control and OAB patients. Retigabine, a K_V7.2- K_V7.5 channel subtype activator, inhibited spontaneous phasic contractions in human DSM. **A)** An original isometric DSM tension recording demonstrating the inhibition of spontaneous phasic contractions by retigabine (10 µM). **B)** Summarized data for the inhibitory effects of retigabine (10 µM) on human DSM contraction parameters including contraction amplitude, muscle force, tone, contraction duration, and frequency (n=9, N=5; ***P<0.001 for each). **C)** An original isometric DSM tension recording demonstrating the inhibition of spontaneous phasic contractions by retigabine (10 µM) in an OAB patient. **D)** Summarized data for the inhibitory effects of retigabine (10 µM) on human DSM contraction parameters in control versus OAB patients (n=3, N=3).

Interestingly, the expression of K_V7.4 and K_V7.5 channel subtype is consistent with emerging reports of K_V7 channel expression in smooth muscle tissues [22, 40, 73]. Nonetheless, conflicting reports exist in the literature concerning which K_V7 channel subtype (i.e. K_V7.4 or K_V7.5) is most highly expressed in human DSM. The most recent of these two reports indicated K_V7.4 channels were most highly expressed, while a separate group demonstrated K_V7.5 channel mRNA as the most highly expressed K_V7 channel subtype in human DSM [61, 74].While K_V7 channel mRNA expression has been emerging, whether corresponding protein expression occurs has not been fully explored.

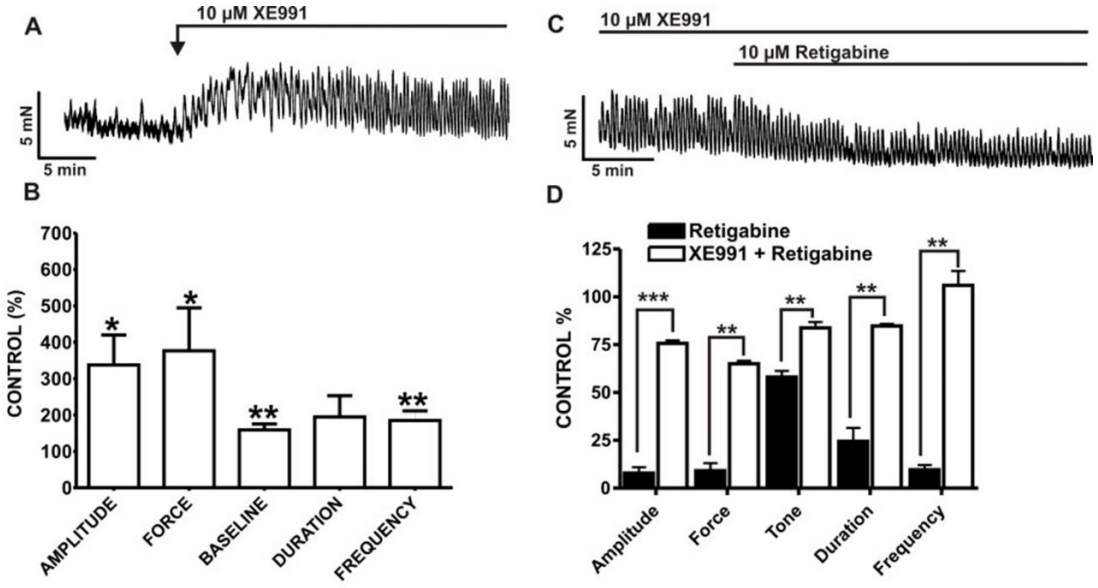

Figure 5.6. XE991, a K_V7.1-K_V7.5 channel subtype inhibitor increased spontaneous phasic contractions and blocked retigabine-induced relaxation in human DSM isolated strips. XE991, a K_V7.1-K_V7.5 channel subtype inhibitor increased spontaneous phasic contractions in human DSM. **A)** An original isometric DSM tension recording demonstrating the augmented spontaneous phasic contractions induced by XE991 (10 µM). **B)** Summarized data for the stimulatory effects of XE991 (10 µM) on human DSM contraction parameters including contraction amplitude, muscle force, tone, contraction duration, and frequency (n=12, N=7; *P<0.05 and **P<0.01). **C)** An original isometric tension recording demonstrating the effect of retigabine (10 µM) upon human DSM spontaneous phasic contractions subject to pretreatment with XE991 (10 µM). **D)** Summarized data comparing the effects of retigabine (10 µM) in the absence or presence of XE991 (10 µM) upon human DSM contraction parameters including contraction amplitude, muscle force, tone, contraction duration, and frequency (n=5-9, N=4-5; **P<0.01 and ***P<0.001).

Our current data reveals the expression of K_V7.4 and K_V7.5 channel subtypes at the mRNA and protein levels (**Figure 5.1-5.4**). This could be very significant as this demonstrates the potential pharmacological efficacy of future selective K_V7.4/K_V7.5 channel activators as effective treatments for OAB, while K_V7.2/K_V7.3 selective modulators may prove better for the treatment of neurological conditions. Thus, this may abolish the large number of adverse effects associated with current OAB treatments and

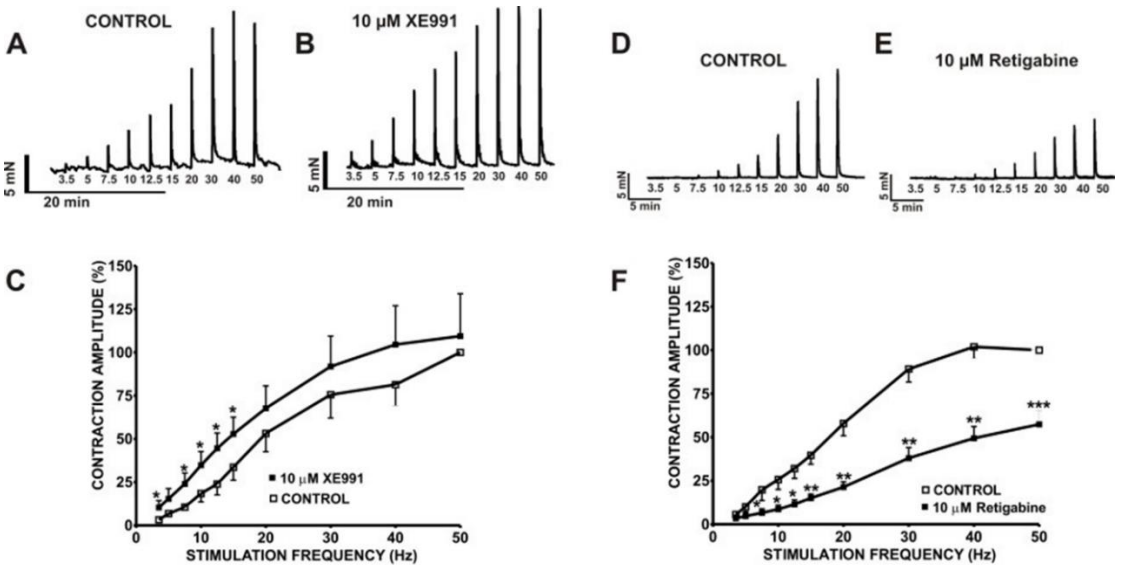

Figure 5.7. Retigabine and XE991 attenuated EFS-induced contractions in human DSM. Original isometric tension recording illustrating 3.5-50 Hz EFS-induced contractions before **(A)** and after **(B)** the addition of retigabine (10 µM). **C)** Frequency-response curves illustrating the inhibitory effects of retigabine on the amplitude of 3.5-50 Hz EFS-induced contractions (n=7, N=4; *P<0.05, **P<0.01, ***P<0.001). **D)** Original isometric tension recording illustrating 3.5-50 Hz EFS-induced contractions before and after **(E)** the addition of XE991 (10 µM). **F)** Frequency-response curves illustrating the inhibitory effects of retigabine on the amplitude of 3.5-50 Hz EFS-induced contractions (n=7, N=4; *P<0.05, **P<0.01, ***P<0.001).

Table 5.1 Human KCNQ Primer Sequences for PCR

Table 5.1 Human KCNQ Primer Sequences for PCR	
KCNQ1 (180 bp)	F: 5'-CTGTCTTTGCCATCTCCTTCT-3'
	R: 5'-GCGTCACCTTGTCTTCTACTC-3'
KCNQ2 (190 bp)	F: 5'-GGCTTCCTTTGTCTCATCCT-3'
	R: 5'-CTGGACTGCAGGCTCTTAAT-3'
KCNQ3 (195 bp)	F: 5'-TCGGGTTCGCCTTTCTAATC -3'
	R: 5'-GTGCCCTTGGTTGGGTAATA-3'
KCNQ4 (201 bp)	F: 5'-CCACCCTGTCCCTATTCTTTG-3'
	R: 5'-GAAGCACTGTCTGGGAGTTT-3'
KCNQ5 (173 bp)	F: 5'-GCACTCCTTGGCATTTCTTTC-3'
	R: 5'-GAGGCTTGTCGGCTCTTAAT-3'

therefore the beneficial implications of this research is incredibly relevant to public health, clinical medicine, and most importantly, quality of life. Based on our data from *in situ* PLA, we provide compelling evidence to confirm the expression of heteromeric K_V7.4/K_V7.5 channel subtypes in human DSM cells (**Fig. 12**). Therefore, heteromeric K_V7.4/KV7.5 channel subtypes may be among the key K_V7 channel subtypes involved in the regulation of DSM function. Although, homomeric K_V7.4 and/or K_V7.5 channel subtypes may also be important for DSM function. Our novel findings concerning the cellular and tissue-level expression of the K_V7 channel, in conjunction with our functional studies of DSM excitability and contractility, our data suggests key physiological roles for the K_V7 channels in human DSM function, with K_V7.4 and K_V7.5-containing channels, including heteromeric K_V7.4/K_V7.5 channels, as potentially the upmost of physiological relevance.

Nonetheless, taken together with our previous studies in the guinea pig (Chapters 3-4), further studies in human DSM will be required using multiple K_V7 channel compound with improved selectivity to that of retigabine. Further, electrophysiological experiments will also prove helpful in human DSM in order to confirm K_V7 channel drug effects are indeed a result of direct modulation of K_V7 current activity. The ability to fine-tune K_V7 channel pharmacological modulators to exhibit improved selectivity between K_V7.4, K_V7.5, and K_V7.4/K_V7.5 channels, may represent a substantial breakthrough in the development of novel and efficacious therapeutic modalities for lower urinary tract dysfunction. These combined studies may help to provide a rationale for further studies in this area of research.

CHAPTER 6

[8]REGULATION OF TRANSIENT RECEPTOR POTENTIAL MELASTATIN 4 CHANNEL BY SARCOPLASMIC RETICULUM INOSITOL TRIPHOSPHATE RECEPTORS: ROLE IN HUMAN DETRUSOR SMOOTH MUSCLE FUNCTION

ABSTRACT

We recently reported key physiological roles for Ca^{2+}-activated transient receptor potential melastatin 4 (TRPM4) channels in detrusor smooth muscle (DSM). However, the Ca^{2+}-signaling mechanisms governing TRPM4 channel activity in human DSM cells are unexplored. As the TRPM4 channels are activated by Ca^{2+}, inositol 1,4,5-trisphosphate receptor (IP_3R)-mediated Ca^{2+} release from the sarcoplasmic reticulum represents a potential Ca^{2+} source for TRPM4 channel activation. We used clinically-characterized human DSM tissues to investigate the molecular and functional interactions of the IP_3Rs and TRPM4 channels. With *in situ* proximity ligation assay (PLA) and perforated patch-clamp electrophysiology, we tested the hypothesis that TRPM4 channels are tightly associated with the IP_3Rs and are activated by IP_3R-mediated Ca^{2+} release in human DSM. With *in situ* PLA, we demonstrated co-localization of the TRPM4 channels and IP_3Rs in human DSM cells. As the TRPM4 channels and IP_3Rs must be located within close apposition to functionally interact, these findings support the concept of a potential Ca^{2+}-mediated TRPM4-IP_3R regulatory mechanism. To investigate IP_3R regulation of TRPM4

[8]Provence, A., E.S. Rovner, and G.V. Petkov, *Regulation of transient receptor potential melastatin 4 channel by sarcoplasmic reticulum inositol trisphosphate receptors: Role in human detrusor smooth muscle function.* Channels (Austin), 2017. **11**(5): p. 459-466.
The following work is currently published in Channels (Austin) [75] and is being reprinted with permission.

channel activity, we sought to determine the consequences of IP_3R pharmacological inhibition on TRPM4 channel-mediated transient inward cation currents (TICCs). In freshly-isolated human DSM cells, blocking the IP_3Rs with the selective IP_3R inhibitor xestospongin-C significantly decreased TICCs. The data suggest that IP_3Rs have a key role in mediating the Ca^{2+}-dependent activation of TRPM4 channels in human DSM. The study provides novel insight into the molecular and cellular mechanisms regulating TRPM4 channels by revealing that TRPM4 channels and IP_3Rs are spatially and functionally coupled in human DSM.

INTRODUCTION

The functions of the urinary bladder – the principle organ charged with the storage and periodic release of urine – are mediated by the activity of detrusor smooth muscle (DSM). In DSM cells, it is well-established that Ca^{2+} influx through L-type voltage-gated Ca^{2+} channels underlies the depolarization phase of spontaneous action potentials whilst the large-conductance voltage- and Ca^{2+}-activated K^+ (BK) channels, in addition to other voltage-gated K_V channels, work in opposition to L-type voltage-gated Ca^{2+} channel activity to promote membrane hyperpolarization[4, 57, 76, 77]. Albeit these mechanisms have been known for many years in DSM, recent studies from our group have identified an important role for an additional Ca^{2+}-sensitive cationic conductance regulating DSM function in rodents and humans[33, 78-80]. Indeed, Ca^{2+}-activated monovalent cation channels known as the transient receptor potential (TRP) melastatin 4 (TRPM4) channels are functionally expressed in rat, guinea pig, and human DSM[33, 78-80].

Of the 28 members that constitute the TRP channel superfamily, TRPM4 channels, in addition to TRPM5, are the only TRP channel members selective for monovalent cations

(K^+ and Na^+)[81, 82]. TRPM4 channel functional roles in excitable cells and tissues, including rodent[33, 79, 80] and human DSM[33, 78-80], have begun to emerge in recent years following studies using the novel and selective TRMP4 channel inhibitor, 9-phenanthrol[33, 79, 80, 83-85]. We recently provided the first detailed study demonstrating the expression and key functional roles for TRPM4 channels in human DSM excitability and contractility using the selective TRPM4 channel inhibitor 9-phenanthrol[78]. Our novel study was the central topic of an editorial focus in the *American Journal of Physiology – Cell Physiology*[86], which highlighted the attractiveness of the TRPM4 channels as potential novel targets for the pharmacological control of the urinary bladder. Under pathophysiological conditions, DSM dysfunction is associated with some forms of overactive bladder[12]. The TRPM4 channels, in addition to the cellular mechanisms regulating their activity, represent an exciting and novel therapeutic approach to the treatment of various bladder disorders and the collateral effects these conditions inflict on patient quality of life. Nonetheless, significant work still remains to ascertain the cellular mechanisms regulating TRPM4 channel activity in human DSM function to further validate their potential therapeutic role for bladder disorders.

It has been suggested that Ca^{2+} release from the sarcoplasmic reticulum (SR) inositol 1,4,5-trisphosphate (IP_3) receptors (IP_3Rs) may constitute a primary Ca^{2+} source for TRPM4 channel activation[87]. The concept of IP_3R-mediated Ca^{2+} release serving as critically important Ca^{2+} source for TRPM4 channel activation, as opposed to Ca^{2+} influx through L-type voltage-gated Ca^{2+} channels, was supported by the observation that removal of extracellular Ca^{2+} had no acute effects on TRPM4 channel activity[87].

Whether this TRPM4-IP_3R regulatory mechanism exists in human DSM, however, is completely unknown.

Therefore, the current study sought to investigate the molecular and functional interaction of the TRPM4 channels and IP_3Rs in human DSM. This was achieved via a combined experimental approach using *in situ* proximity ligation assays (PLA) and perforated patch-clamp electrophysiology in combination with pharmacological tools. This study reveals the novel mechanism whereby SR IP_3Rs regulate the excitability of human DSM through molecular and functional interactions with TRPM4 channels.

MATERIALS AND METHODS

Human DSM tissue acquisition. Human DSM tissues were acquired from donor patients undergoing routine open bladder surgeries as previously described[78, 88, 89]. All procedures attendant upon the collection of human DSM tissues have been reviewed and approved by the Institutional Review Board of the Medical University of South Carolina (protocol number Pro00045232). 6 Caucasian patients (3 men and 3 women; average age 64.5±11.2 years) without preoperative histories of overactive bladder and American Urological Association symptom scores <8 were used for this study. Following surgeries, human DSM tissues were stored on ice in a container containing HEPES-buffered dissection solution (see *Solutions and Drugs*) for immediate transport to the laboratory for DSM cell isolation.

DSM cell isolation. Human DSM single cells were enzymatically isolated using a combination of papain and collagenase as previously described[78, 88, 89]. Freshly-isolated DSM cells were used for *in situ* PLA or electrophysiological experiments within 12 h following isolation.

***In situ* Proximity Ligation Assay (PLA).** *In situ* PLA was performed on freshly-isolated DSM cells using the Duolink® *in situ* orange starter kit goat/rabbit (Cat. No: DUO92106, Sigma-Aldrich, St. Louis, MO) according to the manufacturer's instructions. DSM cells underwent fixation in 2% paraformaldehyde (10 min, 37°C) followed by two 15-min washes in phosphate buffered saline. DSM cells were blocked in Duolink blocking solution (30 min, 37°C). Subsequently, DSM cells were incubated with the anti-rabbit IP_3R and goat anti-TRPM4 channel antibodies (Santa Cruz Biotechnology, Dallas, TX; catalog numbers SC-27540 TRPM4; SC-28614 IP_3R), respectively, in Duolink antibody diluent solution overnight at 4°C, followed by 2x5 min washes in Duolink 1x wash buffer A solution. DSM cells were then incubated with the Duolink PLA probe anti-rabbit MINUS and anti-goat PLUS oligonucleotide-conjugated secondary antibodies (1 h, 37°C), followed by 2x5 min washes in Duolink 1x wash buffer A solution. DSM cells then underwent incubation in ligase-ligation solution (30 min, 37°C), which hybridizes the two PLA MINUS and PLUS probes when in close proximity (<40 nm). Following ligation, DSM cells were washed 2x2-min in Duolink 1x wash buffer A solution. Finally, DSM cells were incubated in amplification-polymerase solution (100 min, 37°C) containing nucleotides and fluorescently-labelled oligonucleotides. The oligonucleotide arm of one PLA probe is a primer for rolling-circle amplification. The fluorescently-labeled oligonucleotides hybridize to the rolling-circle amplification product thus permitting detection. Following amplification, DSM cells were washed 2x10 min in 1x wash buffer B and then a 1 min wash in 0.01x wash buffer B. Slides were then mounted using minimal volume of Duolink *in situ* mounting medium with 4',6-diamidino-2-phenylindole (DAPI). PLA signals (Duolink *In Situ* Detection Reagents Orange ($\lambda_{excitation/emission}$=554/576 nm))

were detected using laser scanning LSM 700 confocal microscope (Carl Zeiss, Germany) with a 63x oil immersion objective.

Patch-clamp electrophysiology. The amphotericin B-perforated whole cell patch-clamp technique was used in all of the electrophysiological recordings as previously described[32, 33, 78, 80]. At the holding potential of -70 mV, the total open channel probability (NP_o) of TRPM4 channel-mediated transient inward cation currents (TICCs) before and after the addition of xestospongin-C was analyzed. A stable recording period of at least 5-10 min before and after the addition of xestospongin-C was utilized for analysis with pCLAMP version 10.2 software (Molecular Devices, Union City, CA).

Solutions and drugs. The Ca^{2+}-free dissection solution had the following composition (in mM): 80 monosodium glutamate, 55 NaCl, 6 KCl, 2 $MgCl_2$, 10 HEPES, and 10 glucose, adjusted to pH 7.3 with NaOH. The extracellular (bath) solution used in the patch-clamp experiments in the gap-free mode (both voltage- and current-clamp) contained (in mM): 134 NaCl, 6 KCl, 1 $MgCl_2$, 2 $CaCl_2$, 10 glucose, and 10 HEPES, pH adjusted to 7.4 with NaOH. The patch-clamp pipette solution for these experiments contained (in mM): 110 potassium aspartate, 30 KCl, 10 NaCl, 1 $MgCl_2$, 10 HEPES, and 0.05 EGTA, pH adjusted to 7.2 with NaOH and supplemented with freshly dissolved (every 1–2 h) 200 μg/ml amphotericin-B in dimethyl sulfoxide. Bovine serum albumin was obtained from Thermo Fisher Scientific (Fair Lawn, NJ). All other compounds were obtained from Sigma-Aldrich.

Data analysis and statistics. The TICCs were analyzed as open channel probability (NP_o) as previously described[78]. Data are summarized as means ± SEM for **n** (the number of

DSM cells) isolated from **N** (the number of patients). Data were compared using a paired Student's *t*-test. A P value <0.05 was considered statistically significant.

RESULTS

TRPM4 channels are colocalized with the IP_3Rs in human DSM cells. In order for the discrete Ca^{2+} release events from SR IP_3Rs to regulate TRPM4 channel activity in human DSM, the IP_3Rs and TRPM4 channels must be located within close apposition. To determine TRPM4 channel colocalization with IP_3Rs, we conducted Duolink *in situ* PLA on freshly-isolated human DSM cells. To elucidate TRPM4/IP_3R colocalization, human DSM cells were incubated with the anti-TRPM4 goat and anti-IP_3R rabbit antibodies, respectively. As shown in **Fig. 6.1A-B**, co-incubation of TRPM4 and IP_3R antibodies positively confirmed that TRPM4 channels and IP_3Rs are located in close proximity (<40 nm) to the cell membrane as indicated by the bright red fluorescence. Fluorescent detection was not observed when the anti-TRPM4 goat antibody was omitted (**Fig. 6.1C**). As a negative control, we utilized a rabbit antibody specific for the voltage-gated K_V7.5 channel subtype, which is expressed in human DSM[90, 91], but not expected to interact with TRPM4 channels. Incubation of human DSM cells with anti-TRPM4 and anti-K_V7.5 rabbit antibodies, respectively, resulted in no observable fluorescent signal (**Fig. 1**). Results were confirmed in at least three human DSM cells.

IP_3R pharmacological inhibition with xestospongin-C decreases transient inward cation current activity in human DSM cells. In non-DSM cells, TRPM4 channels have been shown to be regulated by Ca^{2+} release events originating from the SR IP_3Rs[92]. Therefore, SR IP_3R Ca^{2+} release activity may constitute a fundamentally important cellular mechanism regulating TRPM4 channel activity in human DSM. To ascertain whether SR

IP_3Rs potentially regulate TRPM4 channel activity in human DSM, we examined the physiological consequences of IP_3R pharmacological inhibition on TRPM4 channel-mediated TICCs. At the holding potential of -70 mV, where BK channel activity is negligible[80], pharmacological inhibition of the IP_3Rs with the selective inhibitor xestospongin-C (1 µM) significantly reduced TICC activity (NP_o) from 2.0±1.1 in control conditions to 1.3±1.0 in the presence of 1 µM xestospongin-C (n=6, N=4; $P<0.05$; **Fig. 6.2**). These results support the concept that Ca^{2+} release events from SR IP_3Rs are involved in the regulation of TRPM4 channel-mediated TICCs in human DSM cells (**Fig. 6.3**).

DISCUSSION

This study sought to determine whether IP_3Rs of the SR regulate TRPM4 channel activity in human DSM function. This was achieved by elucidating IP_3R-TRPM4 channel spatial and functional interactions in human DSM by utilizing *in situ* PLA and perforated patch-clamp electrophysiology in combination with the IP_3R inhibitor xestospongin-C. *In situ* PLA confirmed co-localization between IP_3Rs and TRPM4 channels in human DSM isolated cells. Further, IP_3R pharmacological inhibition with xestospongin-C led to the attenuation of TICCs. This study established the novel finding that TRPM4 channels and SR IP_3Rs are physically and functionally coupled in the regulation of human DSM excitability.

Several studies from our laboratory have revealed key roles for the TRPM4 channels in regulating the excitability and contractility of DSM in rodents[33, 79, 80]. More recently, we further explored the translational implications of our findings in rodents by investigating the physiological roles for the TRPM4 channels in clinically-characterized human DSM [78]. As summarized in a recent editorial article in the *American Journal of*

Physiology Cell Physiology[86], our group revealed critical roles for the TRPM4 channels in regulating DSM function. TRPM4 channel expression is abundant in human DSM and species-related differences in the functional roles of the TRPM4 channels have been reported between human and rodents[78]. This previous report by our group provided compelling evidence at the cellular level in human DSM demonstrating the TRPM4 channel inhibitor 9-phenanthrol had a substantially greater inhibitory effect on DSM cell excitability in human versus rodent DSM cells[78].

Utilizing the selective TRPM4 channel inhibitor 9-phenanthrol, we reported that the pharmacological inhibition of the TRPM4 channels hyperpolarized the membrane potential in human DSM cells and caused inhibition of spontaneous phasic, pharmacologically-induced, and nerve-evoked contractions in human DSM isolated strips[78]. Among the mechanisms underlying the inhibitory effects of 9-phenanthrol on human DSM excitability and contractility includes the attenuation of TICCs[33, 78-80]. TICCs are caused by Na^+ influx following Ca^{2+}-dependent TRPM4 channel activation which, under physiological conditions, functions to enhance DSM cell excitability[78, 93, 94]**.**

As TRPM4 channels are activated by Ca^{2+}, it was critically important to determine the specific Ca^{2+}-dependent molecular and cellular mechanisms involved in the regulation of TRPM4 channel activity. Albeit well-known, there are two key sources for the elevation of intracellular Ca^{2+} concentrations, including: 1) Ca^{2+} entry through L-type voltage-gated Ca^{2+} channels at the cell membrane, or 2) Ca^{2+} release events through SR ryanodine receptors or IP_3Rs[57, 94]. In particular, emerging evidence from non-DSM cell types have shown that members of the TRP channel family, including TRPM4, can be activated by

intracellular Ca^{2+} released from SR IP_3Rs. IP_3R-mediated activation of adjacent TRPM4 channels, as has been reported in non-DSM cell types[87, 95], would lead to depolarization of the cell membrane potential, activation of L-type voltage-gated Ca^{2+} channels, an increase in global intracellular Ca^{2+} concentrations, and thus the activation of DSM contractions. In fact, in cerebral artery myocytes, sustained TRPM4 channel activity was shown to be dependent on Ca^{2+} released from the SR IP_3Rs[96].

Given the critically important role for the TRPM4 channels in human DSM excitability and contractility, we sought to examine whether IP_3Rs and TRPM4 channels functionally interact to regulate human DSM function. Our results demonstrated that xestospongin-C, a selective IP_3R inhibitor, significantly decreased TICC activity in human DSM cells (**Fig. 6.2**). These results are consistent with IP_3R-dependent regulation of TRPM4 channels in human DSM by a similar mechanism as was suggested for cerebral artery myocytes. Ca^{2+} released from the SR IP_3Rs are localized and transient events as has been demonstrated in murine colonic myocytes and rabbit portal vein myocytes[84, 97]. Hence, localized Ca^{2+} release events for the SR IP_3Rs must be in close apposition to the plasmalemmal TRPM4 channels in order for IP_3R-TRPM4 channel functional coupling. Thus, to ascertain the potential co-localization for the TRPM4 channels and IP_3Rs, we utilized the Duolink *in situ* PLA technique in combination with TRPM4 channel and IP_3R-specific antibodies. As illustrated by **Fig. 6.1**, *in situ* PLA experiments demonstrated the co-localization of IP_3Rs and TRPM4 channels in freshly-isolated human DSM cells within the vicinity of the cell membrane. These results are in contrast to findings from arterial myocytes, where IP_3R co-localization was confirmed with TRPC3 channels, while no co-localization with either the TRPM4 or TRPC6 channels was found[98]. The existence of

IP_3R co-localization with TRPM4 channels in DSM, but not in arterial myocytes, may suggest TRPM4 channel-IP_3R spatial interactions follow, to an extent, a certain level of tissue-specific expression.

While our current data provide strong evidence to support the spatial and functional coupling of the IP_3Rs and TRPM4 channels in human DSM (**Fig. 6.3**), we cannot exclude potential involvement of alternative signaling pathways. IP_3 and Ca^{2+} are the two central modulators of SR IP_3R activity[99]. Indeed, IP_3R activity has been shown to be regulated by IP_3 generated downstream from the activation of $G_{q/11}$-coupled muscarinic receptor pathways involving phospholipase C hydrolysis of phosphatidylinositol bisphosphate (PIP_2)[99]. Further, more recent studies have shown Ca^{2+}-permeable TRPC6 channels are spatially and functionally coupled with the SR IP_3Rs in cerebral arterial myocytes[100]. Thus, TRPC6 activation of the IP_3Rs lead to Ca^{2+} release events from the SR IP_3Rs, which then activate adjacent TRPM4 channels at the cell membrane[100]. Also, in the vasculature, protein kinase C was shown to modulate vascular myogenic tone in a TRPM4 channel-dependent manner[101, 102]. Consistently, in a separate study on HEK cells expressing cloned TRPM4 channels, the sensitivity for TRPM4 channels to Ca^{2+}-dependent activation is enhanced by PKC phosphorylation[103]. Whether these potential TRPM4 channel regulatory mechanisms exist in human DSM is yet to be explored. However, as our data confirm IP_3R-TRPM4 channel functional coupling, this work represents a foundational study in the human urinary bladder and provides a solid platform for subsequent mechanistic studies in human DSM (**Fig. 6.3**).

The key functional role of the TRPM4 channels in promoting DSM excitability has provided an intriguing opportunity for potential therapeutic exploitation in the context of

overactive bladder syndrome. Specifically, pharmacological modulators of the TRPM4 channels or mechanisms controlling their activity may represent a promising novel approach for treatment of bladder dysfunction. Given the critical role of the TRPM4 channels in human DSM function and dysfunction, further efforts to ascertain TRPM4 channel regulatory mechanisms are critical for confirming and validating their potential therapeutic utility. The current study has provided novel mechanistic insight into TRPM4 channel regulation by SR IP_3Rs in human DSM. As current treatments for overactive bladder lack efficacy, research efforts to identify novel therapeutic modalities are urgently needed and examining TRPM4 channel physiologic roles and mechanisms of regulation is of scientific and clinical relevance.

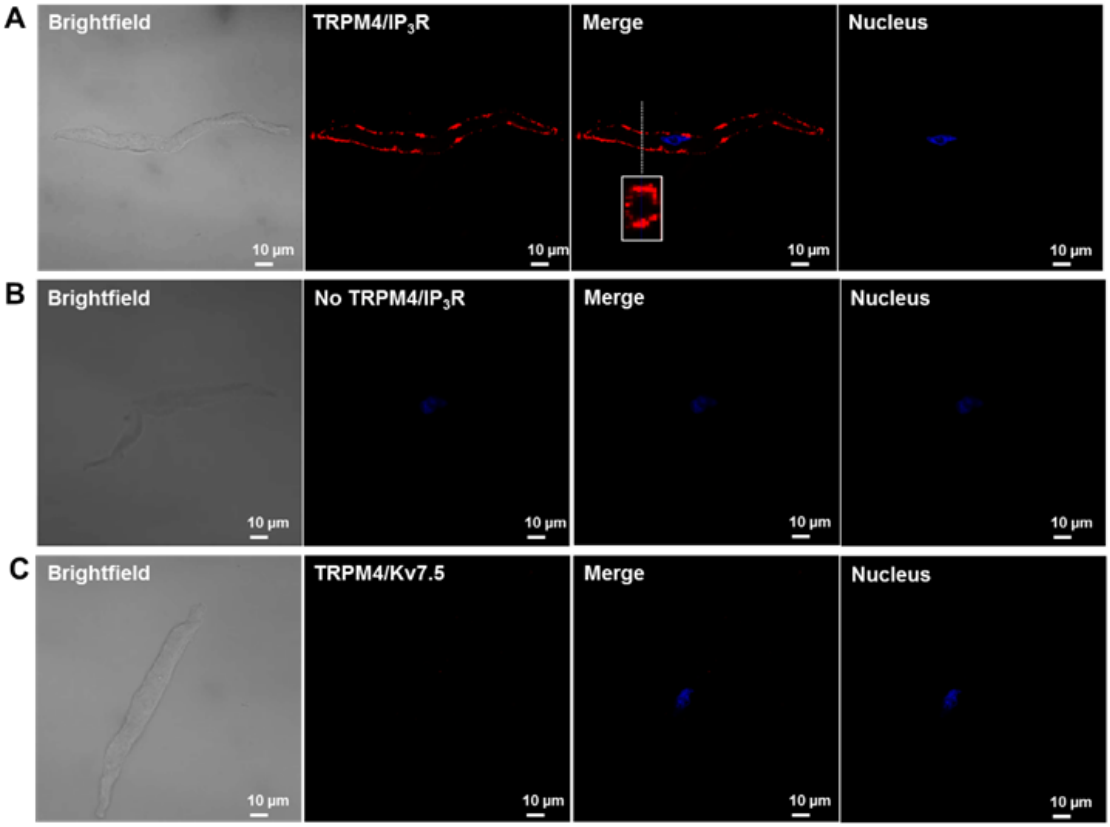

Figure 6.1. TRPM4 channels are colocalized with the IP_3R of the sarcoplasmic reticulum in freshly-isolated human DSM cells. A) Representative image of a human DSM cell stained with the anti-TRPM4 goat polyclonal antibody and anti-IP_3R rabbit polyclonal antibody. As demonstrated in the *merge* panel in **A**, the orthogonal cross-section image of the human DSM cell is shown in the rectangular box and represents the cross-sectional plane as indicated by the white dashed line. **B**) Representative image of a human DSM cells stained with only the anti-IP_3R rabbit polyclonal antibody (negative control, no signal detected). **C**) Representative image of a human DSM cell stained with the anti-TRPM4 goat polyclonal antibody and the anti-$K_V7.5$ rabbit polyclonal antibody (negative control, no signal detected). As shown in **A**, positive co-localization of anti-TRPM4 and anti-IP_3R antibodies is exemplified by red fluorescent staining Results were confirmed in at least three human DSM cells isolated from three different patients.

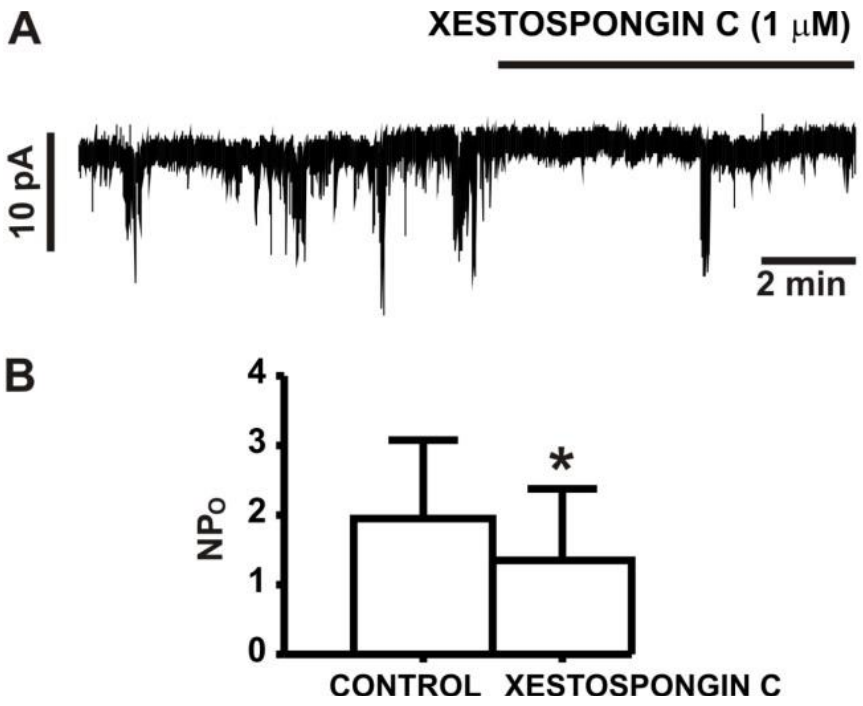

Figure 6.2. IP_3R inhibition with xestospongin-C decreased TICC activity in human DSM cells. A) An original recording showing the inhibitory effect of xestospongin-C (1 μM) on TICCs in a human DSM single cell recorded at a holding potential of -70 mV. **B)** Summary data illustrating the inhibitory effects of xestospongin-C (1 μM) on TICCs, analyzed as single channel open probability (NP_o) (n=6, N=4; *P<0.05).

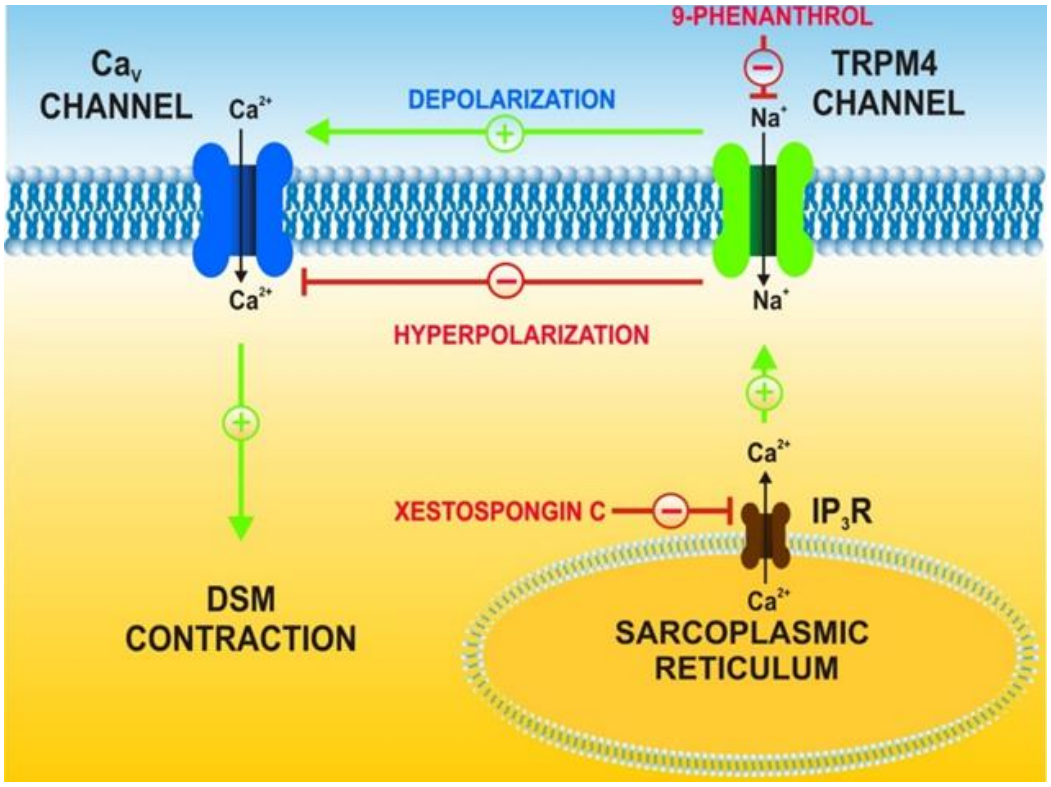

Figure 6.3. Illustration of the IP_3R regulatory role of TRPM4 channels in human DSM function. TRPM4 channels conduct monovalent cations and control human DSM membrane potential. TRPM4 channels are controlled by IP_3R-mediated Ca^{2+} release from the sarcoplasmic reticulum as inhibition of the IP_3Rs with xestospongin-C reduces TRPM4 channel activity. Pharmacological blockade of TRPM4 channels with 9-phenanthrol hyperpolarizes the DSM cell membrane, inhibits the Ca^{2+} channels, reduces intracellular Ca^{2+} levels and promotes DSM relaxation[78].

CHAPTER 7

[9]REGULATION OF GUINEA PIG DETRUSOR SMOOTH MUSCLE EXCITABILITY BY 17B-ESTRADIOL: THE ROLE OF THE LARGE CONDUCTANCE VOLTAGE- AND CA^{2+}-ACTIVATED K^+ CHANNELS

ABSTRACT

Estrogen replacement therapies have been suggested to be beneficial in alleviating symptoms of overactive bladder. However, the precise regulatory mechanisms of estrogen in urinary bladder smooth muscle (UBSM) at the cellular level remain unknown. Large conductance voltage- and Ca^{2+}-activated K^+ (BK) channels, which are key regulators of UBSM function, are suggested to be non-genomic targets of estrogens. This study provides an electrophysiological investigation into the role of UBSM BK channels as direct targets for 17β-estradiol, the principle estrogen in human circulation. Single BK channel recordings on inside-out excised membrane patches and perforated whole cell patch-clamp were applied in combination with the BK channel selective inhibitor paxilline to elucidate the mechanism of regulation of BK channel activity by 17β-estradiol in freshly-isolated guinea pig UBSM cells. 17β-Estradiol (100 nM) significantly increased the amplitude of depolarization-induced whole cell steady-state BK currents and the frequency of spontaneous transient BK currents in freshly-isolated UBSM cells. The increase in whole cell BK currents by 17β-estradiol was eliminated upon blocking BK channels with

[9]Provence A, Hristov KL, Parajuli SP, Petkov GV (2015) Regulation of Guinea Pig Detrusor Smooth Muscle Excitability by 17β-Estradiol: The Role of the Large Conductance Voltage- and Ca^{2+}-Activated K^+ Channels. PLoS ONE 10(11): e0141950

The following work is currently published in Plos One[104], which is an open access journal allowing reprinting.

paxilline. 17β-Estradiol (100 nM) significantly increased (~3-fold) the single BK channel open probability, indicating direct 17β-estradiol-BK channel interactions. 17β-Estradiol (100 nM) caused a significant hyperpolarization of the membrane potential of UBSM cells, and this hyperpolarization was reversed by blocking the BK channels with paxilline. 17β-Estradiol (100 nM) had no effects on L-type voltage-gated Ca^{2+} channel currents recorded under perforated patch-clamp conditions. This study reveals a new regulatory mechanism in the urinary bladder whereby BK channels are directly activated by 17β-estradiol to reduce UBSM cell excitability.

Abbreviations: BK channels, large conductance voltage- and Ca^{2+}-activated K^+ channels; Ca_V channels, L-type voltage-gated Ca^{2+} channels; DMSO, dimethyl sulfoxide; UBSM, urinary bladder smooth muscle; EGTA, ethylene glycol-bis(2-aminoethylether)-N,N,N',N'-tetraacetic acid; HEPES, 4-(2-Hydroxyethyl)piperazine-1-ethanesulfonic acid; P_o, single channel open probability; NP_o, single channel total open probability of each excised patch; OAB, overactive bladder; RyRs, ryanodine receptors; SR, sarcoplasmic reticulum; TBKCs, transient BK currents

INTRODUCTION

The functions of the urinary bladder, which are to store and periodically release urine, are facilitated by the contraction and relaxation of urinary bladder smooth muscle (UBSM). Overactive bladder (OAB), a highly prevalent chronic health condition in the United States, is often associated with increased UBSM contractility. The primary treatment for OAB involves antimuscarinic agents, which have limited efficacy and tolerability [12]. Many forms of OAB have been linked directly to UBSM dysfunction [12,

105]. Therefore, novel therapeutic modalities for OAB, targeting UBSM directly, are urgently needed.

Sharing a common embryonic origin, the genital and lower urinary tract systems are both regulated by sex hormones, including estrogens [106, 107]. Systemic and vaginal estrogen therapies have been considered beneficial in alleviating symptoms of OAB in postmenopausal women [106, 107]. Epidemiological studies have also linked post-menopausal estrogen deficiencies with the increased risk for OAB [106]. Despite these observations, conflicting evidence in the literature exists concerning the role of estrogen as a treatment for OAB [106]. Some studies suggest beneficial effects of estrogen replacement therapies for controlling symptoms of OAB, while other studies report the opposite [106-108]. Thus, there remains the need for an improved understanding of the mechanisms by which estrogens regulate UBSM function [108].

The predominant estrogen in human circulation is 17β-estradiol, a potent hormone known to regulate urinary bladder function [106, 107, 109, 110]. 17β-Estradiol-induced UBSM relaxation has long been established *in vitro* [111-113] and *in vivo* [114]. The cellular mechanisms of these functional effects of 17β-estradiol in UBSM are not well understood, but several mechanisms have been suggested, including L-type voltage-gated Ca^{2+} (Ca_V) channel inhibition [105, 112] and K^+ channel activation [115]. Among the K^+ channel targets of 17β-estradiol are the large conductance voltage- and Ca^{2+}-activated K^+ (BK) channels [116-119]. A previous study in guinea pigs [115] suggested the possible involvement of the BK channels in 17β-estradiol-induced UBSM relaxation as the relaxant effects of 17β-estradiol were concentration-dependently blocked by the specific BK

channel inhibitor iberiotoxin. However, the role of the BK channels as targets for 17β-estradiol has never been investigated at the cellular level in UBSM.

BK channels are among the most physiologically-relevant K^+ channels regulating UBSM excitability and contractility [4, 11]. As both a Ca^{2+} and voltage sensor, BK channels work to oppose UBSM excitability by promoting cell membrane hyperpolarization, which in turn precludes Ca^{2+} influx through L-type Ca_V channels to promote UBSM relaxation [4, 11]. In UBSM, BK channels are activated by either Ca^{2+} influx through L-type Ca_V channels or by Ca^{2+} released from the sarcoplasmic reticulum (SR) ryanodine receptors (RyRs), known as "Ca^{2+} sparks" [11]. BK channel activation by Ca^{2+} sparks triggers transient BK currents (TBKCs), also known as spontaneous transient outward currents (STOCs) [11], which regulate UBSM excitability. Given the key role of the BK channels in UBSM function [4, 11], their potential regulation by 17β-estradiol represents a critically important mechanism in UBSM cell physiology. Indeed, an earlier study proposed a potential role for the BK channels in 17β-estradiol-mediated UBSM relaxation [115]. However, in UBSM, the existence of a 17β-estradiol-BK channel functional interaction has not been investigated at the cellular level. Therefore, this study aimed to elucidate the functional role of the BK channels as non-genomic targets of 17β-estradiol in guinea pig UBSM cell excitability. We employed multiple electrophysiological protocols including single BK channel recordings on inside-out excised membrane patches and the amphotericin-B perforated whole cell patch-clamp technique in combination with the selective BK channel inhibitor paxilline.

MATERIALS AND METHODS

UBSM tissue acquisition and single cell isolation. All experimental procedures were conducted in accordance with the animal use protocol #2186 reviewed and approved by the Institutional Animal Care and Use Committee (IACUC) of the University of South Carolina. Only male animals were used in this study to avoid changes in the estrogen levels that occur during the menstrual cycle of the females. Forty-six adult male Hartley-Albino guinea pigs (Charles River Laboratories, Raleigh, NC) of average weight 740±177 g were euthanized by CO_2 inhalation using a SMARTBOX™ automated CO_2 delivery system (Euthanex Corp, Palmer, PA) followed by thoracotomy. Subsequently, the urinary bladder was removed after a transverse incision superior to the bladder neck. Dissection of UBSM tissues was performed as previously described [120]. UBSM single cells were isolated from UBSM tissues by enzymatic digestion using a combination of collagenase and papain as previously described [120]. Freshly-isolated UBSM cells were used for patch-clamp experiments within 12 h of isolation.

Patch-clamp electrophysiology. UBSM cell suspension (0.3-0.5 ml) was placed in a glass-bottom chamber to settle for at least 20-30 min. We applied the amphotericin-B perforated whole cell patch-clamp technique as previously described [120] to record voltage-step depolarization-induced whole cell BK currents, TBKCs, L-type Ca_V currents, and the resting membrane potential of freshly-isolated guinea pig UBSM cells. To determine the effects of 17β-estradiol on whole cell steady-state BK currents, UBSM cells were voltage-clamped at a holding potential of -70 mV. Subsequently, voltage-step depolarizations were applied from -40 to +80 mV at 20 mV intervals for 200 ms.

Membrane potential recordings were performed in current-clamp mode (*I=0*) of the patch-clamp technique. The effects of 17β-estradiol on peak L-type Ca_V channel currents were recorded at 0 mV in voltage-clamp mode of the amphotericin-B perforated patch-clamp technique in the presence of paxilline (1 μM). Single BK channel recordings were performed on inside-out excised membrane patches as previously described [120]. Single BK channel currents were measured at -60 mV with bath and pipette solutions containing symmetrical 140 mM KCl and ~300 nM free [Ca^{2+}] (see **§Solutions and drugs**). These experiments were conducted using pCLAMP version 10.2 software (Molecular Devices, Sunnyvale, CA) with an Axopatch 200B amplifier (Digidata 1322A). Currents were filtered using an eight-pole Bessel filter (model 900CT/9L8L, Frequency Devices, Ottawa, IL). Borosilicate glass patch-clamp pipettes (Sutter Instruments, Novato, CA) were pulled using a Narishige glass micropipette puller (model PP-830, Narishige Group, Tokyo, Japan) and polished with a Microforge (model MF-830, Narishige Group). The final pipette resistance was 4-6 MΩ for whole cell patch-clamp and 6-15 MΩ for single BK channel recordings. All patch-clamp experiments were conducted at room temperature (22-23°C).

Solutions and drugs. Ca^{2+}-free dissection solution contained (in mM): 80 monosodium glutamate; 55 NaCl; 6 KCl; 10 glucose; 10 N-2-hydroxyethylpiperazine-N'-2-ethanesulphonic acid (HEPES); 2 $MgCl_2$; NaOH was administered to attain pH 7.3. The extracellular solution for whole cell patch-clamp experiments had (in mM): 134 NaCl, 6 KCl, 1 $MgCl_2$, 2 $CaCl_2$, 10 glucose, and 10 HEPES, pH adjusted to 7.4 with NaOH. The patch-pipette solution contained (in mM): 110 potassium aspartate; 30 KCl; 10 NaCl; 1 $MgCl_2$; 10 HEPES; 0.05 ethylene glycol-bis(2-aminoethylether)-N,N,N',N'-tetraacetic acid

(EGTA); NaOH was used to adjust the pH to 7.2. Symmetrical K^+ solution used for single BK channel recordings contained (in mM): 140 KCl, 1.08 $MgCl_2$, 5 EGTA, and 3.16 $CaCl_2$, adjusted to pH 7.2 with NaOH. Stock amphotericin-B solution was freshly prepared daily in dimethyl sulfoxide (DMSO) and was added to the

pipette solution (200-300 μg/ml) prior to the experiment. 17β-Estradiol and paxilline were purchased from Sigma-Aldrich (St. Louis, MO) and were dissolved in DMSO. The final concentration of DMSO in the bath solution did not exceed 0.01%.

Data analysis and statistics. Single BK channel openings were analyzed over 5-10 min intervals before and after the addition of 17β-estradiol (100 nM). The values for single BK channel open probability [107] of each excised patch (NP_o) were calculated using Clampfit 10.2 software as previously described [120]. Single BK channel P_o for each patch was calculated as NP_o where N refers to the number of channels in the patch. The effects of 17β-estradiol on whole cell steady-state BK currents and the cell membrane potential were analyzed using Clampfit 10.2 software. The effects of 17β-estradiol on voltage-step depolarization-induced whole cell BK currents were analyzed by taking the average value of the last 50 ms of each pulse before and after the application of 17β-estradiol (100 nM). The effects of 17β-estradiol on the amplitude and frequency of TBKCs were analyzed using Minianalysis software (Synaptosoft, Decatur, GA). The threshold of TBKCs was set at 9 pA, which is equal to three times the single BK channel amplitude at -20 mV. Data are presented as the means ± SEM. In the summarized data, "**n**" indicates the number of UBSM cells used and "**N**" represents the total number of guinea pigs. CorelDraw Graphics Suite X3 software (Corel Co., Mountain View, CA) and GraphPad Prism 4.03 software (GraphPad Software, Inc., La Jolla, CA) were used for statistical analysis and data

illustration. Paired Student's t-test was used for statistical analysis. P values <0.05 were considered statistically significant.

RESULTS

17β-Estradiol enhanced whole cell depolarization-induced steady-state K^+ currents in freshly-isolated UBSM cells. The average whole cell capacitance of all cells used in the present study was 29.8±2.2 pF (n=64, N=46). 17β-Estradiol (100 nM) caused a significant increase in whole cell steady-state K^+ currents (n=11, N=10; P<0.05, **Fig. 1A-B**). As illustrated in **Fig. 1A-B**, the density of whole cell steady-state K^+ currents at +80 mV were 30.1±14.6 pA/pF for the controls and 35.8±16.0 pA/pF in the presence of 17β-estradiol. To determine whether these stimulatory effects were mediated by the BK channels, we examined the effects of 17β-estradiol in the presence of the BK channel inhibitor paxilline (1 μM). As shown in **Fig. 1C-D**, when BK channels were blocked with 1 μM paxilline, 17β-estradiol had no significant effects on the residual whole cell steady-state K^+ currents. The density of whole cell steady-state K^+ currents at +80 mV was 13.5±2.3 pA/pF for the controls (paxilline only) and after the application of 17β-estradiol in the continued presence of paxilline was 13.4±2.4 pA/pF (n=14, N=12; P>0.05; **Fig. 1C-D**). These results indicate that in UBSM cells, the increase in whole cell steady-state K^+ currents by 17β-estradiol is mediated by the BK channels

17β-Estradiol increased the frequency of TBKCs in freshly-isolated UBSM cells. TBKCs have a key role in regulating UBSM cell excitability [4, 11]. We sought to elucidate the regulation of TBKC activity by 17β-estradiol in UBSM cells. TBKCs were recorded at a holding potential of -20 mV. As illustrated in **Fig. 2**, 17β-estradiol (100 nM) significantly increased the frequency of TBKCs from 0.48±0.15 Hz (control) to 0.59±0.18 Hz (n=9,

N=9; P<0.05), without effecting TBKC amplitude (n=9, N=9; P>0.05). Collectively, these data indicate that 17β-estradiol regulates TBKC activity in UBSM cells.

17β-Estradiol increased single BK channel P_o in UBSM cell excised membrane patches. To elucidate if 17β-estradiol has a direct effect on the BK channels, we conducted single BK channel recordings on inside-out excised membrane patches. 17β-Estradiol (100 nM) increased the mean BK channel NP_o from the control value of 0.05±0.03 to 0.20±0.07 (n=13, N=11; P<0.05). Further, as illustrated in **Fig. 3**, single BK channel opening events were completely abolished by 1 μM paxilline in all excised membrane patches. These data provide strong support that 17β-estradiol directly and rapidly activates BK channels in UBSM cells.

17β-Estradiol hyperpolarized the resting membrane potential of UBSM cells. Next, we aimed to elucidate the BK channel-dependent regulation of the UBSM cell membrane potential by 17β-estradiol in UBSM cells. 17β-Estradiol (100 nM) significantly hyperpolarized the UBSM cell membrane potential to -25.8±2.3 mV from the control value of -22.1±2.4 mV (n=12, N=11; P<0.05; **Fig. 4A-B**). The BK channel inhibitor paxilline (1 μM) reversed the hyperpolarizing effects of 17β-estradiol on the UBSM cell membrane potential to -22.2±1.9 mV (n=12, N=11; P<0.05; **Fig. 4A-B).** As shown in **Fig. 4C-D**, 17β-estradiol had no effects on the UBSM cell membrane potential when administered in the presence of paxilline (1 μM), with the membrane potential of -19.3±6.7 mV in comparison to the control (paxilline only) value of -20.0±7.0 mV (n=7, N=7; P>0.05). These data support the concept that 17β-estradiol regulates the UBSM cell membrane potential through a mechanism involving the modulation of BK channel activity.

17β-Estradiol did not inhibit L-type Ca_V currents in freshly-isolated UBSM cells. In guinea pig UBSM cells, the inhibition of L-type Ca_V currents by 17β-estradiol has been reported at micromolar concentrations using the conventional patch-clamp technique [112], which does not maintain the native physiological environment of UBSM cells. Thus, we sought to determine whether nanomolar concentrations of 17β-estradiol (100 nM) modulates L-type Ca_V channel activity in UBSM cells in the presence of the BK channel inhibitor paxilline (1 μM) using the perforated patch-clamp technique. As exemplified by **Fig. 5**, 17β-estradiol (100 nM) had no effect on L-type Ca_V channel currents. At 0 mV, the average inward current density under control conditions was -1.4±0.3 pA/pF and after the addition of 100 nM 17β-estradiol was -1.6±0.4 pA/pF (n=5, N=5; P>0.05; **Fig. 5**). These results support the novel concept that under physiological conditions of the perforated patch-clamp, nanomolar concentrations of 17β-estradiol do not directly affect L-type Ca_V channel activity.

DISCUSSION

The current study provided the first electrophysiological evidence establishing the novel regulatory mechanism by which the BK channels are direct targets for 17β-estradiol at nanomolar concentrations in guinea pig UBSM cells. Our results demonstrate that 17β-estradiol: 1) rapidly increases the amplitude of whole cell steady-state BK currents; 2) rapidly increases the frequency of TBKCs; 3) rapidly increases single BK channel NP_o; and 4) hyperpolarizes the UBSM cell membrane potential; and 5) does not directly inhibit L-type Ca_V channel currents at nanomolar concentrations. 17β-Estradiol is most widely known for its long-term genomic mechanisms involving gene expression and the promotion of female sexual and reproductive health.

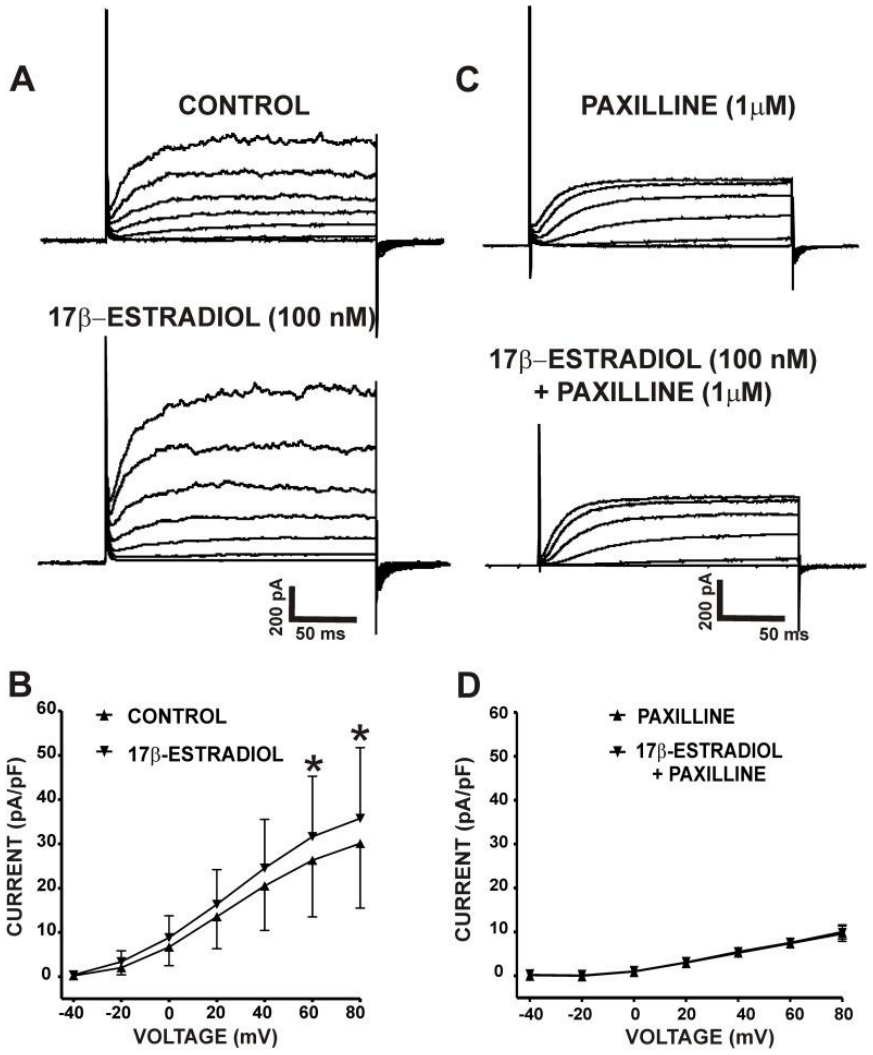

Figure 7.1 17β-Estradiol increases depolarization-induced whole cell steady-state BK currents in freshly-isolated UBSM cells. A) Representative traces from a voltage-clamp experiment illustrating that 17β-estradiol (100 nM) increases whole cell steady-state BK currents in an isolated UBSM cell. **B)** The current-voltage relationship curves illustrate the 17β-estradiol (100 nM)-mediated increase of whole cell steady-state BK currents in isolated UBSM cells (n=11, N=10; *P<0.05). **C)** Representative traces from a voltage-clamp experiment illustrating the lack of effects of 17β-estradiol (100 nM) on whole cell steady-state BK currents in the presence of the BK channel inhibitor paxilline (1 μM). **D)** The current-voltage relationship curves illustrate that 17β-estradiol (100 nM) had no significant effects on whole cell steady-state BK currents in the presence of 1 μM paxilline (n=14, N=12; P>0.05).

However, emerging evidence in UBSM and other cell types suggests the existence of several non-genomic mechanisms of 17β-estradiol, which may acutely influence cell excitability and contractility.

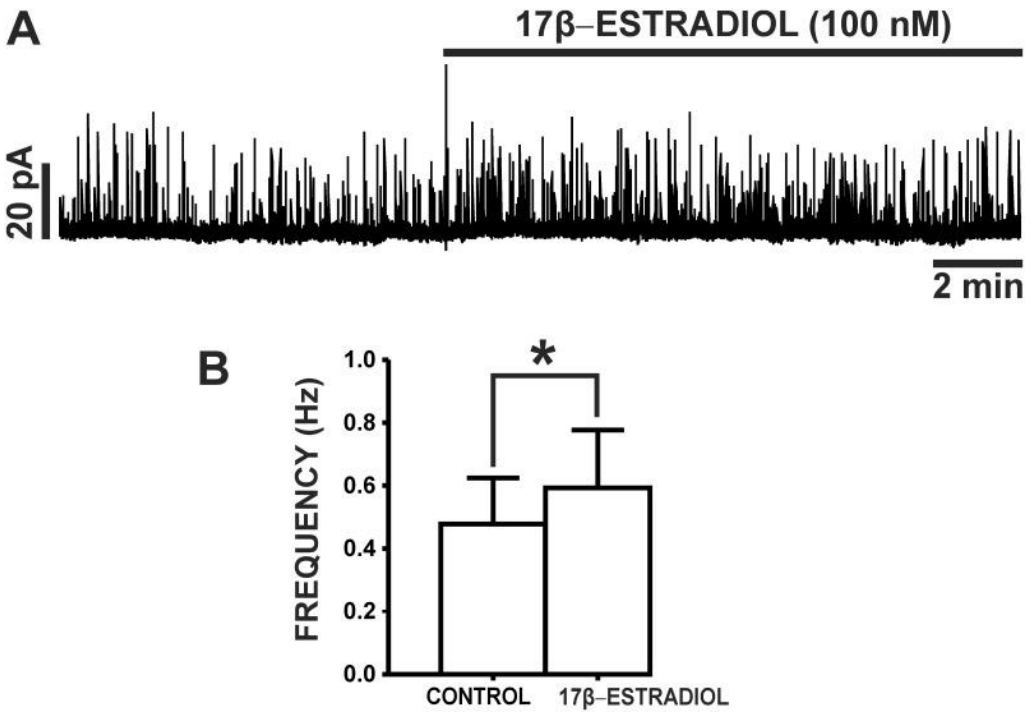

Figure 7.2 17β-Estradiol increases the frequency of TBKCs in freshly-isolated UBSM cells. A) An original representative recording illustrating the stimulatory effects of 17β-estradiol (100 nM) on TBKC activity in an isolated UBSM cell. **B)** Summarized data illustrating the increase in TBKC frequency by 17β-estradiol (100 nM) in UBSM cells (n=9, N=9; *P<0.05).

These non-genomic mechanisms include: inhibition of L-type Ca_V channels [112, 121, 122], endothelial-dependent release of nitric oxide [123], activation of protein kinases [124], and activation of the BK channels [116, 125]. Involvement of the BK channels in the mechanism of 17β-estradiol-induced response is supported by studies from non-UBSM cell types and recombinant systems expressing BK channels, which indicate the activation of BK channels by 17β-estradiol is dependent on their regulatory β1-subunit [108, 116-119]. The role of the regulatory β1-subunit was also supported by studies from freshly-isolated murine colonic myocytes, where the increase in BK channel P_o by 17β-estradiol was not observed in excised membrane patches from β1-subunit knockout ($\beta1^{-/-}$) mice [126].

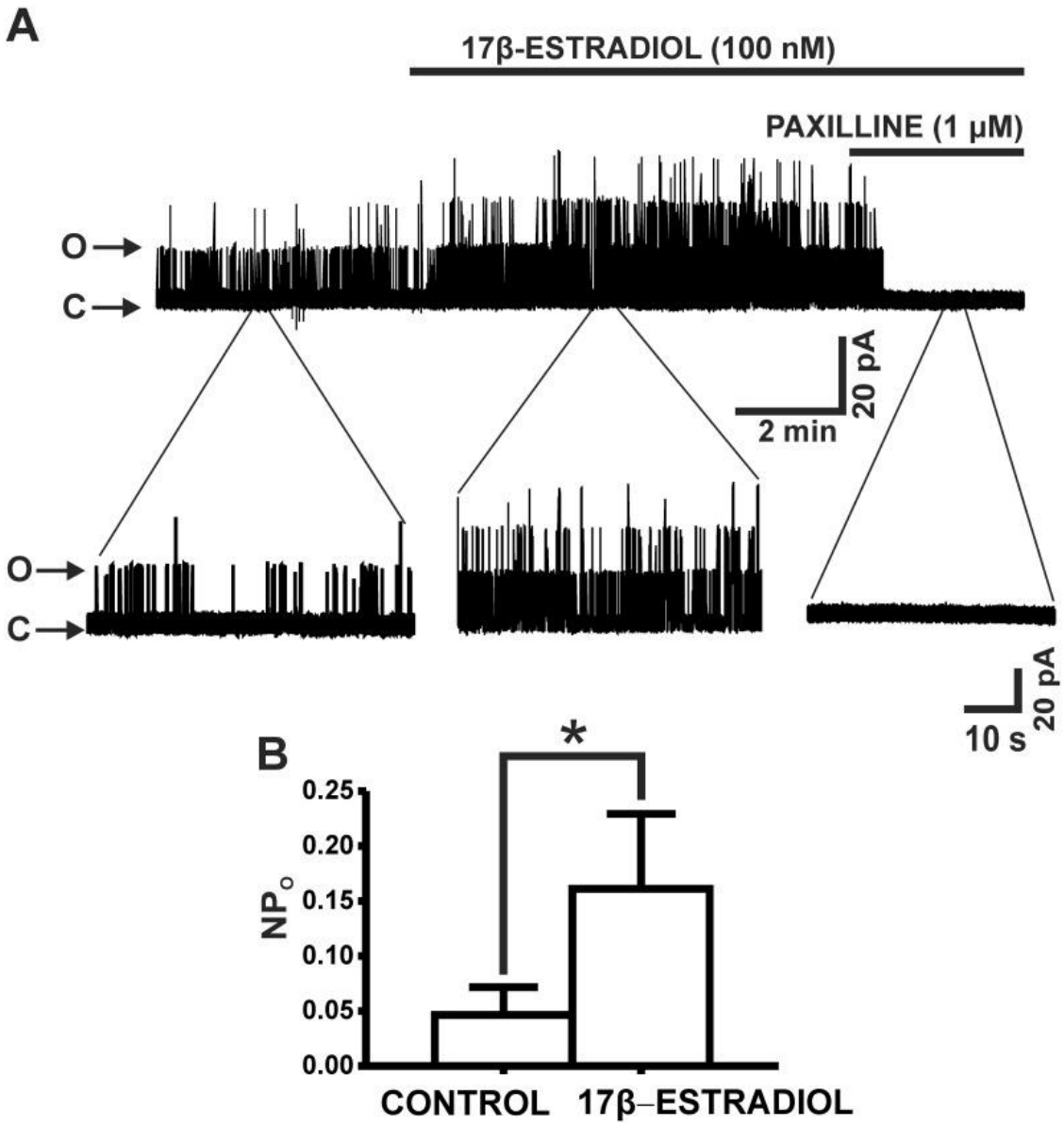

Figure 7.3. 17β-Estradiol increases single BK channel P_o in excised patches from freshly-isolated UBSM cells. A) An original representative recording of BK channel currents recorded in the inside-out configuration of the patch-clamp technique before and after the addition of 100 nM 17β-estradiol in an excised patch from an isolated UBSM cell. Single channel activity was completely abolished by 1 μM paxilline. "**O**" indicates open channel state and "**C**" indicates closed channel state. **B)** Summarized data for the effects of 17β-estradiol (100 nM) on the BK channel NP_o (n=13, N=11; *P<0.05). Single BK channel recordings were performed at a holding potential of -60 mV.

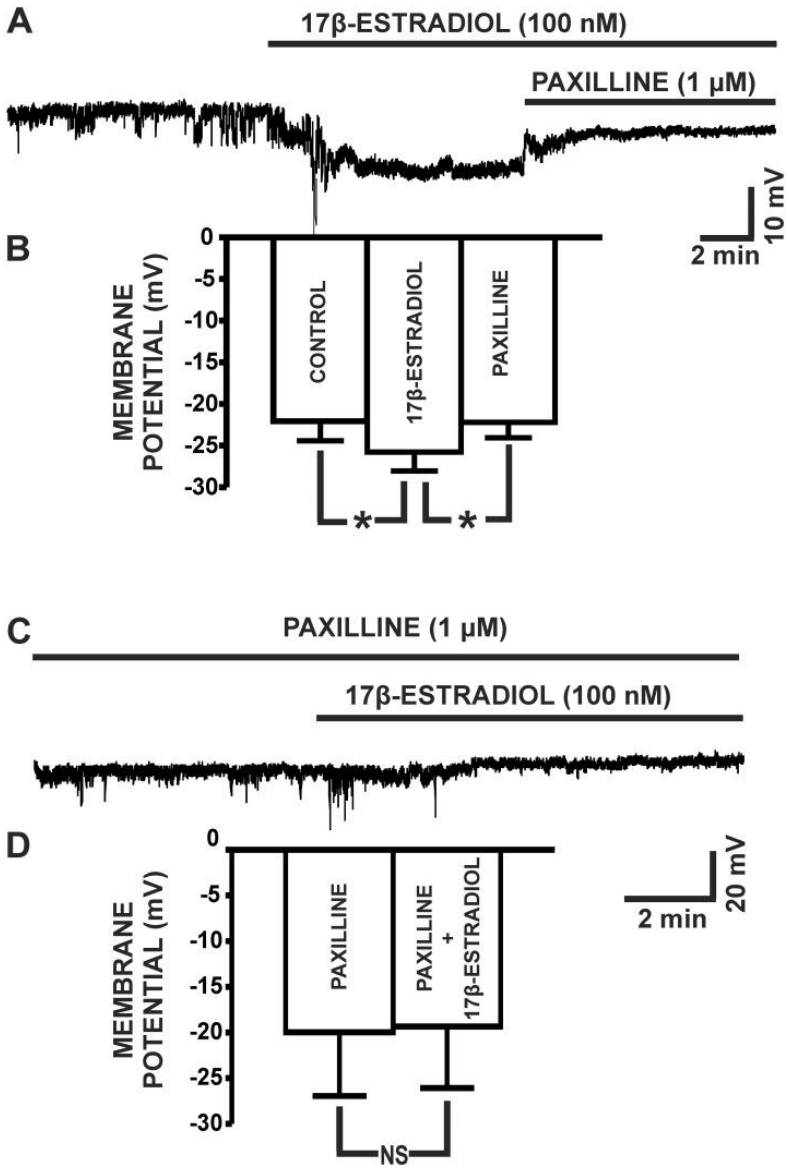

Figure 7.4. 17β-Estradiol hyperpolarized the membrane potential of freshly-isolated UBSM cells. A) A representative trace of a membrane potential recording in current-clamp mode (*I=0*) demonstrating the hyperpolarizing effects of 17β-estradiol (100 nM) in an isolated UBSM cell. The hyperpolarizing effect of 17β-estradiol (100 nM) was reversed by 1 μM paxilline. **B)** Summarized data illustrating the hyperpolarizing effects of 17β-estradiol on the UBSM cell membrane potential and that 1 μM paxilline reverses the 17β-estradiol-induced hyperpolarization (n=12, N=11; *P<0.05). **C)** A representative trace of a membrane potential recording in current-clamp mode demonstrating that when the BK channels are blocked with 1 μM paxilline, 17β-estradiol (100 nM) did not cause membrane hyperpolarization in an isolated UBSM cell. **D)** Summarized data illustrating that 17β-estradiol had no effect on the UBSM cell membrane potential in the presence of 1 μM paxilline (n=7, N=7; P>0.05).

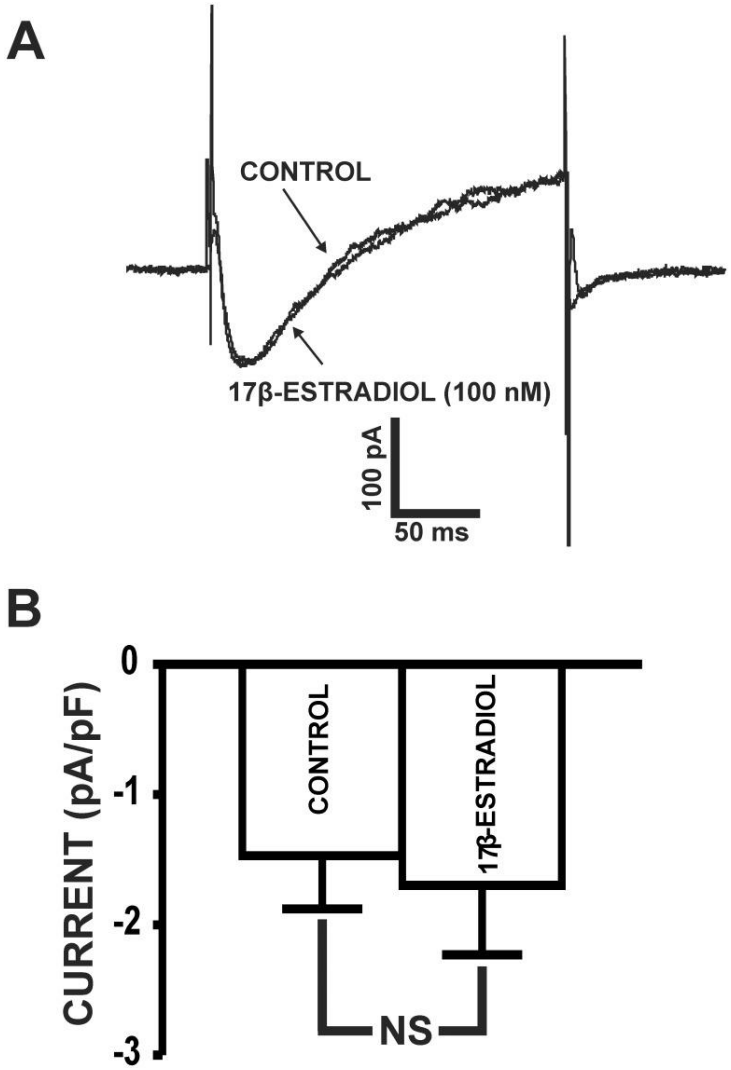

Figure 7.5. 17β-Estradiol does not inhibit L-type Ca_V channel activity in freshly-isolated UBSM cells. A) A representative recording of the peak L-type Ca_V channel currents recorded at 0 mV in a freshly-isolated UBSM cell in the absence (control) or presence of 17β-estradiol (100 nM). **B)** Summary data of the current density of L-type Ca_V channel currents in the absence (control) or presence of 100 nM 17β-estradiol (n=5, N=5; P>0.05).

In UBSM, *in vitro* functional studies have demonstrated the inhibition of rodent and pig UBSM contractility by 17β-estradiol [111, 113, 115]. These observations correspond to reports in rat UBSM, where 17β-estradiol decreased the amplitude and frequency of spontaneous Ca^{2+} flashes [113]. A previous study showed that 17β-estradiol-induced inhibition of UBSM contractility was still achieved in the presence of the estrogen receptor antagonist ICI-182,780 [113]. This finding supports a non-genomic

mechanism for 17β-estradiol in controlling UBSM contractility that is independent of estrogen receptor activation. In guinea pig UBSM, it has been suggested that 17β-estradiol acts as both an L-type Ca_V channel inhibitor and K^+ channel activator [115]. It has been shown that micromolar concentrations of 17β-estradiol inhibit L-type Ca^{2+} currents in guinea pig UBSM cells [112], while a separate study showed the relaxant effects of 17β-estradiol on guinea pig UBSM contractility were blocked in a concentration-dependent manner by the selective BK channel inhibitor iberiotoxin [115]. As BK and L-type Ca_V channels are functionally coupled [4, 11], it was important to elucidate these pathways at the cellular level in UBSM using nanomolar concentrations of 17β-estradiol under physiological experimental conditions.

Our results show that 17β-estradiol increased the amplitude of whole cell steady-state K^+ currents (**Fig. 1**) consistent with reports in non-UBSM cell types [117, 126]. The rapid effects of 17β-estradiol on whole cell K^+ currents were blocked by the BK channel inhibitor paxilline, suggesting a BK channel-dependent mechanism.

Directly confirming the 17β-estradiol-BK channel functional interactions, we found that 17β-estradiol (100 nM) significantly increased the single BK channel NP_o of inside-out excised membrane patches of UBSM cells (**Fig. 3**). These results are in support of earlier electrophysiological reports in non-UBSM cell types showing activation of the BK channels by 17β-estradiol [116-119, 127]. Our single BK channel recordings were performed using symmetrical K^+ solutions with fixed Ca^{2+} concentration and in the absence of signaling pathways that may alter BK channel P_o. The rapid effects of 17β-estradiol on the UBSM BK channels further indicate direct non-genomic mechanisms. Thus, our data

provide clear-cut evidence that 17β-estradiol directly activates BK channels in UBSM cells.

In UBSM cells, Ca^{2+} sparks released from the SR RyRs activate TBKCs, which fundamentally regulate UBSM cell excitability [4, 11]. Activation of TBKCs hyperpolarizes the UBSM cell membrane potential and decreases Ca^{2+} influx through L-type Ca_V channels [4, 11]. 17β-Estradiol (100 nM) caused a significant increase in the frequency of TBKCs **(Fig. 2)**. While we cannot completely exclude the possibility that 17β-estradiol may regulate BK channel activity indirectly through modulating the SR Ca^{2+} sparks, the current data (**Fig. 3**) are in support of a non-genomic mechanism involving a direct 17β-estradiol-BK channel interaction. Thus, the increase in TBKC frequency could be explained by an increase in BK channel NP_o by 17β-estradiol, which can thus increase the number of single BK channel opening events at -20 mV (**Fig. 2**). Therefore, 17β-estradiol increased the number of small BK channel opening events reaching the TBKC threshold of 9 pA, (see **Materials and Methods**) as a result of direct modulation of BK channel NP_o while having no statistically significant effect on TBKC amplitude.

The negative feedback mechanism by which BK channels limit UBSM excitability originates from its ability to control the cell membrane potential [11]. 17β-Estradiol (100 nM) caused a BK channel-dependent cell membrane hyperpolarization in UBSM cells (**Fig. 4**). 17β-Estradiol-mediated hyperpolarization in UBSM cells is consistent with the stimulatory effects of 17β-estradiol on TBKCs and whole cell steady-state BK currents.

Our study is the first to reveal a direct functional role for the BK channels in mediating the effects of 17β-estradiol in UBSM at the cellular level. Importantly, the effects of 17β-estradiol on BK channel activity in the current study were achieved using a

nanomolar concentration, well below the micromolar concentrations previously used in UBSM functional

studies [111-113, 115]. In particular, it was previously reported using the conventional patch-clamp technique that 17β-estradiol, at much higher non-physiological micromolar concentrations (1 μM), inhibited peak Ca^{2+} currents by 50% in guinea pig UBSM cells [112]. However, 17β-estradiol never reaches micromolar concentrations in the blood plasma even under pathophysiological conditions. We demonstrated here for the first time using the perforated whole cell patch-clamp technique, that 17β-estradiol (100 nM) had no direct effects on L-type Ca_V channel activity in freshly-isolated guinea pig UBSM cells (**Fig. 5**). These data suggest that 17β-estradiol directly activates the BK channels at nanomolar concentrations, which are insufficient to affect L-type Ca_V channel activity. Unlike our study, previous studies that showed L-type Ca_V channel inhibition by 17β-estradiol in guinea pig UBSM cells have used physiologically-irrelevant high micromolar concentrations [112]. Thus, our study reveals the novel findings that L-type Ca_V channel inhibition by 17β-estradiol is not involved in UBSM relaxation under normal physiological conditions.

The current study provides strong evidence supporting a role for the BK channels as low-affinity non-genomic targets for 17β-estradiol in UBSM. Our study does not exclude the possibility that 17β-estradiol may exert genomic effects on the BK channels directly through estrogen receptor stimulation. However, the rapid increase in single BK channel NP_o by 17β-estradiol (Fig. 3) clearly indicates that the BK channels are direct non-genomic targets for 17β-estradiol. As the role of estrogens in UBSM physiology and pathophysiology is not fully understood, the current study provides a foundational basis

for future studies in human UBSM. Indeed, decreased estrogen levels have been associated with the increased occurrence of urinary urgency and frequency in post-menopausal women [106-108, 128]. Thus, the activation of the BK channels by 17β-estradiol, which in turn hyperpolarizes the membrane potential to cause UBSM relaxation, may underlie some of the observed benefits of estrogen replacement therapies in alleviating symptoms of OAB [108].In conclusion, we reveal a new paradigm in UBSM cell physiology, indicating a direct role for the BK channels in mediating the inhibitory effects of 17β-estradiol on UBSM cell excitability.

REFERENCES

1. Andersson, K.E. and A. Arner, *Urinary bladder contraction and relaxation: physiology and pathophysiology.* Physiological reviews, 2004. **84**(3): p. 935-86.
2. Heppner, T.J., et al., *Nerve-evoked purinergic signalling suppresses action potentials, Ca^{2+} flashes and contractility evoked by muscarinic receptor activation in mouse urinary bladder smooth muscle.* The Journal of physiology, 2009. **587**(Pt 21): p. 5275-88.
3. Nausch, B., T.J. Heppner, and M.T. Nelson, *Nerve-released acetylcholine contracts urinary bladder smooth muscle by inducing action potentials independently of IP_3-mediated calcium release.* American journal of physiology. Regulatory, integrative and comparative physiology, 2010. **299**(3): p. R878-88.
4. Petkov, G.V., *Role of potassium ion channels in detrusor smooth muscle function and dysfunction.* Nature reviews. Urology, 2012. **9**(1): p. 30-40.
5. Firth, A.Y., Jason. , *Ion Channels and Transporters in the Pulmonary Vasculature: A Focus on Smooth Muscle.* . Textbook of Pulmonary Vascular Disease, DOI 10.1007/978-0-387-87429-6_13, © Springer Science+Business Media, LLC 2011, 2011.
6. Fowler, C.J., D. Griffiths, and W.C. de Groat, *The neural control of micturition.* Nat Rev Neurosci, 2008. **9**(6): p. 453-66.
7. Afeli, S.A., J. Malysz, and G.V. Petkov, *Molecular expression and pharmacological evidence for a functional role of Kv7 channel subtypes in Guinea pig urinary bladder smooth muscle.* PloS one, 2013. **8**(9): p. e75875.
8. Anderson, U.A., et al., *Functional expression of KCNQ (Kv7) channels in guinea pig bladder smooth muscle and their contribution to spontaneous activity.* British journal of pharmacology, 2013. **169**(6): p. 1290-304.
9. Svalo, J., et al., *Functional and molecular evidence for Kv7 channel subtypes in human detrusor from patients with and without bladder outflow obstruction.* PloS one, 2015. **10**(2): p. e0117350.
10. Chen, M., W.F. Kellett, and G.V. Petkov, *Voltage-gated K^+ channels sensitive to stromatoxin-1 regulate myogenic and neurogenic contractions of rat urinary bladder smooth muscle.* American journal of physiology. Regulatory, integrative and comparative physiology, 2010. **299**(1): p. R177-84.
11. Petkov, G.V., *Central role of the BK channel in urinary bladder smooth muscle physiology and pathophysiology.* American journal of physiology. Regulatory, integrative and comparative physiology, 2014. **307**(6): p. R571-R584.
12. Andersson, K.E. and A.J. Wein, *Pharmacology of the lower urinary tract: basis for current and future treatments of urinary incontinence.* Pharmacological reviews, 2004. **56**(4): p. 581-631.

13. Robbins, J., *KCNQ potassium channels: physiology, pathophysiology, and pharmacology.* Pharmacology & therapeutics, 2001. **90**(1): p. 1-19.
14. Soldovieri, M.V., F. Miceli, and M. Taglialatela, *Driving with no brakes: molecular pathophysiology of Kv7 potassium channels.* Physiology, 2011. **26**(5): p. 365-76.
15. Abbott, G.W. and S.A. Goldstein, *Potassium channel subunits encoded by the KCNE gene family: physiology and pathophysiology of the MinK-related peptides (MiRPs).* Molecular interventions, 2001. **1**(2): p. 95-107.
16. Wrobel, E., D. Tapken, and G. Seebohm, *The KCNE Tango - How KCNE1 Interacts with Kv7.1.* Frontiers in pharmacology, 2012. **3**: p. 142.
17. Brueggemann, L.I., et al., *Kv7 potassium channels in airway smooth muscle cells: signal transduction intermediates and pharmacological targets for bronchodilator therapy.* American journal of physiology. Lung cellular and molecular physiology, 2012. **302**(1): p. L120-32.
18. Chadha, P.S., et al., *Contribution of Kv7.4/Kv7.5 heteromers to intrinsic and calcitonin gene-related peptide-induced cerebral reactivity.* Arteriosclerosis, thrombosis, and vascular biology, 2014. **34**(4): p. 887-93.
19. Jepps, T.A., et al., *Downregulation of Kv7.4 channel activity in primary and secondary hypertension.* Circulation, 2011. **124**(5): p. 602-11.
20. Brueggemann, L.I., et al., *KCNQ (Kv7) potassium channel activators as bronchodilators: combination with a beta2-adrenergic agonist enhances relaxation of rat airways.* American journal of physiology. Lung cellular and molecular physiology, 2014. **306**(6): p. L476-86.
21. Mani, B.K., et al., *Vascular KCNQ (Kv7) potassium channels as common signaling intermediates and therapeutic targets in cerebral vasospasm.* Journal of cardiovascular pharmacology, 2013. **61**(1): p. 51-62.
22. Ng, F.L., et al., *Expression and function of the K^+ channel KCNQ genes in human arteries.* British journal of pharmacology, 2011. **162**(1): p. 42-53.
23. Jepps, T.A., et al., *Vasorelaxant effects of novel Kv7.4 channel enhancers ML213 and NS15370.* British journal of pharmacology, 2014. **171**(19): p. 4413-4424.
24. Jepps, T.A., et al., *Molecular and functional characterization of Kv7 K^+ channel in murine gastrointestinal smooth muscles.* American journal of physiology. Gastrointestinal and liver physiology, 2009. **297**(1): p. G107-15.
25. Brickel, N., et al., *The urinary safety profile and secondary renal effects of retigabine (ezogabine): a first-in-class antiepileptic drug that targets KCNQ (Kv7) potassium channels.* Epilepsia, 2012. **53**(4): p. 606-12.
26. Streng, T., T. Christoph, and K.E. Andersson, *Urodynamic effects of the K^+ channel (KCNQ) opener retigabine in freely moving, conscious rats.* The Journal of urology, 2004. **172**(5 Pt 1): p. 2054-8.
27. Svalo, J., et al., *Kv7 Positive Modulators Reduce Detrusor Overactivity and Increase Bladder Capacity in Rats.* Basic & clinical pharmacology & toxicology, 2011. **110**: p. 145-153.
28. Svalo, J., et al., *Bladder contractility is modulated by Kv7 channels in pig detrusor.* European journal of pharmacology, 2013. **715**(1-3): p. 312-20.
29. Xiong, Q., et al., *Activation of Kv7 (KCNQ) voltage-gated potassium channels by synthetic compounds.* Trends in pharmacological sciences, 2008. **29**(2): p. 99-107.

30. Amato, G., et al., *N-Pyridyl and Pyrimidine Benzamides as KCNQ2/Q3 Potassium Channel Openers for the Treatment of Epilepsy.* ACS medicinal chemistry letters, 2011. **2**(6): p. 481-4.
31. Brueggemann, L.I., et al., *Differential Activation of Vascular Smooth Muscle Kv7.4, Kv7.5, and Kv7.4/7.5 Channels by ML213 and ICA-069673.* Molecular pharmacology, 2014. **86**(3): p. 330-41.
32. Hristov, K.L., et al., *Expression and function of K_V2-containing channels in human urinary bladder smooth muscle.* American journal of physiology. Cell physiology, 2012. **302**(11): p. C1599-608.
33. Smith, A.C., et al., *Novel role for the transient potential receptor melastatin 4 channel in guinea pig detrusor smooth muscle physiology.* American journal of physiology. Cell physiology, 2013. **304**(5): p. C467-77.
34. Rode, F., et al., *Functional effects of the KCNQ modulators retigabine and XE991 in the rat urinary bladder.* European journal of pharmacology, 2010. **638**(1-3): p. 121-7.
35. Roeloffs, R., et al., *In vivo profile of ICA-27243 [N-(6-chloro-pyridin-3-yl)-3,4-difluoro-benzamide], a potent and selective KCNQ2/Q3 (Kv7.2/Kv7.3) activator in rodent anticonvulsant models.* The Journal of pharmacology and experimental therapeutics, 2008. **326**(3): p. 818-28.
36. Wickenden, A.D., et al., *N-(6-chloro-pyridin-3-yl)-3,4-difluoro-benzamide (ICA-27243): a novel, selective KCNQ2/Q3 potassium channel activator.* Molecular pharmacology, 2008. **73**(3): p. 977-86.
37. Gunthorpe, M.J., C.H. Large, and R. Sankar, *The mechanism of action of retigabine (ezogabine), a first-in-class K^+ channel opener for the treatment of epilepsy.* Epilepsia, 2012. **53**(3): p. 412-24.
38. Peretz, A., et al., *Targeting the voltage sensor of Kv7.2 voltage-gated K^+ channels with a new gating-modifier.* Proceedings of the National Academy of Sciences of the United States of America, 2010. **107**(35): p. 15637-42.
39. Greenwood, I.A. and S. Ohya, *New tricks for old dogs: KCNQ expression and role in smooth muscle.* British journal of pharmacology, 2009. **156**(8): p. 1196-203.
40. Stott, J.B., T.A. Jepps, and I.A. Greenwood, *K_V7 potassium channels: a new therapeutic target in smooth muscle disorders.* Drug discovery today, 2014. **19**(4): p. 413-24.
41. Evseev, A.I., et al., *Functional effects of KCNQ K^+ channels in airway smooth muscle.* Frontiers in physiology, 2013. **4**: p. 277.
42. Provence, A., J. Malysz, and G.V. Petkov, *The Novel K_V7.2/K_V7.3 Channel Opener ICA-069673 Reveals Subtype-Specific Functional Roles in Guinea Pig Detrusor Smooth Muscle Excitability and Contractility.* The Journal of pharmacology and experimental therapeutics, 2015. **354**(3): p. 290-301.
43. Mani, B.K., et al., *K_V7.5 Potassium Channel Subunits Are the Primary Targets for PKA-Dependent Enhancement of Vascular Smooth Muscle K_V7 Currents.* Molecular pharmacology, 2016. **89**(3): p. 323-34.
44. Bientinesi, R., et al., *K_V7 channels in the human detrusor: channel modulator effects and gene and protein expression.* Naunyn-Schmiedeberg's archives of pharmacology, 2017. **390**(2): p. 127-137.

45. Brown, A.M., et al., *Ion migration and inactivation in the calcium channel.* Journal de physiologie, 1980. **76**(5): p. 395-402.
46. Barhanin, J., et al., *K(V)LQT1 and lsK (minK) proteins associate to form the I(Ks) cardiac potassium current.* Nature, 1996. **384**(6604): p. 78-80.
47. Brown, D.A. and G.M. Passmore, *Neural KCNQ (K_V7) channels.* British journal of pharmacology, 2009. **156**(8): p. 1185-95.
48. Haick, J.M. and K.L. Byron, *Novel treatment strategies for smooth muscle disorders: Targeting K_V7 potassium channels.* Pharmacology & therapeutics, 2016. **165**: p. 14-25.
49. Yu, H., et al., *A small molecule activator of KCNQ2 and KCNQ4 channels*, in *Probe Reports from the NIH Molecular Libraries Program*. 2010: Bethesda (MD).
50. Yu, H., et al., *Discovery, Synthesis, and Structure Activity Relationship of a Series of N-Aryl- bicyclo[2.2.1]heptane-2-carboxamides: Characterization of ML213 as a Novel KCNQ2 and KCNQ4 Potassium Channel Opener.* ACS chemical neuroscience, 2011. **2**(10): p. 572-577.
51. Hristov, K.L., et al., *$K_V2.1$ and electrically silent K_V channel subunits control excitability and contractility of guinea pig detrusor smooth muscle.* American journal of physiology. Cell physiology, 2012. **302**(2): p. C360-72.
52. Mani, B.K., et al., *Activation of vascular KCNQ (Kv7) potassium channels reverses spasmogen-induced constrictor responses in rat basilar artery.* British journal of pharmacology, 2011. **164**(2): p. 237-49.
53. Brueggemann, L.I., et al., *Exploring arterial smooth muscle K_V7 potassium channel function using patch clamp electrophysiology and pressure myography.* Journal of visualized experiments : JoVE, 2012(67): p. e4263.
54. Werner, M.E., et al., *Frequency encoding of cholinergic- and purinergic-mediated signaling to mouse urinary bladder smooth muscle: modulation by BK channels.* American journal of physiology. Regulatory, integrative and comparative physiology, 2007. **292**(1): p. R616-24.
55. Delmas, P. and D.A. Brown, *Pathways modulating neural KCNQ/M (Kv7) potassium channels.* Nature reviews. Neuroscience, 2005. **6**(11): p. 850-62.
56. Petkov, G.V., et al., *Low levels of K(ATP) channel activation decrease excitability and contractility of urinary bladder.* American journal of physiology. Regulatory, integrative and comparative physiology, 2001. **280**(5): p. R1427-33.
57. Petkov, G.V., *Central role of the BK channel in urinary bladder smooth muscle physiology and pathophysiology.* American journal of physiology. Regulatory, integrative and comparative physiology, 2014. **307**(6): p. R571-84.
58. Gamper, N. and M.S. Shapiro, *KCNQ channels. In Handbook of Ion Channels, J. Zheng and M. Trudeau, eds. (CRC press).* . 2015: p. 275-306.
59. Jepps, T.A., et al., *Fundamental role for the KCNE4 ancillary subunit in $K_V7.4$ regulation of arterial tone.* The Journal of physiology, 2015. **593**(24): p. 5325-40.
60. Bientinesi, R., et al., *K_V7 channels in the human detrusor: channel modulator effects and gene and protein expression.* Naunyn-Schmiedeberg's archives of pharmacology, 2016.
61. Argentieri, T., J. Sheldon, and M. Bowlby, *inventors, Methods for modulating bladder function. U.S. patent 6348486.* American Home Products Corporation, assignee, 2002.

62. Mani, B.K. and K.L. Byron, *Vascular KCNQ channels in humans: the sub-threshold brake that regulates vascular tone?* British journal of pharmacology, 2011. **162**(1): p. 38-41.
63. Xu, Q., et al., *Structure of a Ca^{2+}/CaM:K_V7.4 (KCNQ4) B-helix complex provides insight into M current modulation.* Journal of molecular biology, 2013. **425**(2): p. 378-94.
64. Jepps, T.A., S.P. Olesen, and I.A. Greenwood, *One man's side effect is another man's therapeutic opportunity: targeting K_V7 channels in smooth muscle disorders.* British journal of pharmacology, 2013. **168**(1): p. 19-27.
65. Brown, D.A. and P.R. Adams, *Muscarinic suppression of a novel voltage-sensitive K+ current in a vertebrate neurone.* Nature, 1980. **283**(5748): p. 673-6.
66. Wang, H.S., et al., *KCNQ2 and KCNQ3 potassium channel subunits: molecular correlates of the M-channel.* Science, 1998. **282**(5395): p. 1890-3.
67. Khanamiri, S., et al., *Contribution of K_V7 channels to basal coronary flow and active response to ischemia.* Hypertension, 2013. **62**(6): p. 1090-7.
68. Joshi, S., et al., *KCNQ modulators reveal a key role for KCNQ potassium channels in regulating the tone of rat pulmonary artery smooth muscle.* The Journal of pharmacology and experimental therapeutics, 2009. **329**(1): p. 368-76.
69. Ipavec, V., et al., *K_V7 channels regulate muscle tone and nonadrenergic noncholinergic relaxation of the rat gastric fundus.* Pharmacological research, 2011. **64**(4): p. 397-409.
70. Brickel, N., et al., *The urinary safety profile and secondary renal effects of retigabine (ezogabine): a first-in-class antiepileptic drug that targets KCNQ (K(v)7) potassium channels.* Epilepsia, 2012. **53**(4): p. 606-12.
71. Evseev, A.I., et al., *Functional effects of KCNQ K(+) channels in airway smooth muscle.* Frontiers in physiology, 2013. **4**: p. 277.
72. Mackie, A.R., et al., *Vascular KCNQ potassium channels as novel targets for the control of mesenteric artery constriction by vasopressin, based on studies in single cells, pressurized arteries, and in vivo measurements of mesenteric vascular resistance.* The Journal of pharmacology and experimental therapeutics, 2008. **325**(2): p. 475-83.
73. Gamper, N. and M.S. Shapiro, *KCNQ channels. In Handbook of Ion Channels, J. Zheng and M. Trudeau, eds. (CRC press).* 2015: p. 275-306.
74. Sheldon, J., et al., *Evidence for KCNQ gene expression and M-current activity in rat and human urinary bladder smooth muscle (Abstract) in ASPET–Ray Fuller Symposium Series: Diseases of Aging-1: Lower Urinary Tract Disorders–Physiology, Pharmacology and Therapeutic Approaches; 2002 Jul 6–7; San Francisco, CA. American Society for Pharmacology and Experimental Therapeutics, Bethesda, MD.* 2002.
75. Provence, A., E.S. Rovner, and G.V. Petkov, *Regulation of transient receptor potential melastatin 4 channel by sarcoplasmic reticulum inositol trisphosphate receptors: Role in human detrusor smooth muscle function.* Channels (Austin), 2017. **11**(5): p. 459-466.
76. Hashitani, H. and A.F. Brading, *Ionic basis for the regulation of spontaneous excitation in detrusor smooth muscle cells of the guinea-pig urinary bladder.* British journal of pharmacology, 2003. **140**(1): p. 159-69.

77. Hashitani, H. and A.F. Brading, *Electrical properties of detrusor smooth muscles from the pig and human urinary bladder.* British journal of pharmacology, 2003. **140**(1): p. 146-58.
78. Hristov, K.L., et al., *Novel regulatory mechanism in human urinary bladder: Central role of transient receptor potential melastatin 4 channels in detrusor smooth muscle function.* American Journal of Physiology. Cell physiology, 2016: p. 310(7): C600-C611.
79. Parajuli, S.P., et al., *Control of urinary bladder smooth muscle excitability by the TRPM4 channel modulator 9-phenanthrol.* Channels, 2013. **7**(6): p. 537-40.
80. Smith, A.C., et al., *TRPM4 channel: a new player in urinary bladder smooth muscle function in rats.* American journal of physiology. Renal physiology, 2013. **304**(7): p. F918-29.
81. Launay, P., et al., *TRPM4 is a Ca^{2+}-activated nonselective cation channel mediating cell membrane depolarization.* Cell, 2002. **109**(3): p. 397-407.
82. Earley, S. and J.E. Brayden, *Transient receptor potential channels in the vasculature.* Physiological reviews, 2015. **95**(2): p. 645-90.
83. Earley, S., *TRPM4 channels in smooth muscle function.* Pflugers Archiv : European journal of physiology, 2013. **465**(9): p. 1223-31.
84. Guinamard, R., T. Hof, and C.A. Del Negro, *The TRPM4 channel inhibitor 9-phenanthrol.* British journal of pharmacology, 2014. **171**(7): p. 1600-13.
85. Gonzales, A.L., et al., *Pharmacological inhibition of TRPM4 hyperpolarizes vascular smooth muscle.* American journal of physiology. Cell physiology, 2010. **299**(5): p. C1195-202.
86. Hamilton, K.L., *New life in overactive bladder. Focus on "Novel regulatory mechanism in human urinary bladder: central role of transient receptor potential melastatin 4 channels in detrusor smooth muscle function".* American journal of physiology. Cell physiology, 2016. **310**(7): p. C597-9.
87. Gonzales, A.L. and S. Earley, *Endogenous cytosolic Ca^{2+} buffering is necessary for TRPM4 activity in cerebral artery smooth muscle cells.* Cell calcium, 2012. **51**(1): p. 82-93.
88. Hristov, K.L., et al., *Neurogenic detrusor overactivity is associated with decreased expression and function of the large conductance voltage- and Ca^{2+}-activated K^+ channels.* PloS one, 2013. **8**(7): p. e68052.
89. Hristov, K.L., et al., *Large-conductance voltage- and Ca^{2+}-activated K^+ channels regulate human detrusor smooth muscle function.* American journal of physiology. Cell physiology, 2011. **301**(4): p. C903-12.
90. Provence, A., et al., *Voltage-gated KCNQ Channels in Human Detrusor Smooth Muscle Contractility: A Novel Target for the Pharmacological Treatment of Overactive Bladder.* The Journal of Urology, 2015. **193**(4): p. e188.
91. Provence, A., et al., *K_V7 Channel Pharmacological Modulation in Human Detrusor: A Promising Two-Way Street for the Potential Treatment of Overactive and Underactive Bladder.* The Journal of Urology, 2017. **197**(4): p. e1353.
92. Gonzales, A.L. and S. Earley, *Regulation of cerebral artery smooth muscle membrane potential by Ca^{2+}-activated cation channels.* Microcirculation, 2013. **20**(4): p. 337-47.

93. Fliegert, R., et al., *Modulation of Ca^{2+} entry and plasma membrane potential by human TRPM4b.* The FEBS Journal

2007. **274**(3): p. 704-13.
94. Amberg, G.C. and M.F. Navedo, *Calcium dynamics in vascular smooth muscle.* Microcirculation, 2013. **20**(4): p. 281-9.
95. Xi, Q., et al., *IP_3 constricts cerebral arteries via IP_3 receptor-mediated TRPC3 channel activation and independently of sarcoplasmic reticulum Ca^{2+} release.* Circulation research, 2008. **102**(9): p. 1118-26.
96. Gonzales, A.L., G.C. Amberg, and S. Earley, *Ca^{2+} release from the sarcoplasmic reticulum is required for sustained TRPM4 activity in cerebral artery smooth muscle cells.* American journal of physiology. Cell physiology, 2010. **299**(2): p. C279-88.
97. Gordienko, D.V. and T.B. Bolton, *Crosstalk between ryanodine receptors and IP_3 receptors as a factor shaping spontaneous Ca^{2+}-release events in rabbit portal vein myocytes.* The Journal of physiology, 2002. **542**(Pt 3): p. 743-62.
98. Adebiyi, A., et al., *Isoform-selective physical coupling of TRPC3 channels to IP3 receptors in smooth muscle cells regulates arterial contractility.* Circulation research, 2010. **106**(10): p. 1603-12.
99. Hill-Eubanks, D.C., et al., *Calcium signaling in smooth muscle.* Cold Spring Harbor perspectives in biology, 2011. **3**(9): p. a004549.
100. Gonzales, A.L., et al., *A PLCgamma1-dependent, force-sensitive signaling network in the myogenic constriction of cerebral arteries.* Science signaling, 2014. **7**(327): p. ra49.
101. Earley, S., S.V. Straub, and J.E. Brayden, *Protein kinase C regulates vascular myogenic tone through activation of TRPM4.* American journal of physiology. Heart and circulatory physiology, 2007. **292**(6): p. H2613-22.
102. Earley, S., B.J. Waldron, and J.E. Brayden, *Critical role for transient receptor potential channel TRPM4 in myogenic constriction of cerebral arteries.* Circulation research, 2004. **95**(9): p. 922-9.
103. Nilius, B., et al., *Regulation of the Ca^{2+} sensitivity of the nonselective cation channel TRPM4.* The Journal of biological chemistry, 2005. **280**(8): p. 6423-33.
104. Provence, A., et al., *Regulation of Guinea Pig Detrusor Smooth Muscle Excitability by 17beta-Estradiol: The Role of the Large Conductance Voltage- and Ca2+-Activated K+ Channels.* PLoS One, 2015. **10**(11): p. e0141950.
105. Hanna-Mitchell, A.T., et al., *Pathophysiology of idiopathic overactive bladder and the success of treatment: a systematic review from ICI-RS 2013.* Neurourology and urodynamics, 2014. **33**(5): p. 611-7.
106. Robinson, D., P. Toozs-Hobson, and L. Cardozo, *The effect of hormones on the lower urinary tract.* Menopause international, 2013. **19**(4): p. 155-62.
107. Robinson, D., et al., *Oestrogens and overactive bladder.* Neurourology and urodynamics, 2014. **33**(7): p. 1086-91.
108. Hanna-Mitchell, A.T., Robinson, D., Cardozo, L., Everaert, K., Petkov, G.V. , *Do we need to know more about the effects of hormones on lower urinary tract dysfunction? ICI-RS 2014.* Neurourology and Urodynamics, 2015. **In Press**.

109. Game, X., et al., *[Role of estrogens in lower urinary tract physiology and physiopathology]*. Progres en urologie : journal de l'Association francaise d'urologie et de la Societe francaise d'urologie, 2013. **23**(8): p. 502-10.
110. Koski, M.E. and C.J. Chermansky, *Does estrogen have any real effect on voiding dysfunction in women?* Current urology reports, 2011. **12**(5): p. 345-50.
111. Dambros, M., et al., *Relaxant effects of estradiol through non-genomic pathways in male and female pig bladder smooth muscle.* Pharmacology, 2004. **72**(2): p. 121-7.
112. Sheldon, J.H. and T.M. Argentieri, *Acute administration of 17 beta-estradiol inhibits calcium currents in isolated guinea pig detrusor myocytes.* The Journal of pharmacology and experimental therapeutics, 1995. **274**(2): p. 723-9.
113. Valeri, A., et al., *Effects of 17beta-oestradiol on rat detrusor smooth muscle contractility.* Experimental physiology, 2009. **94**(7): p. 834-46.
114. Patra, P.B., K.S. Thorneloe, and N.J. Laping, *Effect of estrogen and progesterone on urodynamics in the conscious rat.* Urology, 2009. **74**(2): p. 463-6.
115. Yasay, G.D., S.T. Kau, and J.H. Li, *Mechanoinhibitory effect of estradiol in guinea pig urinary bladder smooth muscles.* Pharmacology, 1995. **51**(5): p. 273-80.
116. Maher, J., et al., *Smooth muscle relaxation and activation of the large conductance Ca^{2+}-activated K^+ BK_{Ca} channel by novel oestrogens.* British journal of pharmacology, 2013. **169**(5): p. 1153-65.
117. Valverde, M.A., et al., *Acute activation of Maxi-K channels (hSlo) by estradiol binding to the beta subunit.* Science, 1999. **285**(5435): p. 1929-31.
118. De Wet, H., et al., *Modulation of the BK channel by estrogens: examination at single channel level.* Molecular membrane biology, 2006. **23**(5): p. 420-9.
119. de Wet, H., J.D. Lippiat, and M. Allen, *Analysing steroid modulation of BK(Ca) channels reconstituted into planar lipid bilayers.* Methods in molecular biology, 2008. **491**: p. 177-86.
120. Malysz, J., et al., *Ethanol-mediated relaxation of guinea pig urinary bladder smooth muscle: involvement of BK and L-type Ca^{2+} channels.* American journal of physiology. Cell physiology, 2014. **306**(1): p. C45-58.
121. Cairrao, E., et al., *Non-genomic vasorelaxant effects of 17beta-estradiol and progesterone in rat aorta are mediated by L-type Ca^{2+} current inhibition.* Acta pharmacologica Sinica, 2012. **33**(5): p. 615-24.
122. Ogata, R., et al., *Oestradiol-induced relaxation of rabbit basilar artery by inhibition of voltage-dependent Ca channels through GTP-binding protein.* British journal of pharmacology, 1996. **117**(2): p. 351-9.
123. Broughton, B.R., A.A. Miller, and C.G. Sobey, *Endothelium-dependent relaxation by G protein-coupled receptor 30 agonists in rat carotid arteries.* American journal of physiology. Heart and circulatory physiology, 2010. **298**(3): p. H1055-61.
124. Kelly, M.J., et al., *Rapid effects of estrogen to modulate G protein-coupled receptors via activation of protein kinase A and protein kinase C pathways.* Steroids, 1999. **64**(1-2): p. 64-75.
125. Rosenfeld, C.R. and T. Roy, *Large conductance Ca^{2+}-activated and voltage-activated K^+ channels contribute to the rise and maintenance of estrogen-induced uterine vasodilation and maintenance of blood pressure.* Endocrinology, 2012. **153**(12): p. 6012-20.

126. Dick, G.M. and K.M. Sanders, *(Xeno)estrogen sensitivity of smooth muscle BK channels conferred by the regulatory beta1 subunit: a study of beta1 knockout mice.* The Journal of biological chemistry, 2001. **276**(48): p. 44835-40.
127. Morrow, J.P., et al., *Defining the BK channel domains required for beta1-subunit modulation.* Proceedings of the National Academy of Sciences of the United States of America, 2006. **103**(13): p. 5096-101.
128. Cardozo, L., et al., *A systematic review of the effects of estrogens for symptoms suggestive of overactive bladder.* Acta obstetricia et gynecologica Scandinavica, 2004. **83**(10): p. 892-7.

APPENDIX A: REPRINT AUTHORIZATIONS

[10]

SPRINGER LICENSE
TERMS AND CONDITIONS

Dec 04, 2017

This Agreement between Aaron Provence ("You") and Springer ("Springer") consists of your license details and the terms and conditions provided by Springer and Copyright Clearance Center.

License Number	4241530280482
License date	Dec 03, 2017
Licensed Content Publisher	Springer
Licensed Content Publication	Springer eBook
Licensed Content Title	Ion Channels and Transporters in the Pulmonary Vasculature: A Focus on Smooth Muscle
Licensed Content Author	Amy L. Firth, Jason X.-J. Yuan
Licensed Content Date	Jan 1, 2011
Type of Use	Thesis/Dissertation
Portion	Figures/tables/illustrations
Number of figures/tables/illustrations	1
Author of this Springer article	No
Order reference number	
Original figure numbers	Figure 7, panel A. Illustration of Kv Channel Structure
Title of your thesis / dissertation	KV7 CHANNELS OF THE URINARY BLADDER SMOOTH MUSCLE: FUNCTIONAL ROLES AND THERAPEUTIC POTENTIAL
Expected completion date	Dec 2017
Estimated size(pages)	175

[10] Reprint authorization applies to the figure represented in Chapter 1

[11]

NATURE PUBLISHING GROUP LICENSE TERMS AND CONDITIONS

Dec 04, 2017

This Agreement between Aaron Provence ("You") and Nature Publishing Group ("Nature Publishing Group") consists of your license details and the terms and conditions provided by Nature Publishing Group and Copyright Clearance Center.

License Number	4241540289660
License date	Dec 03, 2017
Licensed Content Publisher	Nature Publishing Group
Licensed Content Publication	Nature Reviews Neuroscience
Licensed Content Title	The neural control of micturition
Licensed Content Author	Clare J. Fowler, Derek Griffiths, William C. de Groat
Licensed Content Date	Jun 1, 2008
Licensed Content Volume	9
Licensed Content Issue	6
Type of Use	reuse in a dissertation / thesis
Requestor type	academic/educational
Format	electronic
Portion	figures/tables/illustrations
Number of figures/tables/illustrations	2
High-res required	no
Figures	Figures 1 and 5
Author of this NPG article	no
Your reference number	
Title of your thesis / dissertation	KV7 CHANNELS OF THE URINARY BLADDER SMOOTH MUSCLE: FUNCTIONAL ROLES AND THERAPEUTIC POTENTIAL
Expected completion date	Dec 2017

[11] Reprint authorization applies to the figure represented on page in Chapter 1

12

Estimated size (number of pages) 175

Copyright Clearance Center RightsLink®

Taylor & Francis Taylor & Francis Group

Journal Reprints

Title: Regulation of transient receptor potential melastatin 4 channel by sarcoplasmic reticulum inositol trisphosphate receptors: Role in human detrusor smooth muscle function

Author: Aaron Provence, Eric S. Rovner, Georgi V. Petkov

Publication: Channels

Publisher: Taylor & Francis

Date: Sep 3, 2017

Rights managed by Taylor & Francis

Logged in as:
Aaron Provence
Account #: 3001224853

LOGOUT

Thesis/Dissertation Reuse Request

Taylor & Francis is pleased to offer reuses of its content for a thesis or dissertation free of charge contingent on resubmission of permission request if work is published.

BACK CLOSE WINDOW

[12] Reprint authorization applies to the reprinted manuscript in Chapter 6.

[13]

November 20, 2017

Aaron Provence
Drug Discovery and Biomedical Sciences Department
University of South Carolina
1062 Koon Rd
Irmo, SC 29063

Email: provenca@sccp.sc.edu

Dear Aaron Provence:

This is to grant you permission to include the following article in your dissertation entitled "K_V7 Channels in Detrusor Smooth Muscle: Functional Roles and Therapeutic Potential" for the University of South Carolina:

> A Provence, J Malysz, and GV Petkov (2015) The Novel $K_V7.2/K_V7.3$ Channel Opener ICA-069673 Reveals Subtype-Specific Functional Roles in Guinea Pig Detrusor Smooth Muscle Excitability and Contractility, *J Pharmacol Exp Ther*, 354(3):290-301; DOI: https://doi.org/10.1124/jpet.115.225268

On the first page of each copy of this article, please add the following:

> Reprinted with permission of the American Society for Pharmacology and Experimental Therapeutics. All rights reserved.

In addition, the original copyright line published with the paper must be shown on the copies included with your thesis.

Sincerely yours,

Richard Dodenhoff
Journals Director

[13] Reprint authorization applies to the reprinted manuscript in Chapter 3.

14

November 20, 2017

Aaron Provence
Drug Discovery and Biomedical Sciences Department
University of South Carolina
1062 Koon Rd
Irmo, SC 29063

Email: provenca@sccp.sc.edu

Dear Aaron Provence:

This is to grant you permission to include the following article in your dissertation entitled "K_V7 Channels in Detrusor Smooth Muscle: Functional Roles and Therapeutics Potential" for the University of South Carolina:

> A Provence, D Angoli, and GV Petkov (2017) K_V7 Channel Activation by the Novel Activator ML213: Role for Heteromeric $K_V7.4/K_V7.5$ Channels in Guinea Pig Detrusor Smooth Muscle Function, *J Pharmacol Exp Ther*, DOI: https://doi.org/10.1124/jpet.117.243162

On the first page of each copy of this article, please add the following:

> Reprinted with permission of the American Society for Pharmacology and Experimental Therapeutics. All rights reserved.

In addition, the original copyright line published with the paper must be shown on the copies included with your thesis.

Sincerely yours,

Richard Dodenhoff
Journals Director

[14] Reprint authorization applies to the reprinted manuscript in Chapter 4.